Tailoring Properties of Polythiophene - based Electrochromic Displays

MPhil Thesis 2021

Shufan Yang
C1892026

Table of Contents

Acknowledgements

I want to thank professor Davide Bonifazi for allowing me to study the field of supermolecules in-depth at Cardiff University. I have gained a deeper understanding of Chemistry and a growing interest in it, which has made me more determined to pursue my future research path.

To all my colleagues in Davide Bonifazi group: Thank you for helping me to adapt quickly to the intense atmosphere of research and helping me a lot when necessary. When I was in trouble, not only in life but also in the lab, you were always there to help me without hesitation. Particularly, Dr. Antoine Stopin, Mr. Jack Fletcher-Charles, Mr. Gianvito Romano, Dr. Grazia Bezzu, Miss. Deborah Romito, Mr. Andre Sequeira, Mr. Luca Guarnieri., Miss. Oliwia Matuszwska and Miss. Stavroula Sakellakou helped me a lot when I need to use the new instruments or new devices. They also gave me tons of suggestions to purify the crude product in some reactions which were difficult to purify. The lab life becomes more exciting and colourful because of you guys.

A special thanks to Dr. Antoine Stopin, who gave guidance and teaching for my thesis. His extensive knowledge of chemistry theory and specialised organic synthesis gave me a lot of ideas and inspiration. Without his guidance, my understanding of many chemical theories and knowledge would probably have remained relatively marginal. In addition, special thanks to Mr. Jack Fletcher-Charles for his extensive proofreading work and valuable advice on the thesis and Mr. Gianvito Romano for carrying out plenty of characterisations of the electrochromic devices.

Last but not least, I would like to thank my family and friends. You have been very supportive throughout my thesis. Thank you for your motivation and patience when I was discouraged, which helped me to remain patient and optimistic during the most challenging times. This work would not have been possible without your full support.

List of Abbreviations

Abs	Absorption
°C	Degrees Celsius
calc.	Calculated
conc.	Concentrated
DCM	Dichloromethane
e^-	Electron
EC	Electrochromic
ECP	Electrochromic polymer
ECD	Electrochromic Device
eq.	Equivalents
ES	Electrospray Ionisation
h	Hours
HOMO	Highest Occupied Molecular Orbital
IR	Infrared
ITO	Indium Tin Oxide
LEDs	Light Emitting Displays
LUMO	Lowest Unoccupied Molecular Orbital
M.p.	Melting Point
MS	Mass Spectroscopy
nm	Nanometres
NMR	Nuclear Magnetic Resonance Spectroscopy
OLEDs	Organic Light Emitting Diodes
PEDOT	Poly(3, 4-ethylenedioxythiophene)
PE	Petroleum ether
PET	Polyethylene terephthalate
PProDOT	Poly(3,4-(propylenedioxy)thiophene)
PPy	Polypyrrole
PT	Polythiophene
Pt	Platinum
PTSA	p-toluenesulfonic acid
r.t.	Room Temperature
Rf	Retention Factor

TLC	Thin Layer Chromatography
UV	Ultra-violet
V	Volts
λ	Wavelength
ν	Frequency

Abstract

The synthesis of sixteen thiophene-based copolymers was achieved, using four known 3,4-bis(alkyloxy)thiophene monomers copolymerised with four novel alkoxybenzyl/alkoxynaphthyl thiophene (3 and 4 position) monomers respectively. The polymerisation was performed using a ratio of known monomer to novel monomer of 10 to 1, using iron (III) chloride as catalyst. The steric hindrance of these copolymers can be changed marginally by varying the different positions of the substituent in the alkoxy thiophene (3 and 4 position) monomers. The colour and the properties of copolymers are also changed through the modulation of the steric hindrance. All synthesised copolymers were used to fabricate prototype electrochromic devices and subjected to spectroelectrochemical analysis. In particular, copolymer **75** exhibited excellent electrochromic properties which can be fully oxidised at very low applied voltage (+ 1.5 V) and exhibited fast switching times (0.6 s). It switched between a purple colour in the neutral state and a highly transparent colour in its oxidised state.

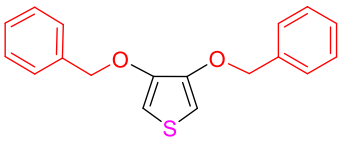

3,4-bis(benzyloxy)thiophene

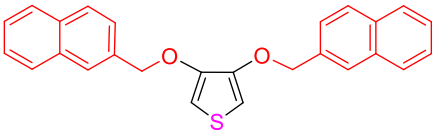

3,4-bis(naphthalen-2-ylmethoxy)thiophene

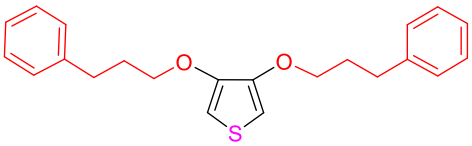

3,4-bis(3-phenylpropoxy)thiophene

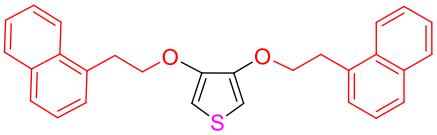

3,4-bis(2-(naphthalen-1-yl)ethoxy)thiophene

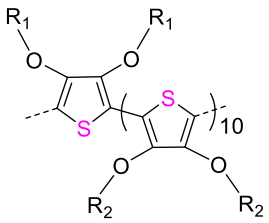

copolymer

R_1: Alkoxybenzyl/alkoxynaphthyl group

R_2: Alkoxyl group

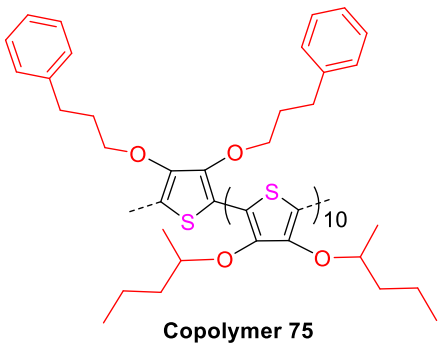

Copolymer 75

1. Introduction

1.1 Electrochromism and Electrochromic devices (ECDs)

Electrochromism can be defined as colour and optical properties of a material that change upon a temporarily applied voltage.[1] In recent years, electrochromic devices (ECD) have received significant attention, and have been used commercially in sensors,[2, 3] smart windows,[4] colour-changing fibers,[5] electronic papers,[6] and displays.[7] In all applications of this technology, the colour change exhibited by an electrochromic device (ECD) needs to be precisely controlled according to its colour saturation and brightness.[2, 8] At a given range of wavelengths, the ECDs responds to the applied voltage by varying the transmittance and switching between different colour states.[8] Generally, ECDs are made up of 7 layers, which is composed of two protective layers, two working electrodes, two electroactive layers and an electrolyte, respectively. As it can be seen in Figure 1, the function of the working electrode is to allow oxidation and reduction of the EC material to proceed at the electrode. After that, there is a counter electrode that acts as a charge balance and ion storage layer. The role of the electrolyte is to maintain the ion migration between the two electrodes.[8]

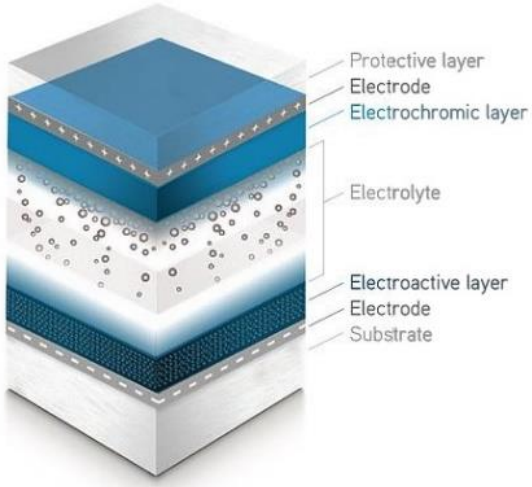

Figure 1: A basic structure of EC window fabricated by Ynvisible.[9]

Electrochromic materials attract a lot of attention because they are valuable in applications. Electrochromic windows are one of the good example of an application where electrochromic materials are added to the window to improve indoor comfort by adjusting the degree of colour change in the material to control the quantity of solar radiation reaching the room.[10] For electrochromic windows, high optical contrast and

long cycle life are necessary, as well as fast switching speeds. Electrochromic materials are being developed that are high-performance, environmentally efficient and low-cost.

1.2 Electrochromic parameters

1.2.1 Electrochromic Contrast

1.2.1.1 Difference of transmittance

Electrochromic contrast of an ECD is usually defined as the percent transmittance change (ΔT, %) between its neutral state and oxidised state at a given wavelength, and is the main parameter for the characterisation of electrochromic materials.[11] The chosen control wavelength is usually the wavelength at which the electrochromic material shows the highest optical contrast. The results can be used to assess the difference of transmittance through a broad range of wavelengths. Notably, the absorbance values acquired by spectroelectrochemical experiments can be converted to percentage of transmittance (%T) because the absorbance and transmittance are reciprocal. Kerszulis *et. al.* reported the spectroelectrochemistry of copolymer Pro-$Ac_{0.65}$/$EBE_{0.35}$ in three different states in three potentials (– 800 mV, 150 mV and 800 mV respectively), as it can be seen in Figure 2.[12] The transmission spectrum of the neutral state can be seen as a blue line, the intermediate state as green, and the oxidised state as red. At the wavelength of ~ 480 nm, the transmittance change reached to around 67 %.

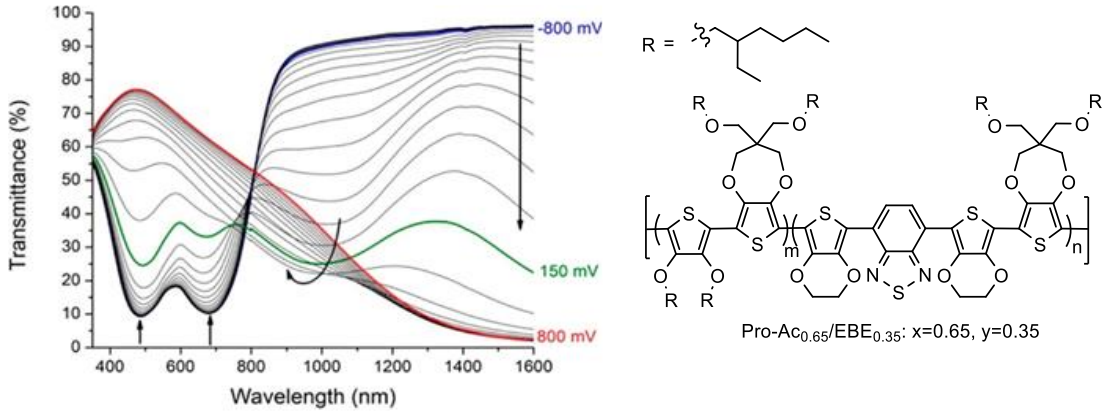

Figure 2: Spectroelectrochemistry of copolymer Pro-$Ac_{0.65}$/$EBE_{0.35}$: x=0.65, y=0.35 by Kerszulis *et al.*[12]

1.2.1.2 Optical contrast

Colourimetry is a technique that converts the spectrum to a physical connection with colour perception.[13] In order to have a better understanding of colourimetry, colour space exhibiting all possible colours in a quantitative form must be introduced. Figure 3 presents two colour spaces commonly used during the analysis of electrochromic material: xyY, and L*a*b*. For the xyY colour space, a straight line between two points

in the colour space means that all possible colours are shown by mixing the edges of the line. The disadvantage of the xyY colour space is that the colour points are only consistent in two-dimensional space, and the geometric distance between the colour points lacks consistency.

When compared with the xyY colour space, the L*a*b* colour space enables 3-dimensional consistency of colour points.[14] In this colour space, L* represents brightness: the value of 0 to100 means the colour from black to white; a* denotes the green to red range of the colour space; and b* describes blue to yellow (negative to positive values, respectively). As the range of a* and b* increases, the colour becomes more saturated, and the colour phase changes as it moves between colour values.[12]

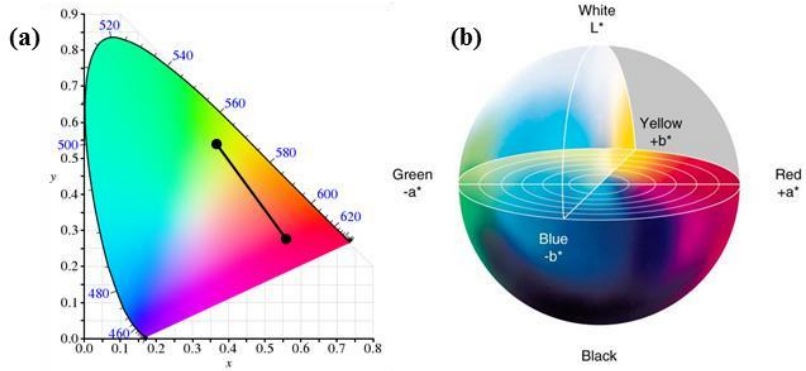

Figure 3: (a) xyY colour space. (b) L*a*b* colour space.[14]

The International Commission on Illumination (CIE) defines the distance metric as the colour contrast (ΔE^*_{ab}).[15, 16] Mathematically, ΔE^*_{ab} represents the distance between any two points in the sphere. Two colours in the sphere are set as (L_1*, a_1*, b_1*) and (L_2*, a_2*, b_2*), respectively. In order to obtain the distance of the line segment (ΔE^*_{ab}) in the sphere, it is necessary to use the distance equation between two points through the use of the Pythagorean theorem. Therefore, given (L_1*, a_1*, b_1*) and (L_2*, a_2*, b_2*) as two colours in colour space, the colour difference formula is defined as:

$$\Delta E^*_{ab} = \sqrt{(L^*_2 - L^*_1)^2 + (a^*_2 - a^*_1)^2 + (b^*_2 - b^*_1)^2}$$

Vice versa, the corresponding colourimetry values of L*, a* and b* can be obtained using the specialised equipment and the ΔE^*_{ab} value of the target object can be identified. Herein, to better understand the colour difference, there is a “game colour test” to distinguish colour differences in Figure 4: The colour difference in figure 4a is the easiest to identify. From figure 4a to figure 4c, it becomes increasingly difficult to recognise the colour difference in an area. The value of L*, a* and b* of this colour were obtained in colour grab.[17] In Figure 4a, the L*, a* and b* values for the lighter

and darker areas are (78.1, - 9.4, - 20.2) and (41.8, - 7.6, -21.8), giving the ΔE^*_{ab} value of 36.37. As for Figure 4b, the L^*, a^* and b^* values for the lighter area is (90.3, - 33.0, 13.1) and darker area is (76.1, - 33.8, 13.9) which gives a ΔE^*_{ab} value of 14.24. In Figure 4c, the L^*, a^* and b^* values for the lighter and darker areas are (84.7, 3.3, - 6.6) and (75.1, 4.2, - 7.1) respectively. The ΔE^*_{ab} value here is 9.65. Therefore, the ΔE^*_{ab} value decreases as it becomes increasingly difficult to distinguish the colour difference from Figure 4a to Figure 4c.

a)

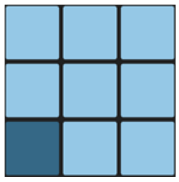

b)

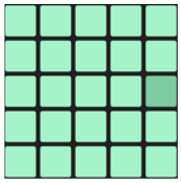

c)

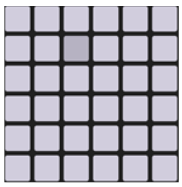

Figure 4: a) Areas that can easily distinguish colours. b) Areas that is not easy to distinguish colours. c) Areas that is difficult to distinguish colours.[18]

1.2.2 Switching Rate

Switching rate is the time it takes for an electrochromic material to complete the process of switching from a redox state to another state.[19] Factors such as device structure, unit configuration and magnitude of the applied external voltage can all affect the switching rate. In particular, the ionic mobility of the electrolyte and the ability of these counterbalancing ions to diffuse through the EC active layer are the determination factors of switching rate.[11, 20]

The switching rate can be analysed by measuring the transmittance at a chosen wavelength of light (λ_{max}) in a repeated redox step experiment. To be specific, through choosing the maxima wavelength of the electrochromic materials, and applying the potential repeatedly between the material's neutral and most oxidise transmissive state,

the time taken to reach the total transmittance change can be measured. Figure 5 demonstrates the switching time for a film of poly(pentadecafluoro-octanoic acid 2,3-dihydro-thieno(3,4-b)(1,4)dioxin-2-ylmethylester) (PEDOT-F) synthesised by Schwendeman *et al.*[21] It shows the change in transmission during switching between neutral and oxidised states. The transmittance contrast (Δ% T) is calculated by subtracting the light transmission of the most oxidised and neutral forms. It exhibited rapid switching times (around 1.2 s) and high transmittance (66%) at 95 % of full contrast.[21]

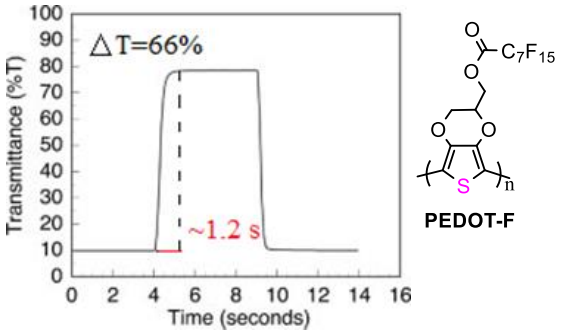

Figure 5: Switching time of PEDOT-F as recorded at λ_{max} = 608 nm by Schwendeman *et al.*[21].

1.2.3 Coloration Efficiency

Coloration efficiency (CE) is defined as the change in optical density (OD) per unit charge (Q) insertion or extraction from an electrochromic film.[22] Optical density is the proportion of the incident light intensity falling on a given substance to the transmitted intensity, which represents a measurement of absorbance.[11] As an inherent property of electrochromic materials, the value of CE reflects the optical modulation range capability of the device. The value of coloration efficiency can be calculated as following formula:

$$CE(\lambda) = \frac{\Delta OD(\lambda)}{Q}, \quad \Delta OD(\lambda) = \log \frac{T_b}{T_c}$$

Specifically, T_b represents the transmittance in bleached state and T_c represents the transmittance in coloured states. Q is the integration of the current with the coloration time, and λ is the given wavelength.[22]

1.2.4 Stability

As mentioned earlier, for many application electrochromic materials such as electrochromic polymers (ECP) must have a long cycle life. Therefore, to achieve this long cycle life, the ECP requires a stable redox process, which allows the electrochromic properties can be reproduced during repeated switching.[23]

Testing of long-term switching stability is generally achieved in a three-electrode electrochemical cell by repeated potential cycles, which can be seen in Figure 6. The switching performance of the electrochromic materials can be assessed after 10,000-100,000 cycles on a transparent conductive substrate (in most cases using ITO coated PET slide).

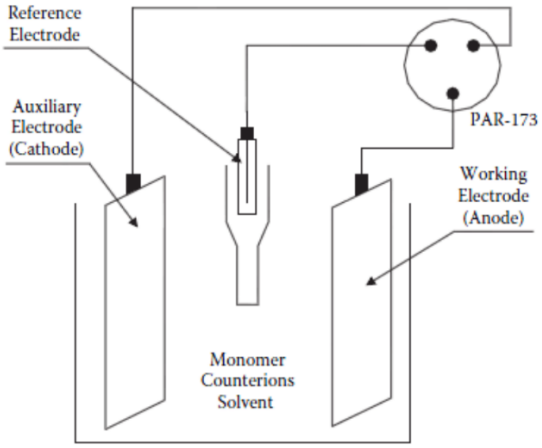

Figure 6: Three electrode electrochemical polymerisation cell by Kashif Iqbal.[24]

In an ECP device, the stability of the ECP is subjected to external and internal disruptions. Externally, the resistance heating during repeated switching can affect its stability. Internally, the interference of water and O_2 with the redox composition of the EC and the self-degradation of the electrode material can have an impact on stability.[11] Poorly stable materials cannot stand up to high-speed switching potentials and will result in the loss of neutral state colour or delamination.

1.3 Electrochromic Materials

1.3.1 Inorganic Electrochromic Materials

The first report of electrochromism was published in 1969 when tungsten oxide (WO_3) was shown to change colour from colourless to blue by Deb *et al.*[5] Since this initial work, the oxides (in film form) of many transition metals, for example, rhodium,[25] ruthenium,[26] manganese,[27] etc. have been studied extensively with each, showing that they have electrochromic properties.[28] These materials have many drawbacks; however, the main issue is that inorganic metal oxides are lacking in terms of material stability and precise colour adjustment. Compared to metal oxides, organic electrochromic materials offer excellent colour efficiency,[29] faster switching time,[30] greater precision in colour modulation,[31] and high stability.[32] As a result, the attention of researchers is increasingly focused on organic electrochromic materials.

1.3.2 Organic Electrochromic Materials

1.3.2.1 Electrochromic Polycyclic Aromatic Hydrocarbons

In recent years, Polycyclic Aromatic Hydrocarbons (PAHs) have distinguished themselves in the area of electrochromic colour change due to their good solubility and precise colour adjustment. In the field of ECD preparation using small molecule PAHs, Stec *et al*.[33] made a nearly transmissive ECD using perylene, which can be changed from royal blue in the neutral state (– 3.5 V) to olive in its oxidised state (+ 4.0 V). The molecule and the electrochromism exhibited by the ECD can be seen in Figure 7. The device requires extremely high potentials due to the formation of polaron and bipolaron that cause colour changes from colourless to blue and colourless to olive.[33] More recently, Corrente *et al.* synthesised a series of EC molecules using dibenzofuran.[34] The absorption and bandgap of the synthesised molecules are modified by changing the degree of conjugation within substituents on the dibenzofuran based-molecule. The synthesised molecules cover a series of colours: colourless, light pink, light orange, orange-red, etc. Figure 8 demonstrates these ECDs with good cyclability (> 10,000 cycles) for the transition from neutral state to oxidised state.[34]

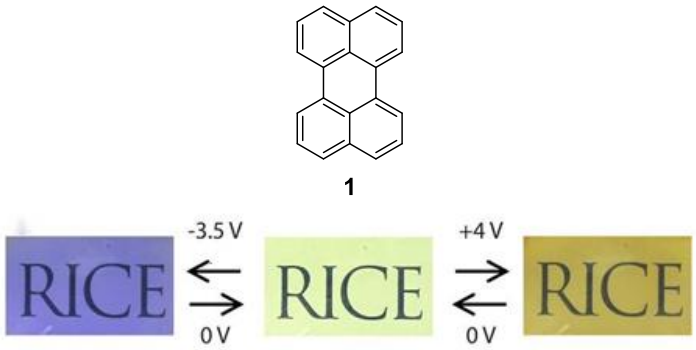

Figure 7: By applying – 3.5, 0 and + 4 V to the ITO electrodes, it is achievable to switch reversibly between the blue, almost colourless and olive.[33]

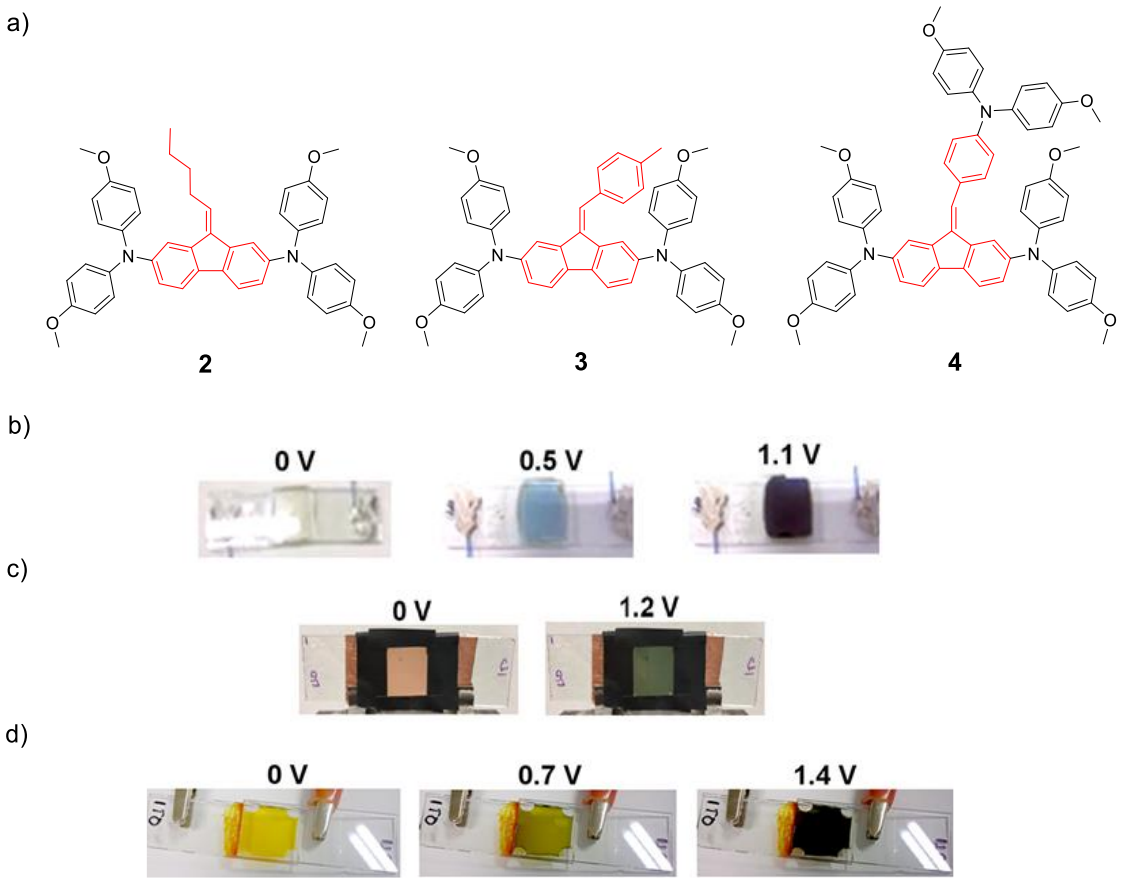

Figure 8: a) Three types of dibenzofulvene derivatives synthesised by Corrente *et al.*; b) Colour switching of the ECD using molecule **2**; c) Colour switching of the ECD using molecule **3**; d) Colour switching of the ECD using molecule **3** and **4**.[34]

1.3.2.2 Organic Electrochromic Polymers

Over the past decades, conductive polymers with polyenes and polyaromatic compounds have attracted more attention. (e.g. polyaniline, polypyrrole, polyfuran, polythiophene, polyphenylene).[3] The derivatives of polypyrrole and polythiophene have shown good prospects.[35] However, the solubility of these polymers is not ideal in organic solvent. In order to address these issues, a series of substituted derivatives of these polymers have been synthesised by attaching functional side chains, such as alkyl/benzyl groups, leading to polymers with good solubility, fast switching time and high optical contrast.[8, 36] The main subject of research regarding the properties of organic electrochromic polymers has been side chain modification, since this modification has been shown to be the main factor affecting the solubility, bandgap, ionic conductivity and morphology of the compound.[37]

1.3.3.2.1 Polypyrrole

Polypyrrole has been of great interest in recent years for its low oxidation potential.[38] Compared with other organic electrochromic polymers, it has better film-forming

properties, low oxidation potential, excellent solubility in organic solvent, excellent compatibility in the aqueous phase, and relatively high electrical conductivity.[3] Functionalisation is usually performed at the 3-position, 4-position, or at the nitrogen position of the pyrrole heterocycle.[11] Diaz *et al.* were focused on forming films with comparison between unsubstituted polypyrrole, N-alkyl polypyrrole and N-phenyl functionalised polypyrrole.[39, 40] As it can be seen in Figure 9, molecule **5** has a bandgap value of 2.7 eV, switching from high transparent yellow in the neutral state to brown-black in its fully oxidised state. Other polypyrrole derivatives investigated (molecules **6**, **7**, **8**, **9**, **10**) were found to switch colour from yellow to black unaffected by N-alkyl and N-phenyl functionalisation of the main chain. These results show that the steric distortion caused by the N-substituted group along the backbone of the corresponding homopolymer is small. Furthermore, structural modifications were capable of lowering the conductivity values of doped polypyrroles, which was proven in the conductivity studies of unsubstituted polypyrroles with different N-substituted polypyrrole derivatives.[11, 41, 42]

In contrast to N-substituted pyrrole, the synthesis of 3- and 4-position substituted pyrrole derivatives is extremely demanding due to the poor stability of the monomers, and the synthesised polymers are sensitive to O_2 and water.[43] Several studies have been reported on the synthesis of C-substituted PPys (**11**-**13**) and the corresponding properties have been investigated.[44]

Pyrrole monomers bridged at the N position by polyether bonds were synthesised by Cihaner *et al.* and the corresponding polymer **14** was characterised.[45, 46] The synthesised polymer can be converted from yellow-green in the neutral state to dark green in its oxidised state. Ak *et al.* reported a star-shaped molecule (2,4,6-tris(4-(1H-pyrrol-1-yl)phenoxy)-1,3,5-triazine) (Tria-Py) and synthesised its corresponding polymer: P(Tria-Py) successfully.[47] After equipping P(Tria-Py) and poly(3,4-ethylenedioxythiophene) (PEDOT) as two different electroactive layers to form the complementary-coloured device, this device exhibited low oxidation potentials (+1.5 V) and fast switching times (2.2 s). It switched from a red colour in the neutral state to a turquoise in its oxidised state.[47]

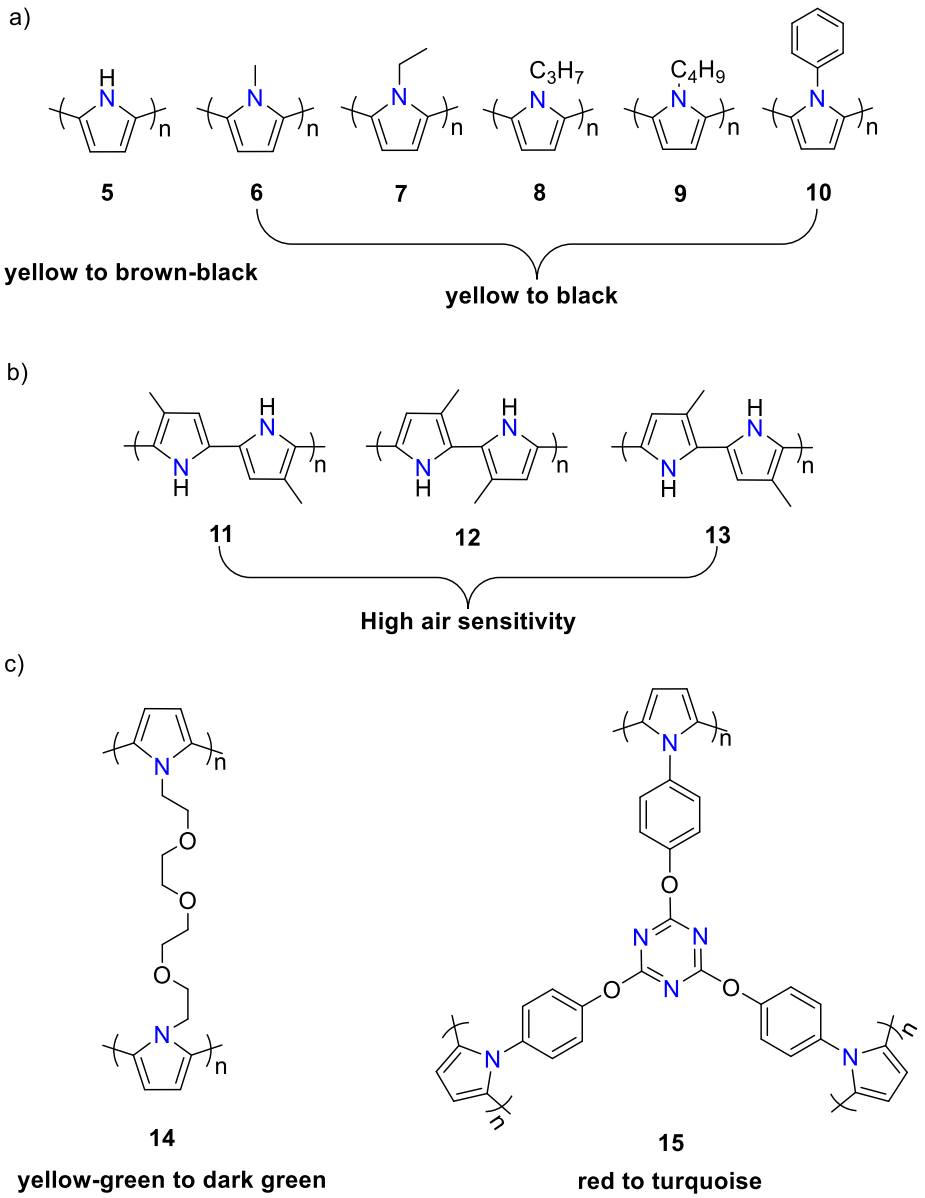

Figure 9: a) Polypyrroles synthesised by Diaz *et al.*[39, 40] b) C-substituted polypyrroles on the 3 and 4 positions synthesised by Benincori *et al.*[44] c) Polypyrrole synthesised by Cihaner and the colour changes.[45, 46] d) The structure of P(Tria-Py) and the colour changes of P(Tria-Py)/(PEDOT) ECD.[47]

1.3.3.2.2 Polythiophene

1.3.3.2.2.1 Poly(alkylthiophene)s

The first utilising polythiophenes (PTs) for EC applications was reported by Garnier *et al.* in 1983.[48, 49] The authors investigated the electrochromic properties of five-membered heterocyclic polymers using the monomers pyrrole, thiophene, 3-methylthiophene, and 3,4-dimethylthiophene. Changes in the colour and performance of the synthesised PTs were achieved through changing the substituent of the monomers and supporting salts. In particular, they were the first to propose that the homogeneity of the polymer film significantly influences the switching time of the polymer: the

higher homogeneity of the polymer, the shorter the switching time. The switching time obtained for polymer attached to the polished Platinum (Pt) surface was about 10 times faster than the switching time (0.1 to 0.5 s) for the polymer attached to the rough Pt electrode.[48] Compared with other electrochromes, polythiophenes offer materials with better stability, excellent coloration efficiency, and easier processing for device fabrication.[50] Unsubstituted polythiophene **16** was electrochemically polymerised on ITO using standard electrochemical equipment, appearing with a red colour in the neutral state switching to a blue in its oxidised state (+ 0.3 V).[51] Figure 10b exhibits the doped and undoped form of unsubstituted polythiophene and its colour in each state. When applying a positive voltage to undoped polythiophene, it goes through an oxidation reaction, losing electrons and forming a dicationic state. In its oxidised state, the conjugation of the polymer increases significantly, narrowing the energy gap, thus red-shifting the absorption wavelength of polythiophene. Substituted polythiophenes were synthesised by Heywang *et al.*[51] and Mastragostino *et al.*[52] When substituted with alkyl group at the 3-position of thiophene such as P3MT (**17**), the electrochromic properties of polymers do not change significantly.[53] P3MT switched between an orange-red colour in the neutral state and a light blue colour in its oxidised state (+ 0.72 V).[52] The structure of P3MT can be seen in Figure 10a. Interestingly, Osaka *et al.* described a range of solution-processable poly(alkylthiophene) derivatives.[54] These materials form high conductivity and stability complexes with electron acceptors. Their conductivities after doping can be seen in Figure 10c. The conductivity of the poly(alkylthiophene) derivatives was found to be lightly affected by the length of the alkyl substituents or by adding different dopants, and the conductivities obtained after their doping were typically high. Therefore, substituting with alkyl side chains of polythiophene improves the solubility of the polymer, making the commercialisation of devices become accessible.[54, 55]

a)

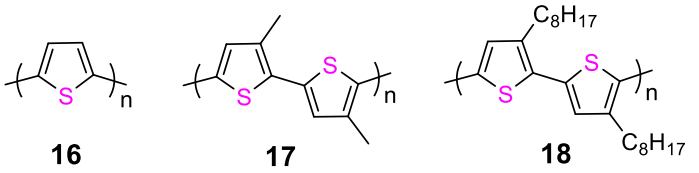

16 red to blue | 17 red to blue purple | 18 orange red to blue

b)

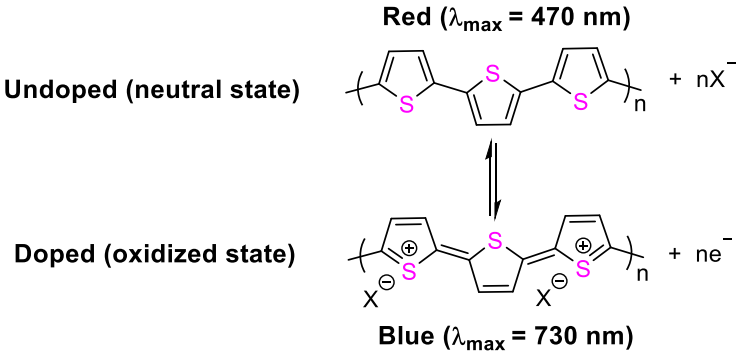

c)

Polymer	Dopant	δ 300K (ohm^{-1} cm^{-1})
Poly (3-Methylthiophene) P3MT	I_2	3
	$NOBF_4$	4
	$NOPF_6$	4
	$NOSbF_6$	3
Poly (3-Ethylthiophene) P3ET	I_2	3
Poly (3-n-Butylthiophene) P3BT	I_2	4
	$NOSbF_6$	6 (Film)
Poly (3 -Thiomethylthiophene) P3TMT	I_2	0.5
Poly (3,4-Dimethylthiophene) PDMT	$NOSbF_6$	0.5
	I_2	—
Poly (3-Methylthiophene-co-3'-n-Butylthiophene) (50:50) P3MTBT	$NOSbF_6$	20 (Film)
	I_2	4
	$FeCl_3$	50 (Film)
Poly (3-Methylthiophene-co-3'-n-Octylthiophene) (60:40) P3MTOT	$NOSbF_6$	5

Figure 10: a) Polythiophenes synthesised by Heywang *et al*. and Mastragostino *et al*. b) Doped and undoped form of unsubstituted polythiophene and colour in either state. c) Conductivities of doped polythiophenes.[54]

1.3.3.2.2.2 Poly(3,4-(ethylenedioxy)thiophene)s

Inganäs *et al.*[56] initially reported the first PEDOT electrochromic device. The synthesised polymer possessed a narrow energy gap (1.6 eV) and a low oxidation potential (+ 1.0 V). The PEDOT produced in this work shows a colour change from deep blue in its coloured state to a transparent light blue in its bleached state. The outstanding transmittance of PEDOT **19** has attracted much attention, as it starts to absorb light in the near infrared region in the neutral state, coupled with a minimal tail

in the charged carrier transition generated by visible electrochemical oxidation.[11] Figure 11b shows the spectroelectrochemical analysis of **19**, by applying a variable voltage to show the various colours. At voltages from – 0.9 V to + 1.0 V, the λ_{max} of PEDOT was approximately 600 nm.

Since 2004, PEDOT and its derivatives have been in the spotlight of numerous publications. The first solution-processable PEDOT derivatives (**20**, **21** and **22**) were produced by Reynolds *et al.*[30, 57, 58] who went on to study the corresponding electrochemical properties. Figure 11c demonstrates the structures of mono alkyl-substituted PEDOT derivatives **20**-**22**. The maximum absorption of wavelength of polymer **19** was observed at 605 nm. The λ_{max} of polymers **21** and **22** was 635 nm and 650 nm separately. Therefore, it can be concluded that the change in wavelength is due to the electronic coupling in the alkyl-substituted PEDOT derivatives. The splitting of the π-π* transition leads to a shift in the λ_{max} of the ECP, which changes optical contrast of λ_{max}. These results indicate that polymer **21** after alkylation can achieve a high electrochromic contrast of 59 % (Δ%T).

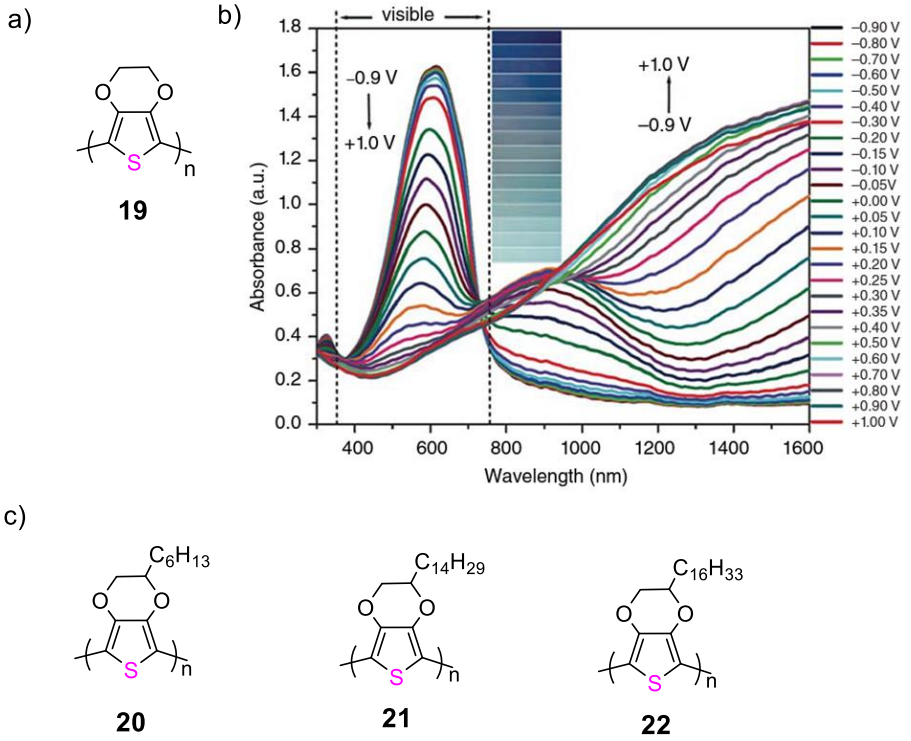

Figure 11: a) Structure of PEDOT (**19**) b) Spectroelectrochemical analysis of **19**. As reported by Sonmez *et al.*[59] (c) Derivatives of PEDOT by Reynolds *et al.*[30, 57, 58]

1.3.3.2.2.3 Poly(3,4-(propylenedioxy)thiophene)s

In 1994, Dietrich and Heinze *et al.* synthesised and characterised Poly(3,4-propylenedioxythiophene) (PProDOT) (**23**), which exhibited excellent stability and optical properties.[60] Building on this, Reynolds *et al.* conducted an in-depth study of the relationship between the structure and electrochromic properties in PXDOTs.[29] In this work, they compared PProDOT (polymer **23**), the poly(3,4-butylenedioxythiophene) (PBuDOT, polymer **24**) and the poly(3,4-(2,2-dimethylpropylenedioxy)thiophene) (PProDOT-Me_2, polymer **25**). The switching time for polymer **24** to complete discolouration by oxidation was found to be almost two times faster than polymer **23** (1.3 s and 2.2 s respectively). This result demonstrates that the larger alkylidene dioxin rings possess a more effective redox process.[29, 57] The structures of PProDOT, analogue of PXDOT and derivatives of PProDOT can be seen in Figure 12. Compared with **23**, the doped state of **25** was found to have a higher transmittance. Therefore, it was experimentally proposed that alkyl substitution impedes interchain charge migration and therefore may attenuate the near-infrared optical leap in visible light region and cause observable residual colour phases.[11]

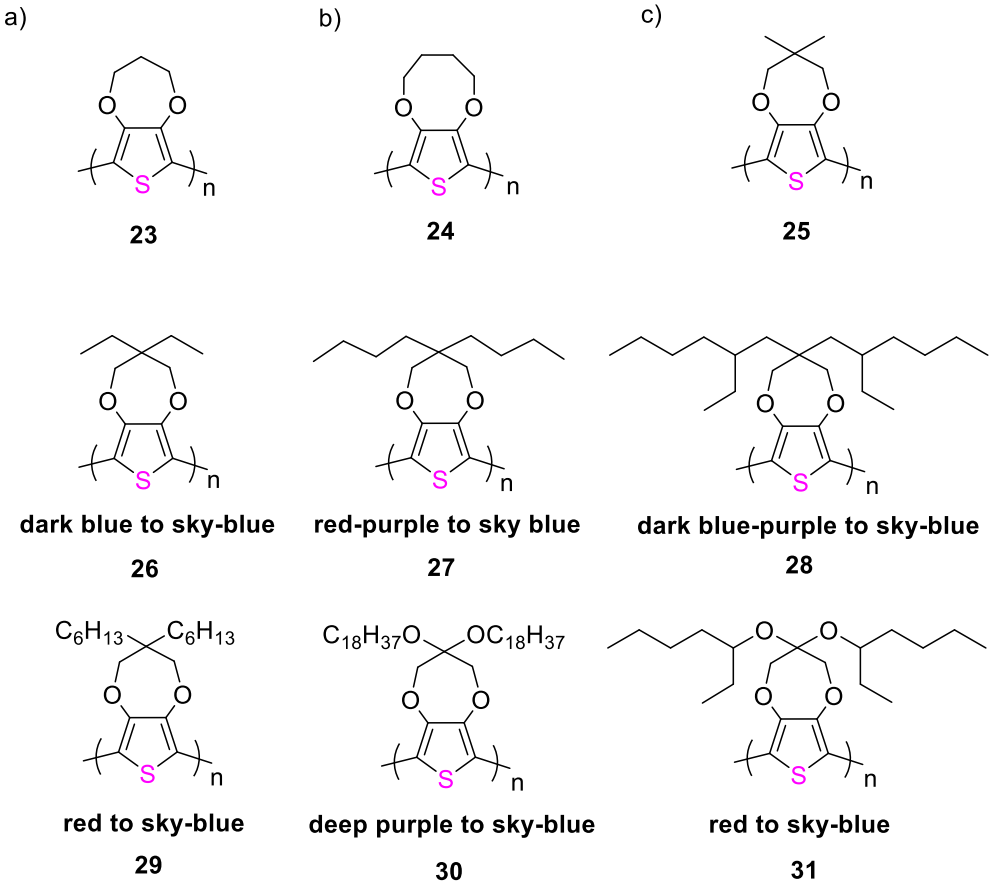

Figure 12: a) PProDOT. b) Analogue of PXDOT. c) Derivatives of PProDOT (**25** to **31**).

In 2002, Carleton *et al.*[61] reported poly(3,4-(2,2-diethylpropylenedioxy)thiophene) (PProDOT-Et_2, polymer **26**) with high transmittance (~ 75 % at λ_{max} = 580 nm) and high colour efficiency (505 cm^2/C). It switched between black blue in the coloured state and light sky-blue in its bleached state. At an applied potential of – 0.1 V, **26** has a maximum absorbance at 580 nm. Figure 13 demonstrates that the energy gap, for the beginning of π-π* transition of PProDOT-Et_2 is 1.75 eV. Compared with unsubstituted PProDOT **23** and PProDOT **24**, PProDOT-Et_2 **26** showed the highest switching speed, 0.3 s to achieve 95 % of its full contrast. Comparing these three PProDOT derivatives, the switching time of PProDOT **23** is the slowest. Therefore, PProDOT derivatives with more substituted alkyl linear chains makes the movement of ion faster, thus giving faster switching speeds.[62] Additional work from Welsh *et al.*[63] synthesised reddish-purple PProDOT-Bu_2 with a wavelength maxima of 544 nm and an energy gap of 1.8 eV. It switches from a red-purple in its neutral state (– 1.0 V) to a transmissive sky blue when oxidised (+ 0.5 V). Other polythiophene-based polymers **28-31** were later reported by the Reynolds group, these polymers were shown to switch from a blue-purple in the neutral state to a transmissive sky blue in its oxidised state, exhibiting high electrochromic contrast of 40-70 %.[64]

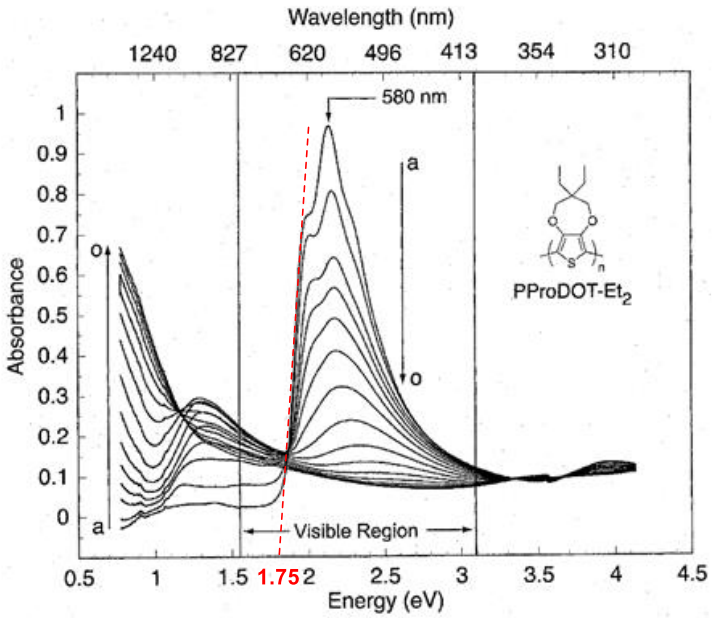

Figure 13: Spectroelectrochemistry of PProDOT-Et_2 **26**. The potential is applied from – 1.0 V to + 0.5 V.

1.3.3.2.2.4 Poly(alkoxythiophene)s

In addition to the conformational changes caused by the insertion of substitution groups along the polythiophene backbone, 3- and 4-position substitutions of thiophene have been shown to increase the rich electronic properties of the thiophene monomer and decrease its oxidation potential, thus preventing the overoxidation process of the polymer that occurs during making films.[65] Daoust *et al.* reported the chemical polymerisation of **32** and **33**.[66] These poly(alkoxythiophene)s were referred to as AcDOT. In figure 14b, the structure of the AcDOT (**34**) is shown, with the material exhibiting low oxidation potentials (around 0.60 V), meaning it possesses more stable conducting states. Polymers **32** and **33** switched between a violet colour in the neutral state and a blue-black colour in its oxidised state. In 2010, Aubrey *et al.*[67] reported a poly(alkoxythiophene) derivative **34** (ECP-orange). The bandgap of ECP-orange is 2.04 eV, the maximum absorption of wavelength centred at 483 nm. Additionally, in Figure 14c, ECP-orange was switched during the applied potentials from − 0.73 V to 0.57 V, achieving 47.2 % transmittance (%T) contrast.

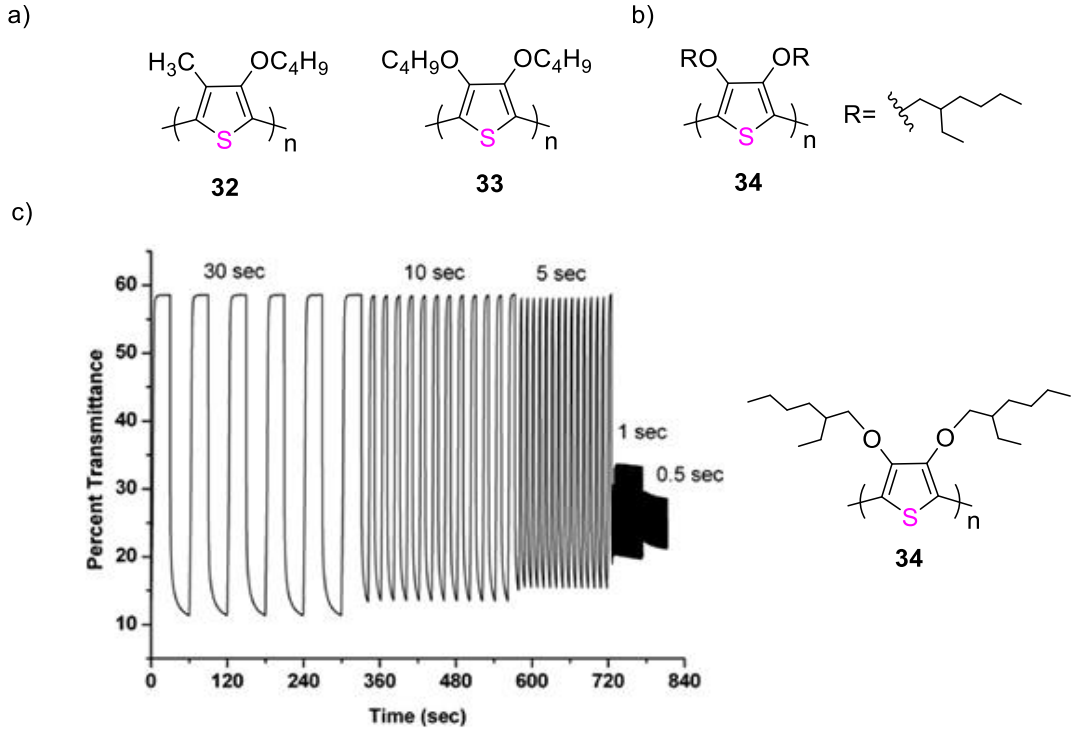

Figure 14: a) Polythiophenes synthesised by Daoust *et al.* b) ECP-orange synthesised by Aubrey *et al.* c) Relationship between transmittance and switching time of ECP-orange at λ_{max} during the potentials from −0.73 V to 0.57 V.[67]

It has been reported in many publications that the polymer backbone affects the mobility and conductivity of the internal solid state charge.[68, 69 70] In addition, the insertion of side chains into the polymer contributes to the modulation of both charge transfer and

redox properties.[71] Therefore, it is necessary to investigate how main and side chain modifications affect the redox properties of conjugated polymers.

Kuei *et al.*[68] provided some insight into this through investigating the effect of persistence length on chain conformation, using experimental and computational means to determine the corresponding parameters for prediction. The persistent length of the conjugated polymer is controlled by the deflection angle and torsional potential of the skeleton, specifically, by the stiffness and linearity of the skeleton.[72, 73] In 2020, Pittelli *et al.* synthesised **34** and **35** with branched and linearly soluble side chains of AcDOT, respectively.[74] They demonstrated that linear side chains of ACDOT decrease the oxidation potential and increase the electrochemical conductivity.[74] In particular, the polymers substituted with linear side chains exhibit better performance in transporting electron carriers via the film. Compared to the branched ethylhexyl chain of **34**, the linear side chain of **35** reduces the AcDOT oxidation potential by 300 mV and improves its electrochemical conductivity. Furthermore, compared to **34** with λ_{max} of 495 nm, the spectrum of **35** is 55 nm red-shifted (Figure 15).

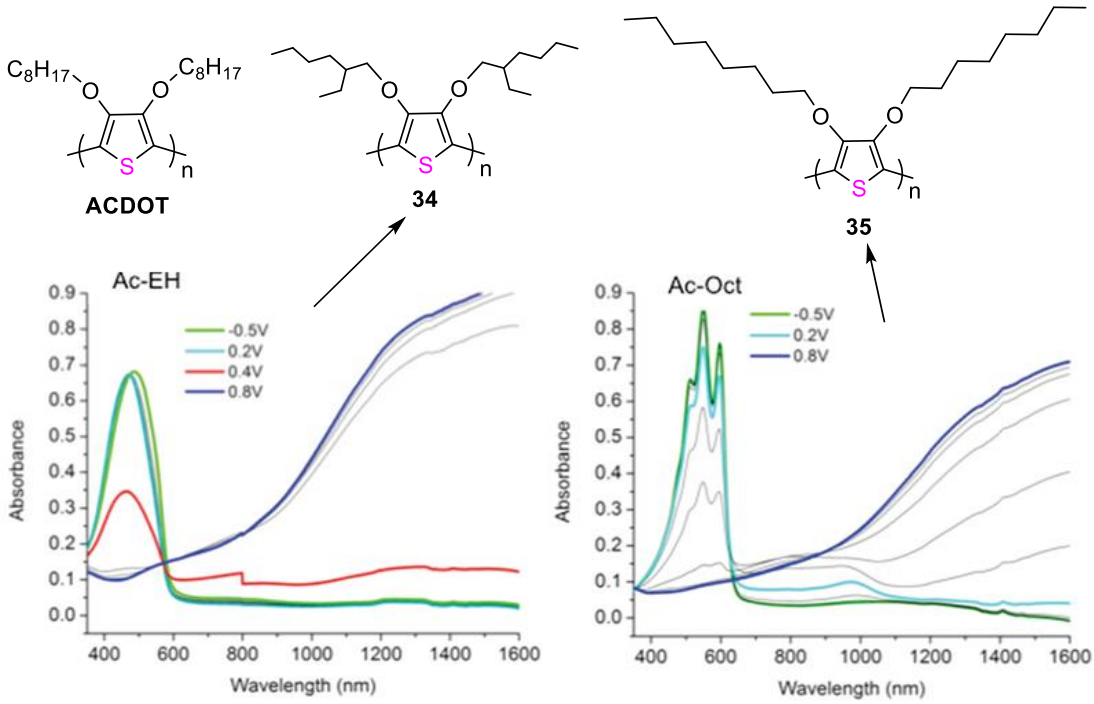

Figure 15: Spectroelectrochemistry of **34** and **35** films during the potentials from −0.5 V to 0.8 V.[74]

1.3.3.2.2.5 Thiophene Copolymers

Recently, thiophene copolymers with donor-acceptor-donor systems have attracted a lot of attention because of their ability to improve performance and modulate colour.[12] The colour of the ECP depends on the effective conjugation length and the degree of the

overlap of π orbitals to reflect different steric hindrance and electron effects.[75] The colour-changing manipulation often results in materials with different electrochemical properties. Copolymers have a broader absorption spectrum covering a wider range of visible light and provide better colour modulation. Therefore, finding EC copolymers with favourable colour and electrochemical properties is considered to be more achievable compared to homopolymers.[75]

As mentioned above, **34** has a maximum absorption wavelength at ~ 490 nm. However, the side chains of the monomer **34** cause steric hindrance, which reduces the effective conjugate length in the homopolymer. Dyer *et al.*[67] randomly doped the dimethoxythiophene units into the backbone of **34**, relaxing the steric hindrance and appropriately reducing the bandgap (by 0.04 eV), with a considerable red shift of λ_{max} to 525 nm.[76] The unit structures of **34** and **36** in Figure 16a reflect the steric hindrance between the side chains and the backbone distortion.

In 2016, Cao *et al.*[77] synthesised copolymers **37**-**39** (Figure 16b), which possess dimethoxyphenylide-based repeating units with AcDOT dimers or ProDOT dimers. They used the incorporation of electron-rich dimethoxyphenylenes to subtly control the bandgap and optical properties of dioxythiophene copolymers. After characterising and analysing their structures, they found that, for the ProDOT system, the introduction of electron-rich methoxy units increased the HOMO level of the polymer. This meant that the polymers could be completely oxidised at lower potentials.[77] On the contrary, for the AcDOT system, the methoxy unit increases the steric hindrance in the backbone and raises the energy gap.

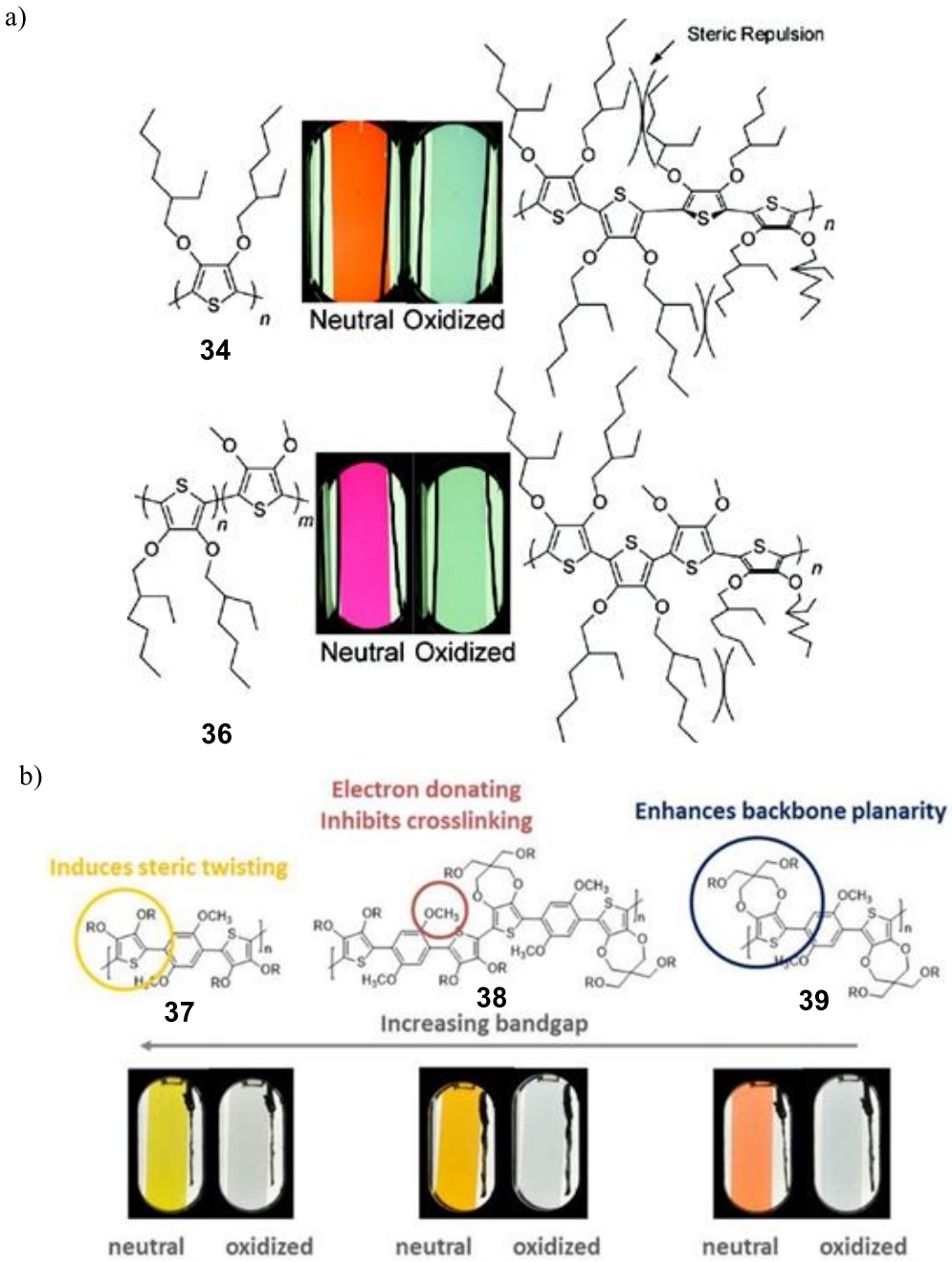

Figure 16: a) Structure of **34** and **36** and polymers converted from neutral states to oxidative states. b) Structure of **37-39** and the colour changes of polymers from neutral states to oxidative states.[67]

Kerszulis *et al.*[12, 78] reported the synthesis of copolymers (**40**-**46**) that contained EDOT(3,4-ethylenedioxythiophene), ProDOT(3,4-propylenedioxythiophene), and AcDOT (acyclic dioxythiophene) alternate repeating units (Figure 17a). The synthesis of these copolymers aimed to investigate the influences of relaxed and twisted structures on electron absorption transitions. Through adjusting the steric hindrance of these copolymer structures to change their configuration, a new colour in the neutral state can be achieved (Figure 17b).

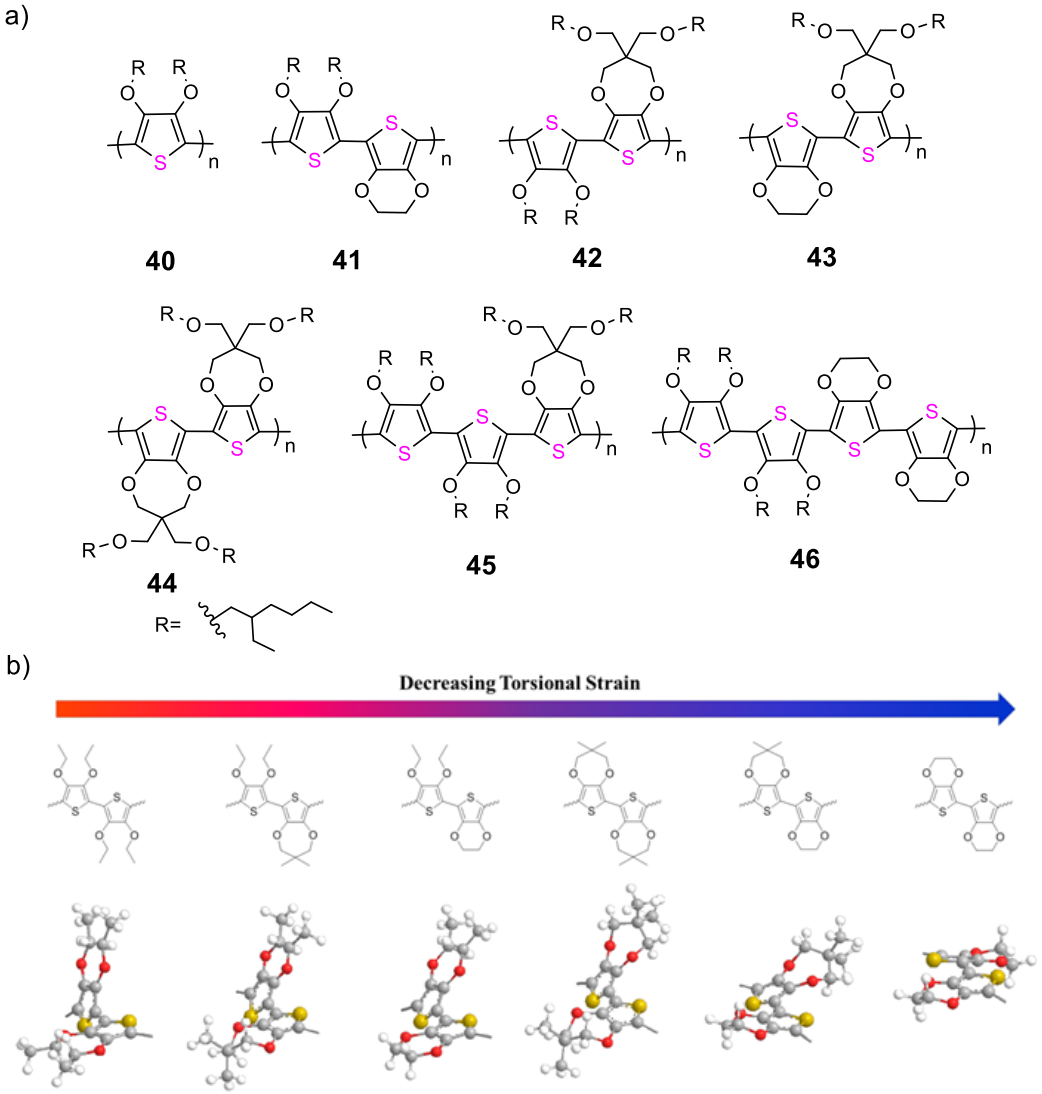

Figure 17: a) Structures of EDOT-, ProDOT-, and AcDOT-based conjugated polymers.[78, 79] b) General model in steric interactions to achieve new neutral state colours by Kerszulis *et al.*[12]

1.3.3 Hybrid Electrochromic Materials

Hybrid electrochromic materials have received much attention in recent years. Compared to inorganic materials, hybrid materials not only have the high processability and functionality from organic materials, but also the outstanding thermostability from inorganic materials. These results provide the hybrid materials with higher colouration efficiency, shorter response times, and excellent device cyclability.[80]

As one of the branches of hybrid materials, nanocomposites are characterised by holding the embedded domains together through van der Waals forces or hydrogen bonds. In recent years, nanocomposites composed by organic polymers and metal oxides such as TiO_2,[81] NiO[82, 83] and IrO_2[84] have been reported. Furthermore, conductive nanoparticles (e.g. Ag,[85] Au[86], carbon nanotubes[87] and graphene[88]) can also be doped in organic polymer as electrochromic nanocomposites.[28] Bhandari *et al.*[89] demonstrated

the synthesis of the nanocomposite film of (PEDOT)-Au-CdSe and the corresponding optoelectronic properties were tested. This film was made by incorporating a porous PEDOT layer into a hybrid gel of Au nanoparticles and CdSe quantum dots (Figure 18). Compared to neat PEDOT, (PEDOT)-Au-CdSe shows higher colouring efficiency (300 cm^2/C), and shorter switching time (4.5 s for colouration and 1.5 s for bleaching).[89]

As for hybrid materials with interfacial chemical bonds, Saxena *et al.*[90] investigated the electrochromic properties of PEDOT nanocomposite assemblies by embedding fluoroalkyl phosphate-based ionic liquid functionalised graphene (ILFG) and reduced graphene oxide (RGO). Compared to PEDOT-RGO, PEDOT-ILFG took only 1.5 s to complete the bleaching process from 0 to 100 % of full optical contrast (2 s faster than PEDOT-RGO). In addition, PEDOT - ILFG exhibited 580 cm^2/C colouring efficiency (211 cm^2/C higher than PEDOT-RGO), and superior conductivity (σ = 0.0022 S cm^{-1}).[28, 90] Figure 19 shows the interactions existing in the PEDOT-ILFG and PEDOT-RGO nanocomposites, respectively.

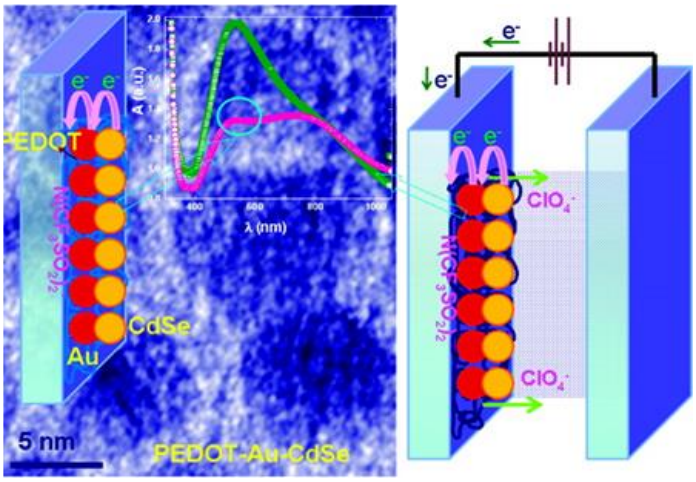

Figure 18: Preparation of PEDOT-Au-CdSe nanocomposites; absorbance versus wavelength curve of PEDOT-Au-CdSe (green line) and pure PEDOT (red line).[89]

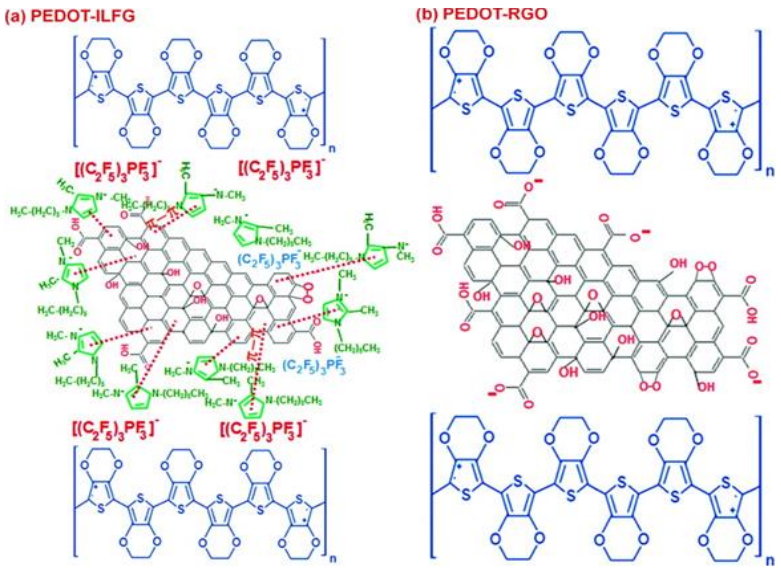

Figure 19: a) Structure of PEDOT−ILFG. b) Structure of PEDOT−RGO.[90]

For the past few years, many studies have shown that thiophene copolymer layers doped with semiconductor materials (carbon nanotubes) make thin films with better mechanical properties, thermal stability and durability.[91] To obtain electrochromic materials with better performance such as increased switching cycles and shorter switching times, the Bonifazi group used multiwalled carbon nanotubes (MWCNTs) to dope copolymer **48**.[92] They used chemical polymerisation to synthesise new copolymers **48**, from monomers **34** and **47** (Figure 20a).

After assembling the material as ECDs, the colour contrast value (ΔE) versus the number of cycles in copolymer **48** with doping from 0 % MWCNT to 10 % MWCNT was tested. Figure 20b shows that with increasing number of cycles, the value of colour contrast decreases. Comparing 0 % MWCNT and 2.5 % MWCNT a significant difference in colour contrast can be seen, while the value of ΔE between 7.5 % MWCNT and 10 % MWCNT declined moderately. Figure 20c demonstrates the switching cycles of the assembled ECDs using copolymer **48** with a doping of 0 % MWCNT and 7.5 % MWCNT. The change of absorbance upon oxidation of the 7.5 % MWCNT sample was considerably larger than that of the 0 % MWCNT ECD. The switching times of the 0 % MWCNT ECD and the 7.5 % MWCNT ECD were shown to be similar (around 4 seconds).

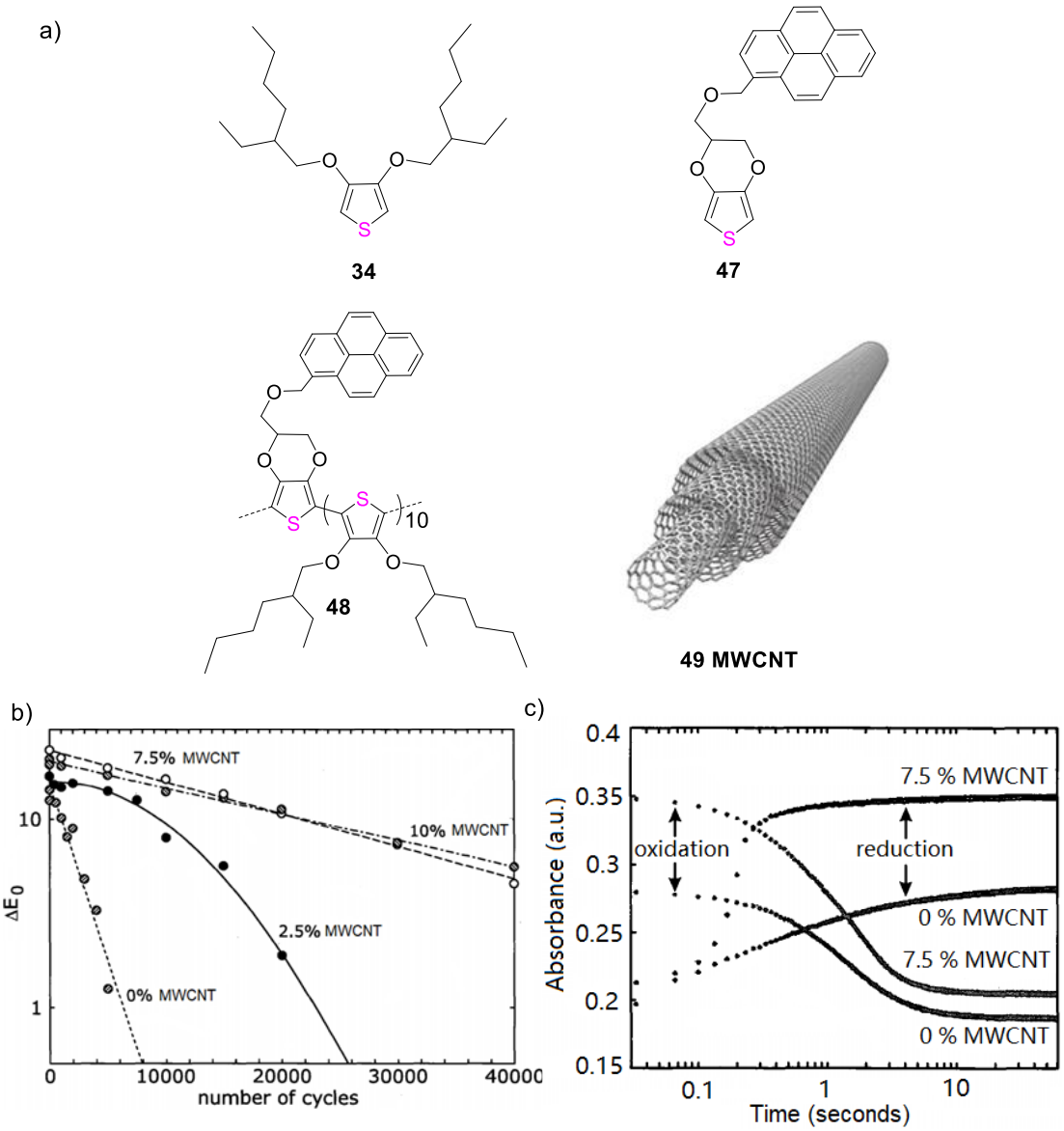

Figure 20: a) The structure of monomers and copolymer **48**. b) Colour contrast value (ΔE) versus the number of cycles by adding different proportion of MWCNT on copolymer **48**. c) Switching cycles of assembled ECDs.

1.4 Aim of the Project

The work of this MPhil aims to form copolymers synthesised from novel thiophene monomers possessing alkoxybenzyl/alkoxynaphthyl branched chains and known thiophene monomers with alkoxyl branched chains. Copolymers will be made into electrochromic devices to observe the colour changes in the oxidised and neutral states, and allow for key characterisation such as spectroelectrochemical analysis to be performed.

In order to control the optoelectronic properties of the copolymers, different branched and linearly soluble side chains of thiophene monomers are used in an attempt to subtly change the steric interactions of copolymers. In addition to this, the introduction of bulky moieties such as fused aromatic rings in thiophene monomers, should lead to an increase in the planarization of copolymer. This increased planarization should lower the energy gap of the polymer due to the increased effective conjugation within the polymer backbone. The relationship of energy gap and conjugation can be seen in Figure 21. The colour of the copolymer will have a red shift in absorption spectrum.

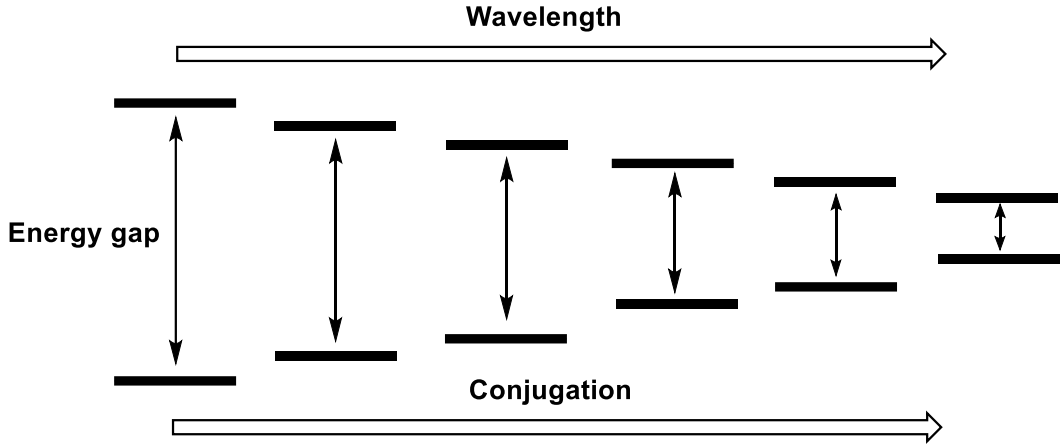

Figure 21: The relationship between conjugation, wavelength and energy gap of conjugated polymer.

After the desired copolymers are synthesised, the ultimate goal of this project is to use spraying technology to prepare ECP films of all copolymers and then fully characterise the ECDs fabricated using these films. Characterisation of the ECDs will include: investigation of its spectroelectrochemistry, and switching time.

2. Results and Discussion

2.1 Synthesis

2.1.1 Monomers

The reaction mechanism for the formation of alkoxyl/alkoxybenzyl/alkoxynaphthyl thiophene monomers is shown in Figure 22. In this reaction, 3,4-dimethoxythiophene and benzyl/naphthyl alcohol derivatives are used as reactants. P-toluenesulfonic acid (PTSA) acts as a catalyst, with no depletion at the end of the reaction.

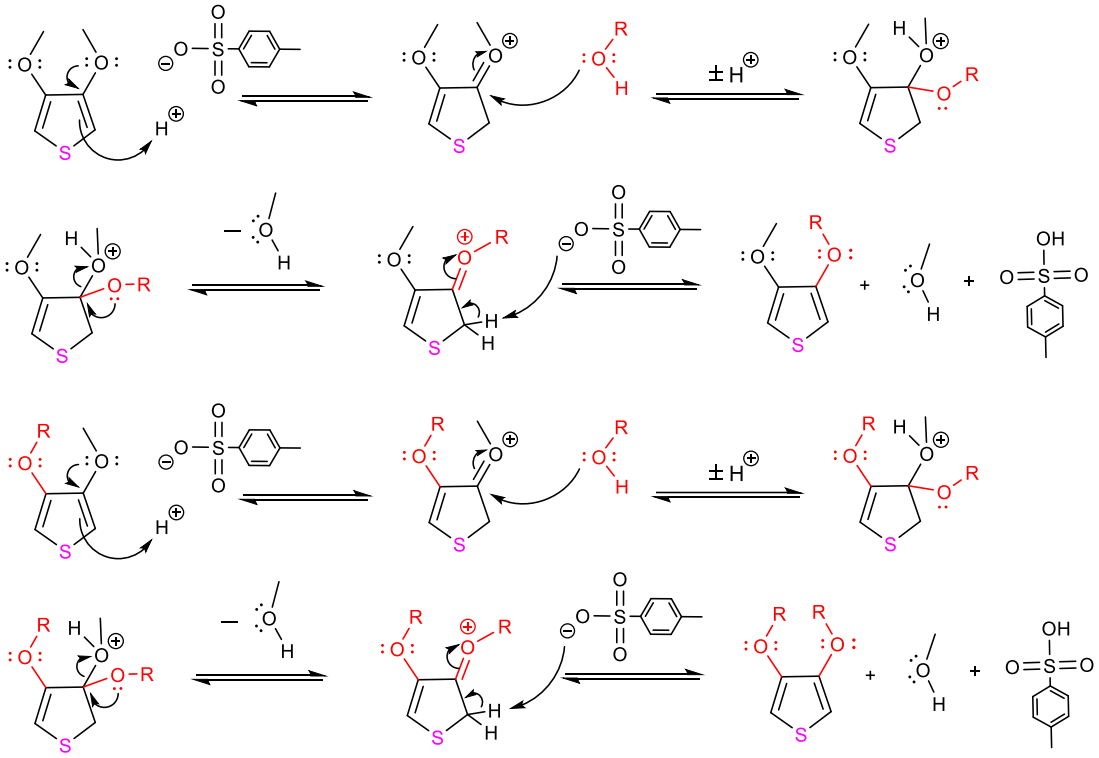

R: alkoxyl/alkoxybenzyl/alkoxynaphthyl group

Figure 22: Mechanism of synthesising alkoxyl/alkoxybenzyl/alkoxynaphthyl thiophene monomers.

2.1.1.1 3,4-bis(benzyloxy)thiophene (51)

The initial idea is to introduce fused aromatic branched chains at 3- and 4-positions of thiophene monomers. As the size of the fused ring increases, the building blocks enhance optical contrast of the conjugated polymers. In addition, the introduction of bulky branched chains into the monomer changes the degree of the conjugation and the energy gap of polymers. Therefore, the synthesis of thiophene monomers with benzene and naphthalene branched chains was attempted. The retrosynthetic analysis of compound **51** to commercially **50** is seen in Figure 23. The target molecule can be synthesised by a nucleophilic substitution reaction between commercially obtainable benzyl alcohol and the 3- and 4-positions of 3,4-dimethoxythiophene.

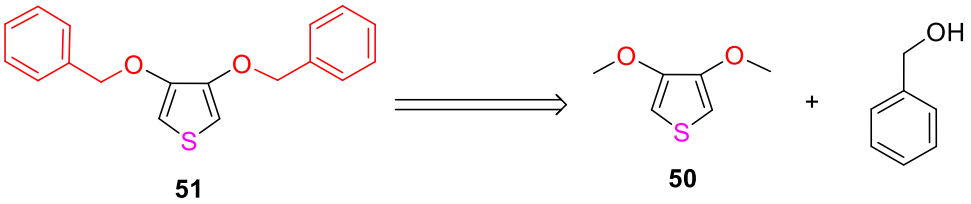

51 **50**

Figure 23: Retrosynthetic analysis for the monomer **51**.

The synthesis of monomer **51** was successful, using modified conditions developed by Qi *et. al.* (Scheme 1).[93] 3,4-dimethoxythiophene along with benzyl alcohol were weighted into a 50 mL over-dried round bottom flask. The flask was flushed with nitrogen and dry toluene was added, followed by PTSA. The reaction mixture was stirred and heated to 110 ℃ for 27 h. While the reaction is in progress, the methoxy group at the 3,4 thiophene position is removed after protonation to form methanol, which appears as the by-product in this reaction. The methanol with a boiling point of 64.7 ℃ is in the form of a gas during the reaction at a reaction temperature of 110 ℃. Therefore, in this thermodynamically reversible reaction, if the formed methanol remains in the reaction flask, a dynamic equilibrium will be reached with time. In order to shift the equilibrium in the direction of the desired molecule and achieve a higher yield, methanol was removed during the reaction. In addition, benzyl alcohol added in this reaction was in excess. When it came to purification of the target molecule, the presence of benzyl alcohol made it hard to separate the target product by column chromatography. TLC demonstrated that the spot of the target compound and benzyl alcohol have the same retention factor, which means that it is difficult to separate the mixture of these two compounds by column chromatography. The solubility of benzyl alcohol in water at 20 ℃ at room temperature was found to be 4.29 g/100 mL after checking the solubility table of organic compounds. Therefore, attempts to remove benzyl alcohol with water were attempted, but were unsuccessful. After a series of attempts of trituration, it was found that benzyl alcohol was fairly soluble in petroleum ether, and the target product was slightly soluble in that solvent, so the pure target product was separated with PE. This gave the monomer **51** in 30% yield.

It was also found that this reaction has strict requirements on the amount of catalyst. In order to increase the yield, initial attempts to raise the equivalents of the catalyst from 0.12 to 0.5 were unsuccessful, the target product was not formed after the reaction. On TLC, there is a major product that is different to the two reactants. However, after the

crude reaction mixture treatment, the ^{1}H NMR demonstrated no signals of the target product. After purifying the major product by column, it was found that this was benzyl ether. Therefore, we hypothesise that an excessive amount of PTSA makes reaction intermediates self-polymerise.

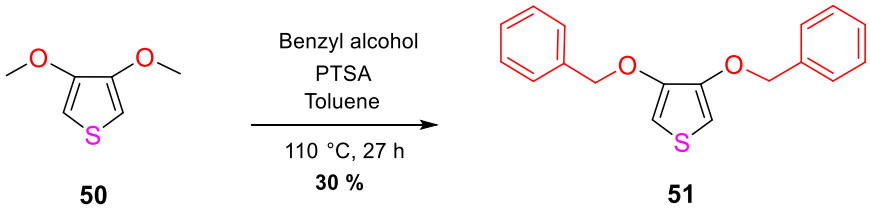

Scheme 1: Synthetic route of **51**.

After the successful synthesis of the colourless 3,4-bis(benzyloxy)thiophene, new ideas began to emerge. If an alcohol substituent or a methoxy substituent is attached to the phenyl branched chain of 3,4-bis(benzyloxy)thiophene, the new compound may take on a different colour and chemical properties because of their addition. Hence, the synthesis route of **52-54** using the same procedure of **51** is demonstrated in Scheme 2. Unfortunately, the initial attempt to synthesise **52** were unsuccessful. When following the same procedure, the starting material (3,4-dimethoxythiophene) cannot be seen on TLC, and there were no other spots in TLC except for one at the bottom. ^{1}H NMR of the crude reaction mixture after treatment showed no signals related to the target molecule. The synthesis of **53** was also not achieved. Starting material (3,4-dimethoxythiophene) cannot be seen on TLC, and there was also no target product peaks in the ^{1}H NMR. According to the approach used to obtain **51**, the original attempt to obtain **54** also failed, resulting in the conversion of the original material ((4-methoxyphenyl)methanol) with almost no target product.

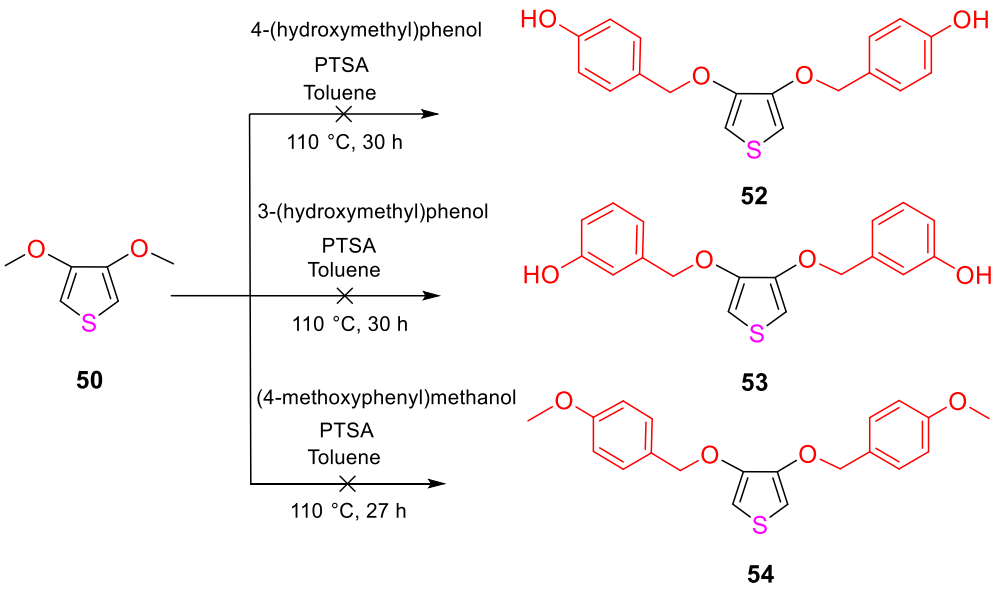

Scheme 2: Failed attempts for the synthesis of **52**-**54**.

2.1.1.2 3,4-bis(3-phenylpropoxy)thiophene (55)

After unsuccessful attempts to synthesise 3,4-bis(benzyloxy)thiophene with alcohol substituents or methoxy groups, ideas began to focus on whether new monomers with more sterically demanding groups and more distorted structures could be synthesised by increasing the alkyl chains of the benzyl alcohol derivatives or by increasing the number of benzene rings present. Therefore, monomer **55** was designed and the synthesis of **55** was achieved successfully. Commercially available 3,4-dimethoxythiophene and 3-phenyl-1-propanol were weighed into an over-dried flask. The system was purged with nitrogen and dry toluene was added, followed by PTSA. The flask was heated to 110 ℃ for 24 h. Methanol was removed from the solution twice per hour during the day and the reaction was given leave to continue overnight. The purification process was very successful, giving the monomer **55** in 40% yield.

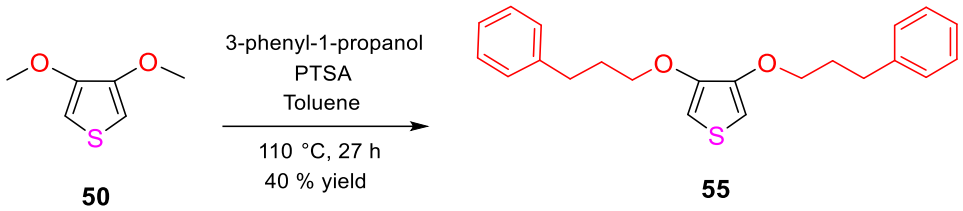

Scheme 3: Synthetic route of **55**.

2.1.1.3 3,4-bis(2-(naphthalen-1-yl)ethoxy)thiophene (56)

The synthesis of **56** following the same procedure for the synthesis **51** was successful (scheme 4). Through analysing and calculating the protons contained in the corresponding functional groups of the crude compound in ^{1}H-NMR spectrum, it can

be determined which peak in the crude product belongs to which compound (Figure 24). For instance, the singlet at ~ 6.24 ppm is associate with the two protons that are attached to the thiophene moiety of the starting material (3,4-dimethoxythiophene) and the singlet at ~ 6.34 ppm is attributed to the two protons bound to the thiophene ring of the target product **56**. After that, two doublets from 6.25 to 6.33 ppm is associate with the two protons bound to the thiophene group of the mono-substituted analogue of **56**. Therefore, through the analysis of NMR, the proportion of the target product **56** was found to be low (8%), with the mono-substituted analogue of **56** around 46% and the original material at around 45%.

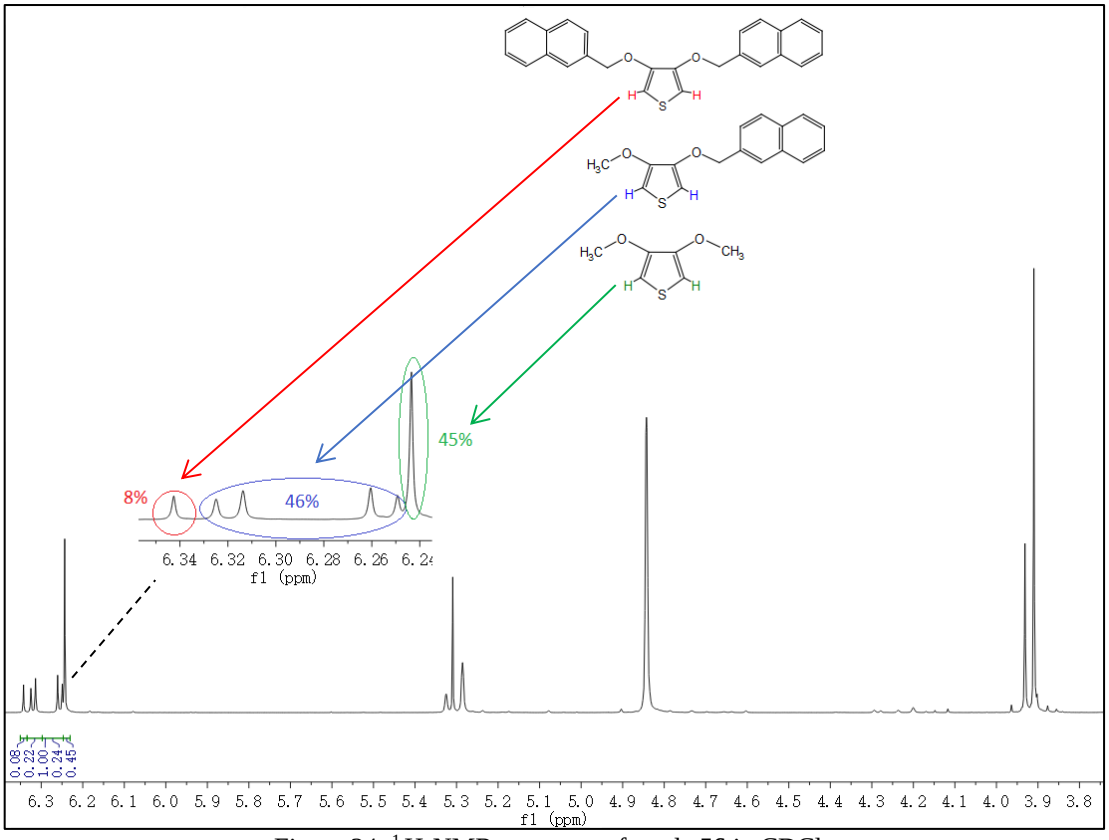

Figure 24: ^{1}H-NMR spectrum of crude **56** in $CDCl_3$.

To increase the yield, initial attempts to raise the equivalents of the catalyst from 0.12 to 0.2, 0.3 and 0.5 respectively were made. When using 0.12 equivalents of the catalyst, 8% of the target product was yield. The attempts using 0.3 and 0.5 equivalents of catalyst were unsuccessful. On TLC, there is a relatively big spot that is different from the 3,4-dimethoxythiophene and 2-naphthalenemethanol starting materials. NMR analysis also demonstrate that there was not target product peak in crude product. Interestingly, there are some peaks corresponding to 2-naphthalenemethanol which occupy a large proportion of the NMR spectrum. Therefore, for these two reactions

using 0.3 and 0.5 equivalents of PTSA, in one case, it is possible for 2-naphthalenemethanol to go through self-polymerised to form naphthalene ether. In another case, these two reactions result in the conversion of the original material with almost no target product and have a large proportion of 2-naphthalenemethanol left. Considering that this reaction has strict requirements on the amount of catalyst, a new attempt to use 0.2 equivalent of the catalyst was successful, increasing the yield to 17%. On TLC, the retention factor of pure 2-naphthalenemathanol is significantly different from that of the target and the mono-substituted products. Through purification by column chromatography and analysis by NMR, it showed that the target product is yielded. However, there was also peak that appears at 4.8 ppm in NMR spectrum. The initial speculation was that the peak signal belongs to the methyl hydrogen of 2-naphthalenemathanol. Therefore, the proportion of target and the crude was calculated separately in NMR spectrum. It was found that after subtracting the integral value of the target product, the ratio of integration of the remaining methyl peak to the naphthalene peak was 2 to 7. In this case, it was assumed that the target product dropped out together with the excess 2-naphthalenemathanol (crude) during the column chromatography treatment.

Therefore, the mixture of target product and crude needed to undergo an extra purification. Firstly, PE was used to try and separate them but the target molecule is also partially soluble in PE. The function of separation is inefficient. After that, ethanol and methanol were used to attempt to separate the mixture because pure 2-naphthalenemethanol is soluble both of them. However, these attempts failed. The method of recrystallisation was also used to purify the target product, but the solubility of the target product and crude in different solvent is so similar that this method also did not work. During multiple attempts at trituration using different organic solvents, it was found that ethanol is able to dissolve pure 2-naphthalenemethanol quickly. If the pure compound **56** was put in ethanol alone, it is almost insoluble. However, when ethanol was added to the mixture, the effect of separation is poor. Therefore, for the rest of the mixture that exited the column together, recrystallisation from ethanol was used in an attempt to further purify the mixture. Unfortunately, this method did not separate compound **56** and crude successfully.

The failure to successfully separate the pure product from the mixture after many attempts was perplexing. It is possible that the crude product of the mixture is not 2-

naphthalenemethanol but naphthalene ether. Hence, after analysing the difference between TLC and column, the target product and the crude both dissolved in PE. The method of purification of column was changed. Solid deposit method was used to prepare the column and then purification of the mixture of target product and crude was performed again. Finally, a part of pure target product was obtained after column.

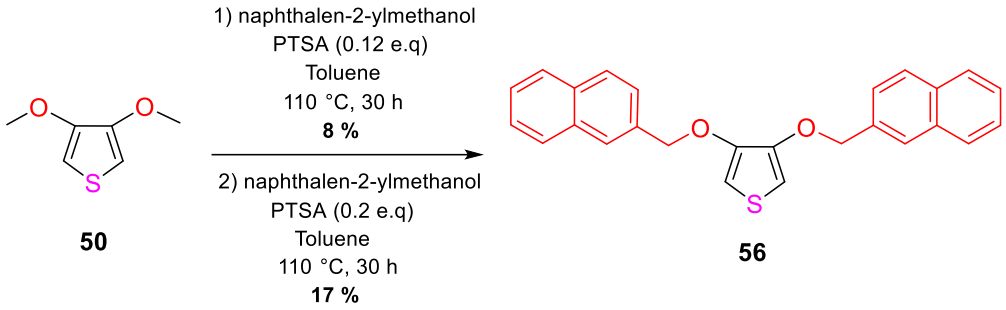

50 **56**

Scheme 4: Synthetic route of **56**.

The synthesis of **57** following the same procedure as **51** was unsuccessful. Analysis of the reaction showed that there were lots of spots appearing on TLC. NMR of the crude product showed that there was no signal of the target product **57**. This reaction was purified by column. After purifying the biggest spot on TLC and analysing by NMR, it demonstrates that the main product of this reaction is bis(α-naphthylmethyl) ether. New attempts to change the equivalent of the catalyst from 0.5 to 0.12 were unsuccessful, there were no signals corresponding to the target product in the NMR spectrum. The synthesis of **58** following the same procedure as **57**, using a solution of 3,4-dimethoxythiophene, anthracen-9-ylmethanol and PTSA was stirred in dry toluene for 27 hours at 110 ℃ was unsuccessful. There were lots of spots in TLC (around 12 spots), and no signal peak of thiophene in the NMR of the crude product. By purifying major spots from the TLC and then using NMR to analyse them respectively, the compounds produced by the reaction cannot be recognised.

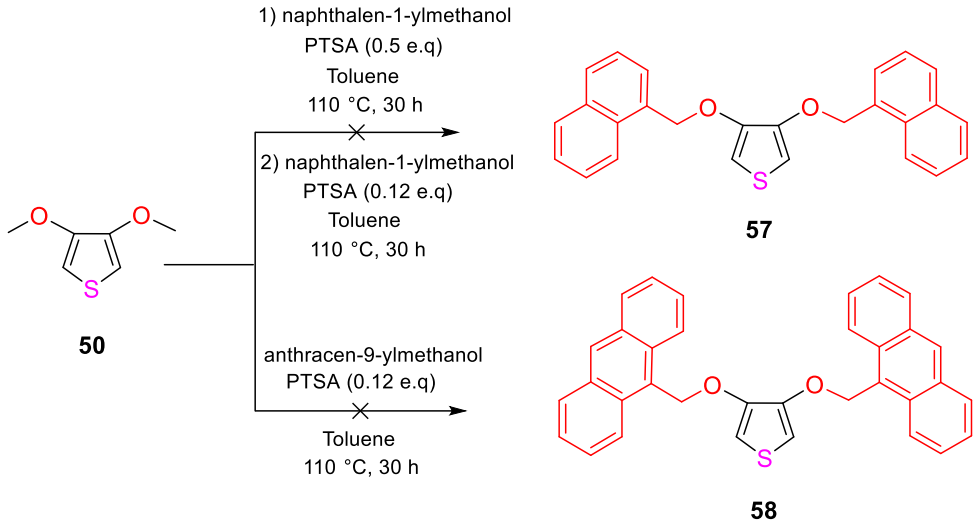

Scheme 5: Failed attempts for the synthesis of **57**-**58**.

2.1.1.3 3,4-bis(2-(naphthalen-1-yl)ethoxy)thiophene (59)

The synthesis of **59** using the same approach than for the synthesis of **51** was successful. A solution of 3,4-dimethoxythiophene and 2-(naphthalen-1-yl)ethan-1-ol and PTSA was stirred in dry toluene for 24 hours at 110 °C. Methanol was removed from the solution during this time. The crude material was purified by silica gel column chromatography. After that, the 2-(naphthalen-1-yl)ethan-1-ol and target molecule drop out together from the column. Attempts to separate the mixture of them by trituration were performed, using methanol, ethanol, diethyl ether and petroleum ether. Finally, it was found that 2-(naphthalen-1-yl)ethan-1-ol dissolved in petroleum ether and the target product partially soluble in petroleum ether. Therefore, the purification process was very successful, giving the desired product in 32% yield.

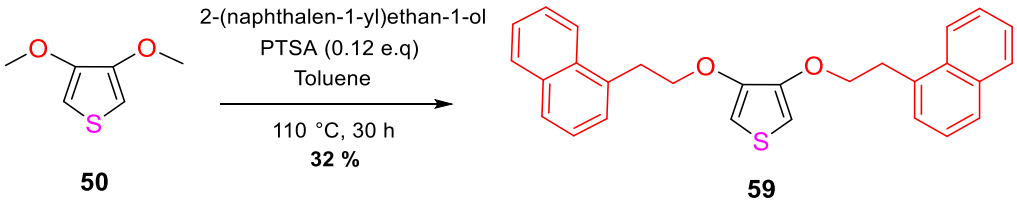

Scheme 6: Synthetic route of **59**.

2.1.1.4 Alkoxylthiophene (3 and 4 position) monomers

The selection of alkyl branched substituents at 3- and 4-position of thiophene can have an effect on the steric interactions of the corresponding homopolymer and copolymer, and also improve the solubility. The synthesis route of **60** to **63** can be seen in scheme 7. As for the synthesis of **60**, 3,4-dimethoxythiophene and pentan-1-ol were weight into a round bottom flask which was flushed with nitrogen. Dry toluene (50 mL) was added,

followed by PTSA. The reaction mixture was heated 110 ℃ for 25 h. Methanol was removed from the solution each hour except when the reaction was left overnight. The mechanism of the reaction was the same as synthesis of alkoxybenzyl thiophene (3 and 4 position) monomers. The synthesis of **61**, **62** and **63** following the same procedure of synthesising **60** was successful. This gave the monomer **60** in 43% yield, monomer **61** in 32% yield, monomer **62** in 28% yield and monomer **63** in 34% yield respectively.

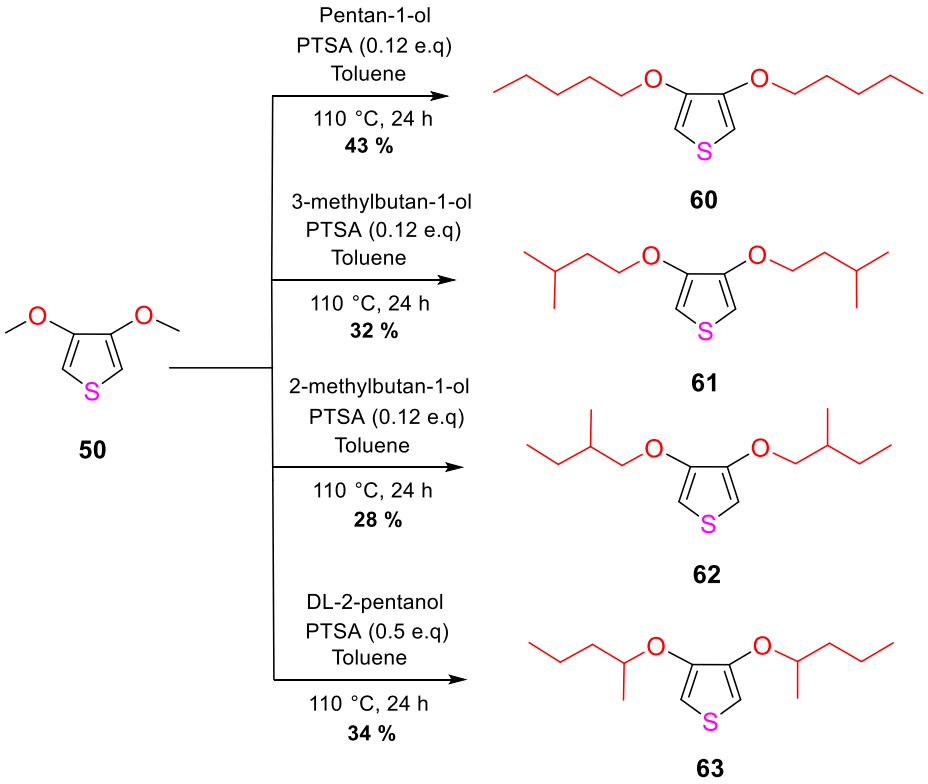

Scheme 7: Synthetic route of monomers **60-63**.

Notably, monomer **62** with two stereogenic centres has several stereoisomers. In Figure 25, A and B are the same molecule while C and D are enantiomers that are mirror images of each other. A and C, D are diastereoisomers that are not identical to each other. The NMR spectrum of **62** shows that at ~ 6.3 ppm, there is one singlet, which is the proton peak of thiophene (Figure 26). It means that the enantiomer and diastereoisomers of monomer **62** have the same chemical shift and their proton signals are superimposed. Interestingly, at ~ 3.8 ppm, there are two doublet of doublets in the NMR spectrum. In Figure 25, the blue proton and red proton of molecule C are different because they are diastereotopic. To be specific, in terms of the red coloured proton, it couples with the blue proton and black proton, causing it to exhibit a doublet of doublets splitting in the NMR spectrum. Same situation happens in regards to the blue proton,

which couples with the black proton and red proton, again exhibiting the doublet of doublets signal that is separate to the signal of red proton.

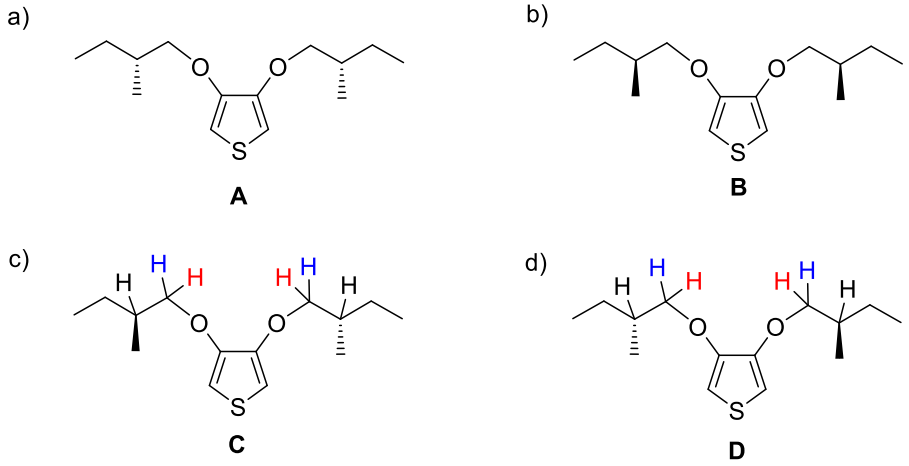

Figure 25: Stereoisomers of monomer **62**.

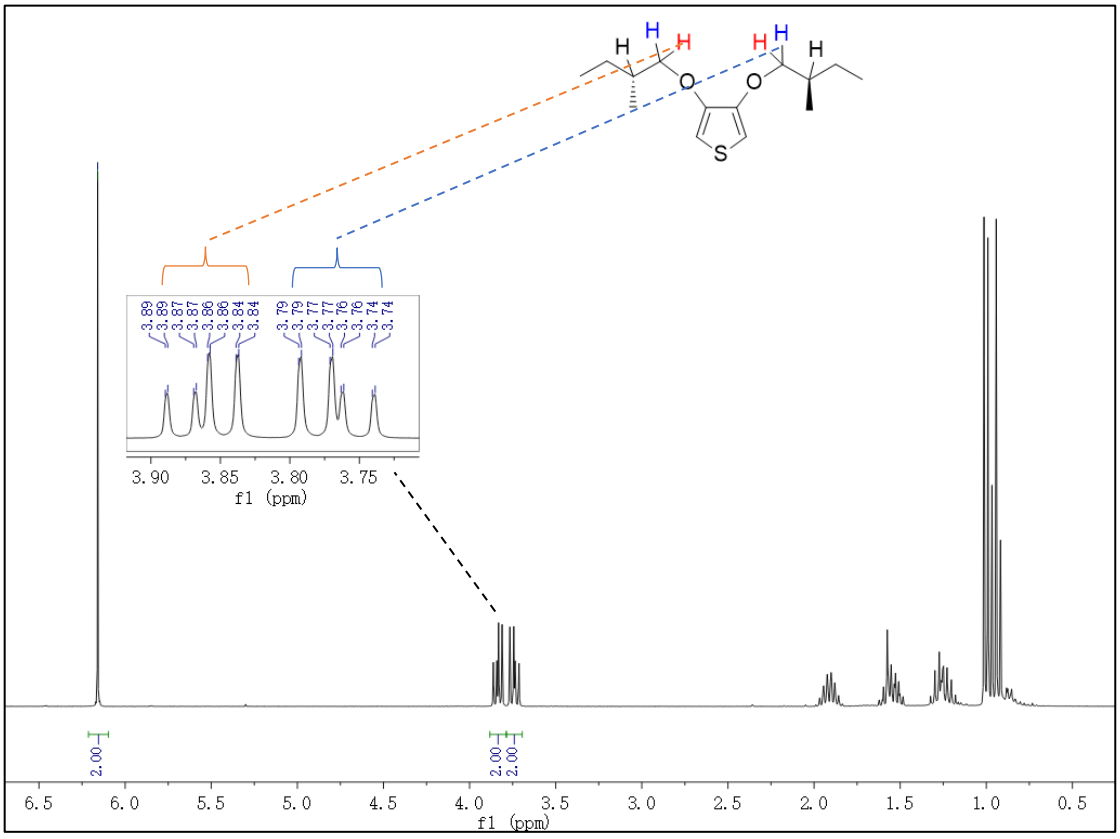

Figure 26: ^{1}H-NMR (300 MHz) spectrum of monomer **62** in $CDCl_3$ solvent.

As for monomer **63**, it has a pair of enantiomers and diastereoisomers because reactant DL-2-pentanol is racemic. In Figure 27, E and F are the same molecule. G and H are enantiomers that are not superimposable on their mirror image. E and G, H are diastereoisomers that are not mirror image to each other. In Figure 28, at ~ 6.2 ppm, there are two singlets, which means that the thiophene protons of diastereoisomers have

a different chemical shift. In addition, at ~ 4.2 ppm of the NMR spectrum, there is a sextet, which is the proton that located on the stereogenic centre. Obviously, the proton attached to the stereogenic centre is affected by three protons of a methyl group and two protons of "-CH_2-", following the "[n+1] rule". Besides, in Figure 28, the phenomenon of the sextet at ~ 4.2 ppm also means that the protons of diastereoisomers and enantiomers of monomer **63** have the same chemical shift. To be specific, the peaks of red, black and blue proton in Figure 27 are superimposed with each other in NMR spectrum.

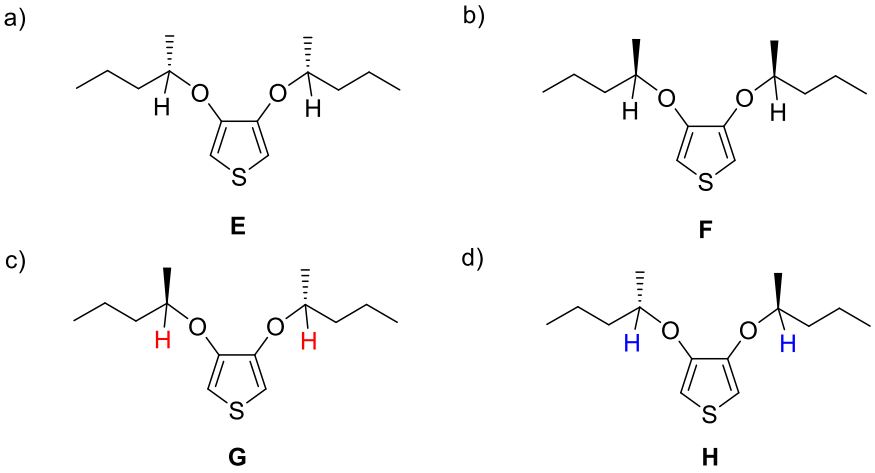

Figure 27: Stereoisomers of monomer **63**.

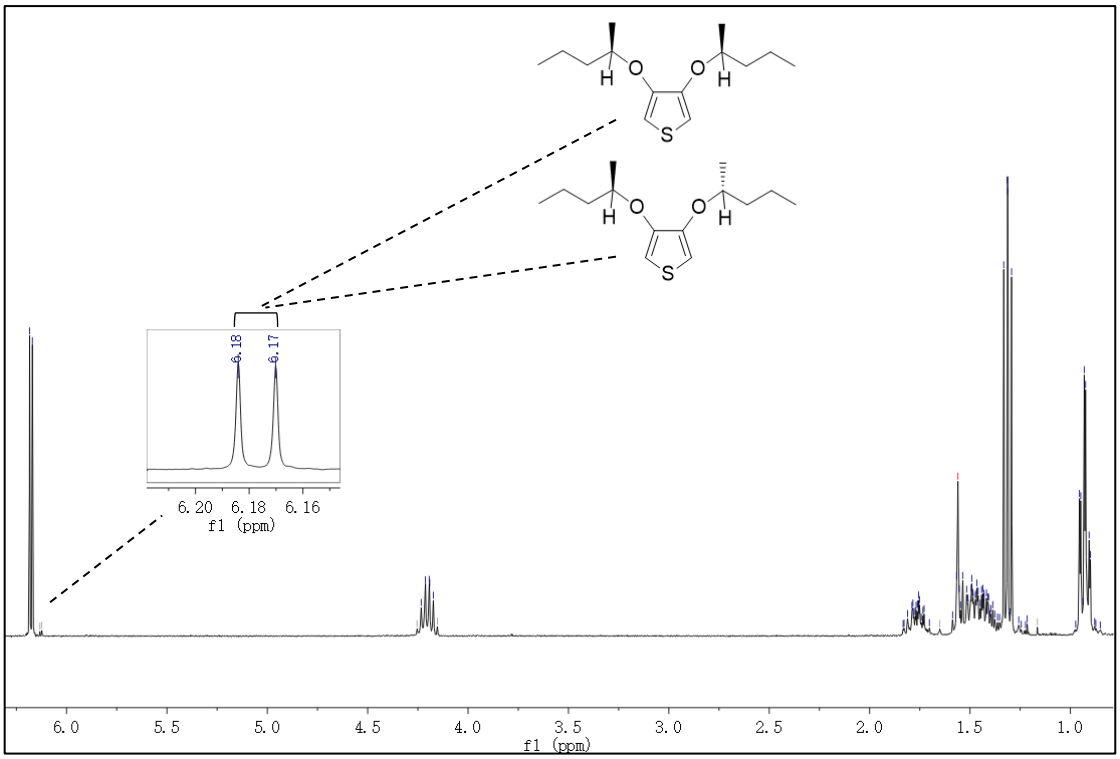

Figure 28: ^{1}H-NMR spectrum of monomer **63** in $CDCl_3$ solvent.

2.1.2 Homopolymers/Copolymers

2.1.2.1 Alkoxybenzyl/alkoxynaphthyl thiophene (3 and 4 position) polymers

After all the thiophene monomers containing alkoxybenzyl and alkoxynaphthyl groups had been synthesised, it was desired to study the properties and colour changes of the homopolymers to which those monomers corresponded. Therefore, attempts to synthesise the homopolymers of these monomers were undertaken. Polymers **64-66** were synthesised successfully through oxidative polymerisation (Scheme 8), using 1 equivalent of monomer (alkoxybenzyl/alkoxynaphthyl thiophene derivatives) and 3 equivalents of iron (III) chloride. Iron (III) chloride was used as an oxidant that removes electrons. Ethyl acetate was used as a solvent because it can dissolve both monomers and iron (III) chloride easily. Ethyl acetate mixed with monomer and iron (III) chloride were stirred for 24 hours at room temperature. After that, the reaction was diluted with chloroform and quenched with water. After chloroform extraction, the desired crude polymer was obtained. The common procedure of purifying the crude is wash them with methanol. Both reactions to form polymer **64** and **65** were set up successfully and purified smoothly using methanol to wash crude product. This gave the polymer **64** in 20% yield, polymer **65** in 22% yield respectively. However, monomer **56** and monomer **59** were only partially soluble in ethyl acetate. In order to dissolve them in the solvent, the sonicator was used for one minute. For crude **66**, methanol was used to wash the crude product four times. However, NMR demonstrated that the purification using methanol was less successful than expected. Signals of dimers and monomer could be seen in the spectrum, meaning that the solubility of the monomer and dimers was not high. Therefore, ethanol was attempted to wash the crude again three times. NMR demonstrated that purification using ethanol is successful. Polymer **66** was then obtained in 14% yield. For crude **67**, methanol was used to wash the product for three times. However, after washing, the NMR showed there were still many impurities in the polymer, which means that methanol cannot dissolve all of the impurities. After trying dichloromethane, ethyl acetate, and acetone, it was found that acetone is an efficient solvent to wash crude **67**. After weighing the resulting pure polymer **66**, the yield is obtained by dividing the mass of monomer **56** initially involved in the reaction, giving the polymer **67** in 12% yield. With the novel homopolymers/copolymers synthesised, their yields were obtained by this method of calculation.

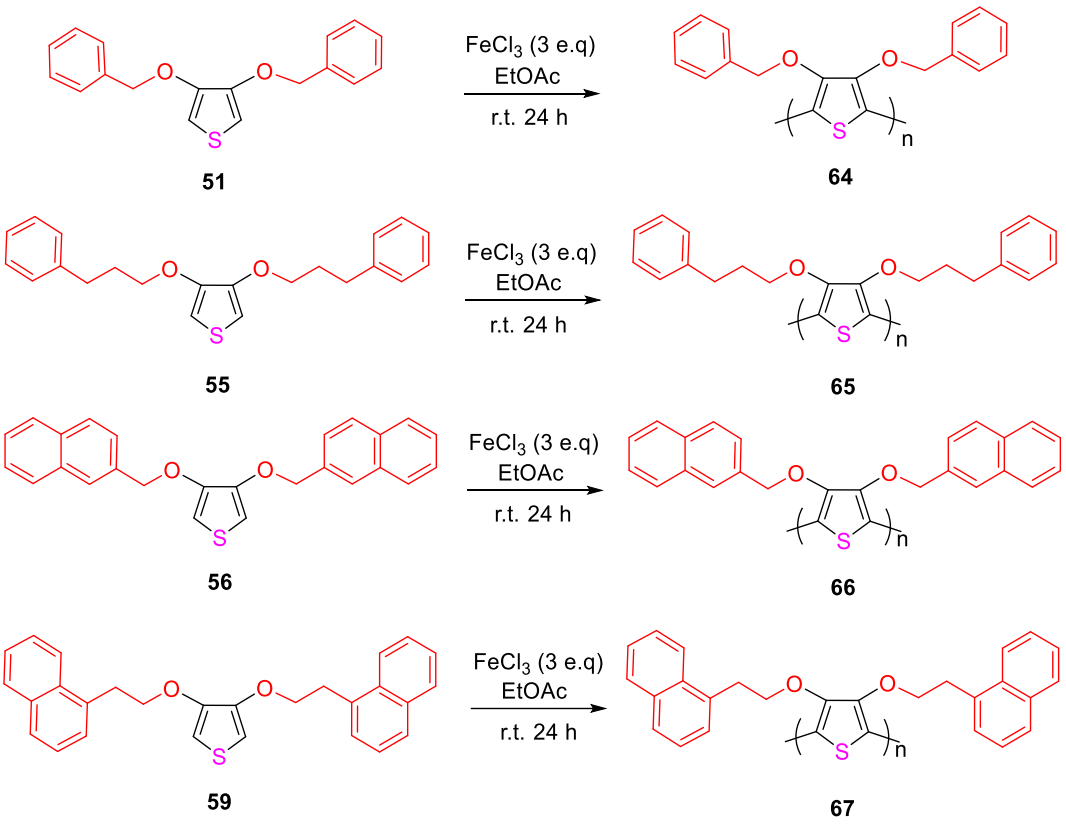

Scheme 8: Synthesis of homopolymer **64-67**.

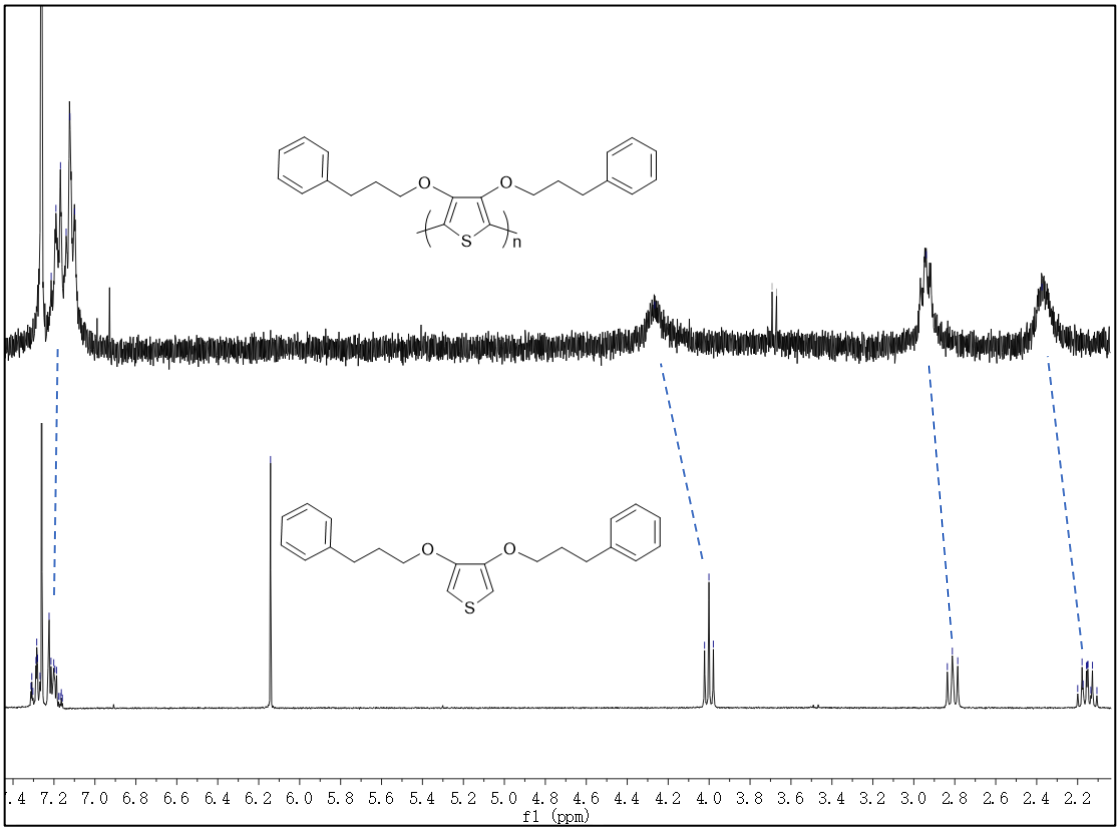

Figure 29: ^{1}H NMR spectra of homopolymer **65** and monomer **55** in $CDCl_3$ solvent.

Since the polymer is composed of multiple repeating monomer units, the peaks of each monomer are located at similar chemically displaced positions. Therefore, comparing to the peaks shown by the monomers, the multiple signals overlapping show a broader signal for the polymer. Therefore, from the comparison of the NMR diagrams of polymer **61** and monomer **51** in Figure 29, it can be determined that the correct polymer is achieved. The polymer signal peaks are less obvious due to the low concentration of the polymer used to do the NMR spectroscopy. NMR analysis software is used to make the peaks look more obvious, although this reduces the resolution of the image.

2.1.2.2 Alkoxybenzyl/Alkoxynaphthyl thiophene (3 and 4 position) copolymers

In order to study the effects of subtle steric hindrance differences on copolymer colours and properties, a series of alkoxybenzyl/alkoxynaphthyl thiophene copolymers were designed and synthesised. Our group has previously performed extensive experiments to demonstrate that the copolymer conjugate lengths obtained after selecting this ratio (10 to 1 equivalent of alkoxythiophene monomers and alkoxybenzyl/alkoxynaphthyl thiophene monomers) are the most favourable and exhibit the best performance in device properties and colour changes. Hence, copolymers **68** to **71** were synthesised successfully through oxidative polymerisation (Scheme 9), using one equivalent of 3,4-bis(benzyloxy)thiophene and 10 equivalents of alkoxythiophene derivatives as monomers. For copolymer **68**, 3,4-bis(pentyloxy)thiophene and 3,4-bis(benzyloxy)thiophene were dissolved in ethyl acetate. Iron (III) chloride was dissolved in ethyl acetate and then added to the stirred solution of two monomers. The reaction mixture was stirred for 24 hours at room temperature. After that, the desired copolymer **68** was obtained after washing with methanol. Subsequently, the synthesis of **69**, **70** and **71** following the same procedure of synthesising **68** was successful. In addition, NMR spectrum demonstrated that the purification using methanol of **68**, **69**, **70** and **71** was suitable to obtain pure polymer. Compared to purifying homopolymers, the purification of copolymers is relatively easier. This is because there is a greater proportion of thiophene monomers with alkoxyl chains inside the copolymers (10 to 1). Therefore, the reaction produces larger proportions of impurities from the thiophene monomers with alkoxyl chains. Thiophene monomers and dimers with alkoxyl chains are easily soluble in organic solvents, which makes methanol particularly effective for the purification of copolymers. Overall, this gave the copolymer **68** in 12% yield,

copolymer **69** in 17% yield, copolymer **70** in 18% yield and copolymer **71** in 15% yield respectively. Figure 30 shows the ^{1}H NMR spectra of monomer **51**, monomer **63** and copolymer **71**. Copolymer **71** is composed of multiple repeating monomer **51** and **63** units. The signal peaks that are associate with the two monomers are exhibited together in the copolymer spectrum. After that, the overlap signals of repeat units of two monomers show a broader signal for the copolymer. Hence, from the comparison of the ^{1}H NMR diagrams of copolymer **71**, monomer **63** and monomer **51** in Figure 30, it can be determined that the right copolymer is yielded.

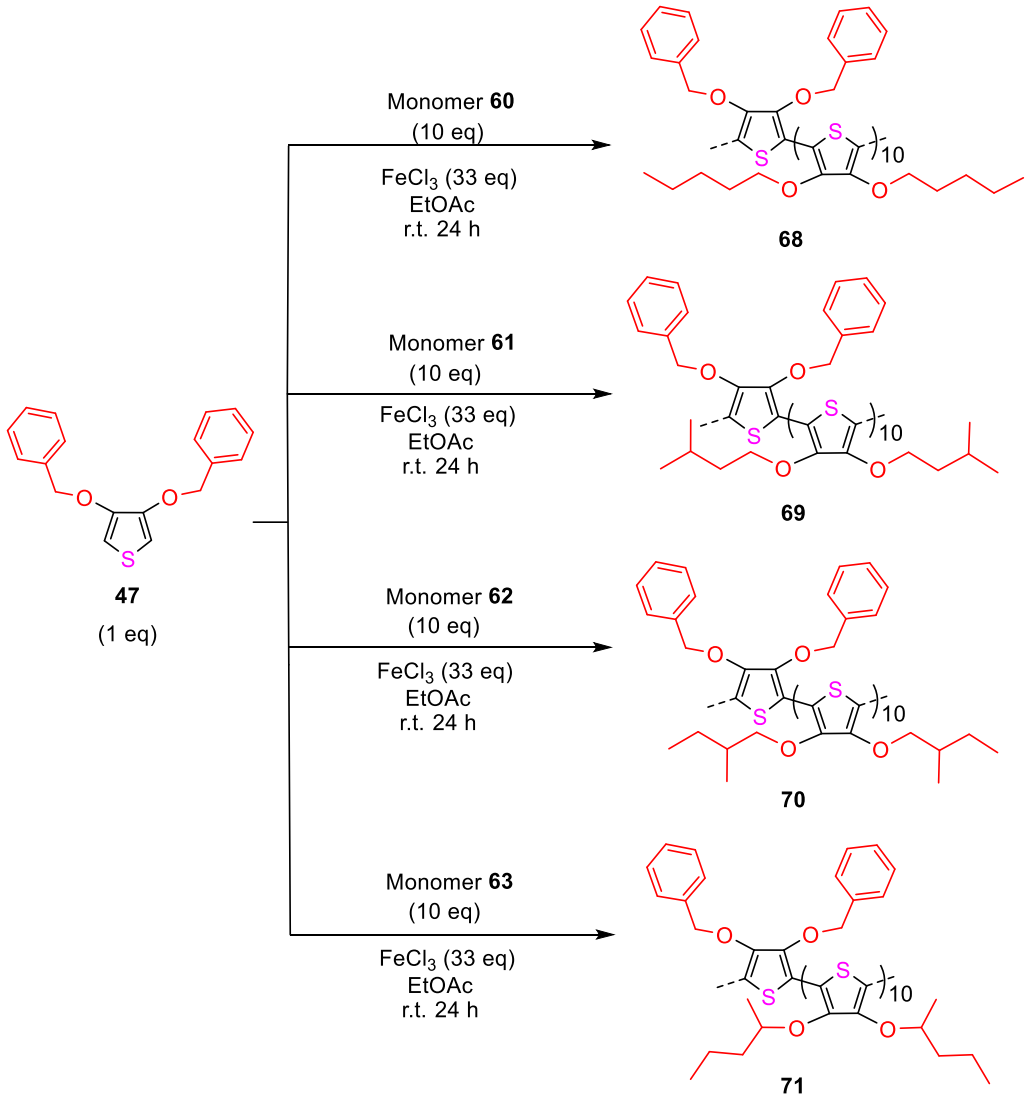

Scheme 9: Synthesis of copolymer **68-71**.

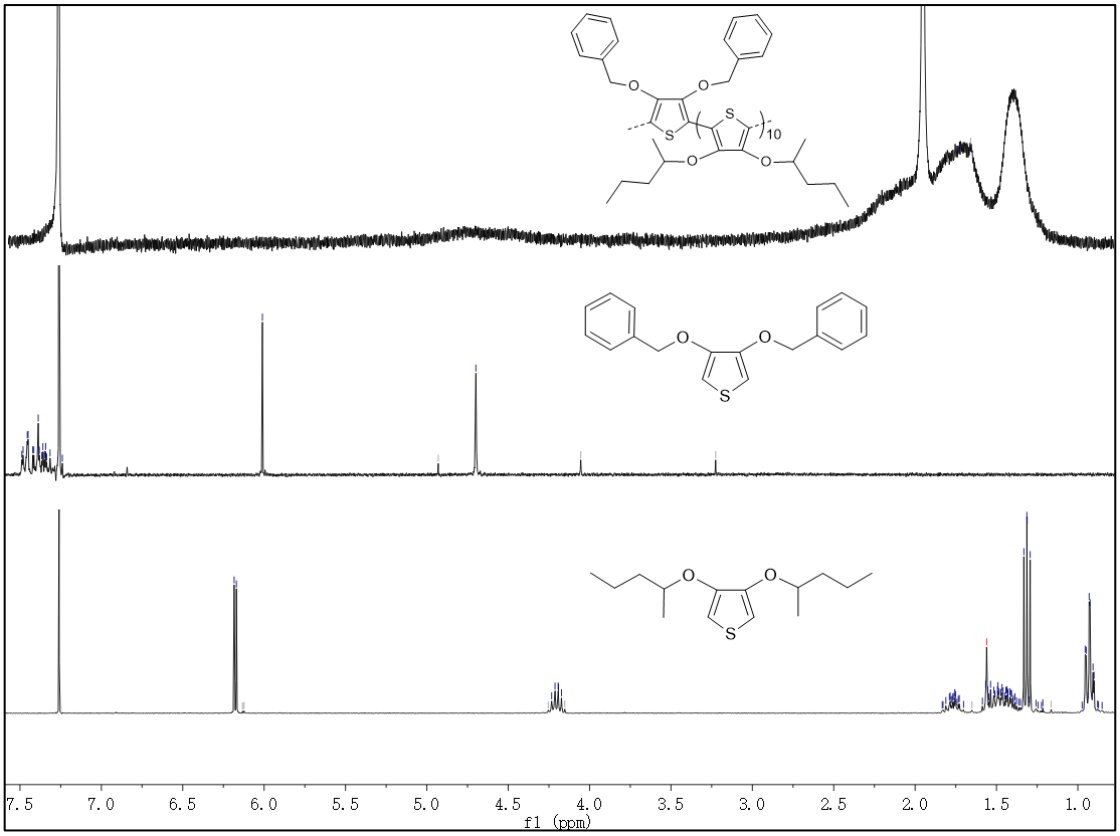

Figure 30: Comparison of ^{1}H NMR spectrum of monomer **51**, monomer **63** and copolymer **71** in $CDCl_3$ solvent.

Copolymers **72** to **75** were synthesised successfully through the same oxidative polymerisation as mentioned above, using 1 equivalent of 3,4-bis(3-phenylpropoxy)thiophene and 10 equivalents of alkoxythiophene derivatives as monomers. 33 equivalent of iron (III) chloride was used as catalyst during this reaction. The synthesis route of copolymers can be seen in Scheme 10. This gave the copolymer **72** in 19% yield, copolymer **73** in 16% yield, copolymer **74** in 15% yield and copolymer **75** in 18% yield, respectively.

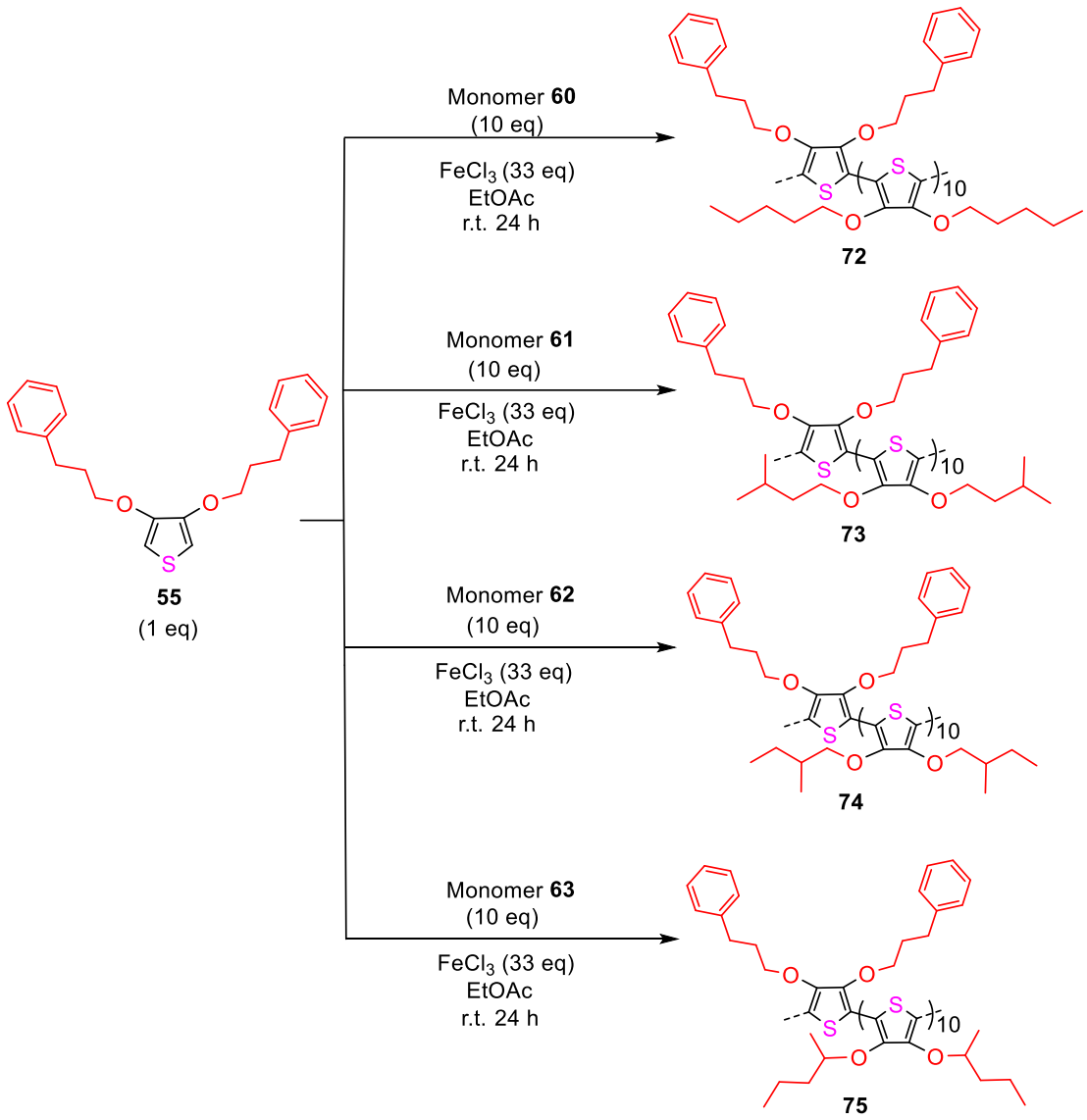

Scheme 10: The synthesis of copolymer **72-75**.

Copolymers **76** to **79** (Scheme 11) were synthesised successfully through the same oxidative polymerisation, using 1 equivalent of 3,4-bis(naphthalen-2-ylmethoxy)thiophene and 10 equivalents of alkoxythiophene derivatives as monomers. This gave the copolymer **76** in 13% yield, copolymer **77** in 15% yield, copolymer **78** in 16% yield and copolymer **79** in 17% yield, respectively.

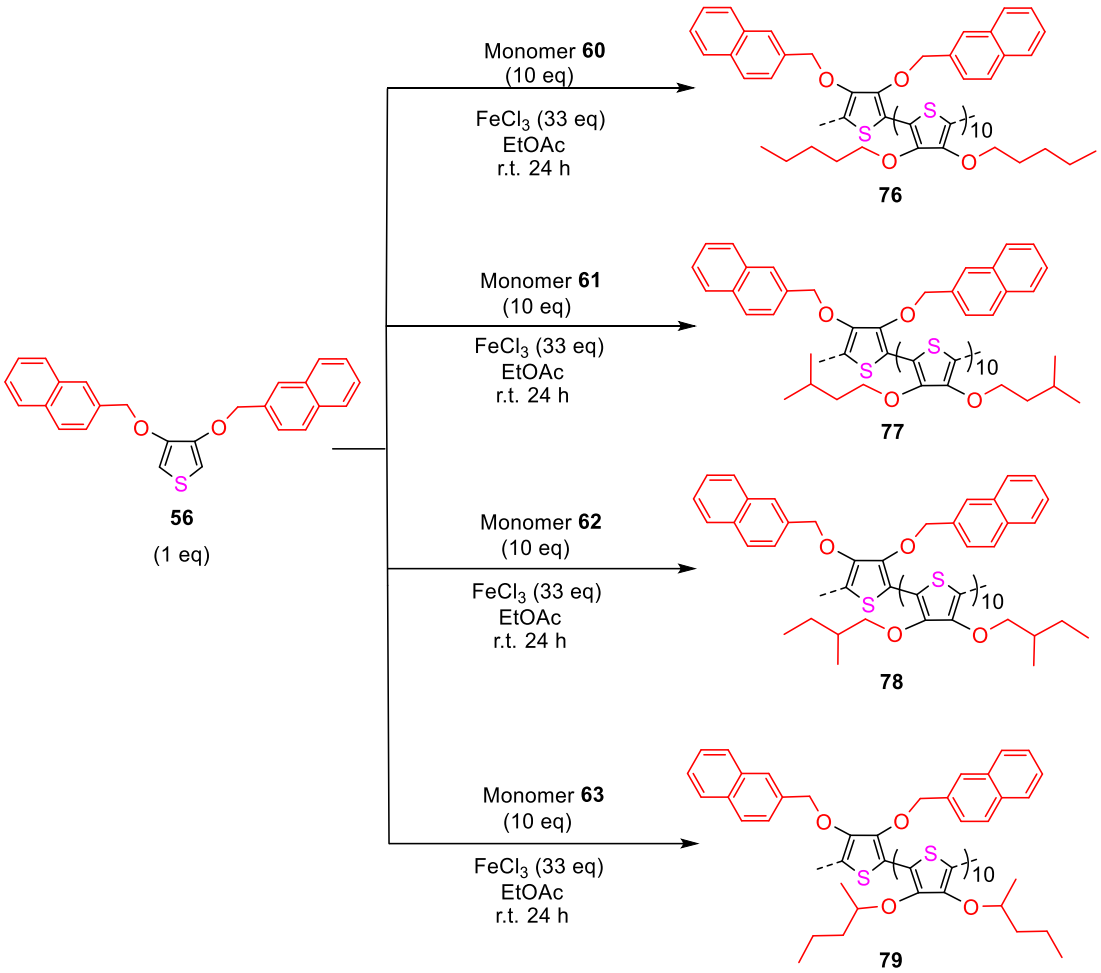

Scheme 11: The synthesis of copolymer **76-79**.

Copolymers **80** to **83** (Scheme 12) were synthesised successfully through the same oxidative polymerisation, using 1 equivalent of 3,4-bis(2-(naphthalen-1-yl)ethoxy)thiophene and 10 equivalents of alkoxythiophene derivatives as monomers. Monomer **59** is slightly soluble in ethyl acetate, which needs to be mixed by sonicator in advance. This gave the copolymer **80** in 14% yield, copolymer **81** in 19% yield, copolymer **82** in 17% yield and copolymer **83** in 17% yield, respectively.

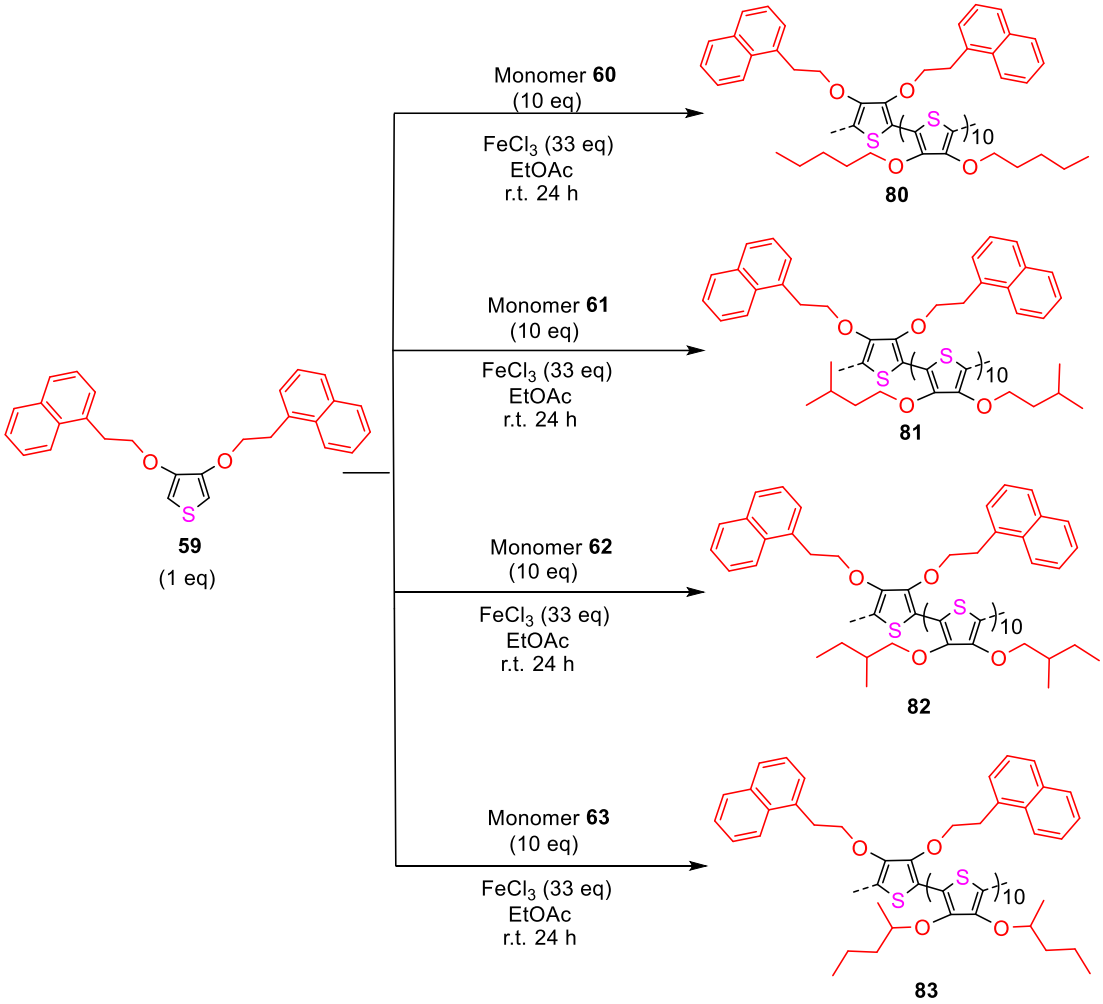

Scheme 12: The synthesis of copolymer **80-83**.

2.2. Characterisation of the electrochromic polymers

2.2.1. Electrochromic Devices

The synthesised polymers were assembled and tested as electrochromic devices by Dr. Antoine Stopin and Mr. Gianvito Romano from the University of Vienna. The main components of the device are: ITO coated PET (polyethylene terephthalate) substrate, copper tape, two working electrodes and an electrolyte. The electrolyte is fully deposited on the ITO/PET inside the bonding template, which is then cured under UV light (365 nm) for around 5 min before starting the assembly of the ECD.[94] The detailed structure of the ECD can be seen in Figure 31. The electrochromic material is dissolved in chloroform (1 mg/mL) using a spray coating method and sprayed onto the prepared device. Wires are connected to the copper tape of each working electrode so that ions can be exchanged from one working electrode to the other when a voltage is applied. The electrolyte is a gel substance with conductive properties, which is responsible for

the exchange of ions between the two electrodes when a voltage is applied to the device. By varying the applied voltage, the material undergoes reduction or oxidation and the optical properties of the ECD are changed.

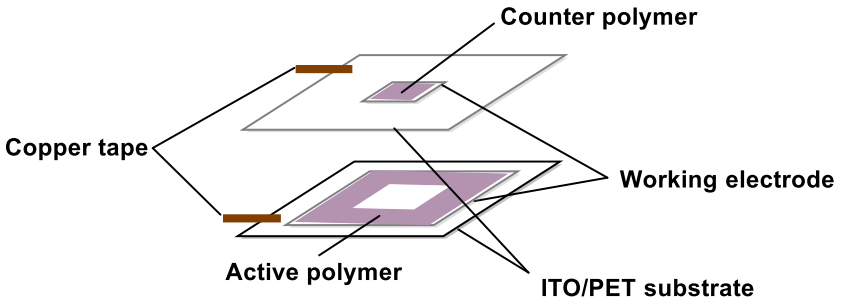

Figure 31: The structure of electrochromic device.

2.2.2. Copolymer spectroelectrochemistry studies

Spectroelectrochemistry of copolymer **71**, **75** and **79** as a function of the applied potential (between − 1.5 V and + 1.5 V) have been tested and analysed. The selected absorbance spectra range from 350 nm to 800 nm (Figure 32). Copolymer **71** demonstrates a maximum absorption wavelength of 546 nm at a voltage of − 0.6 V, this was calculated to have a transmittance of 13%. When applying the potential of + 1.5 V, the polymer reached a bleached state and the film exhibited 52% transmittance at 546 nm with 39% transmittance contrast (Δ%T). Compared with copolymer **71**, copolymers **75** and **79** show similar properties. They both reach their maximum absorption wavelengths of 545 nm and 547 nm at a − 0.6 V, demonstrating transmittances of 42% and 37% respectively. When applying the potential to + 1.5 V, polymer **75** reached a bleached state at 545 nm with 74% transmittance and copolymer **79** has a transmittance of 69% at 547 nm. Interestingly, the transmittance contrast for both **75** and **79** were calculated to be 32% (Δ%T).

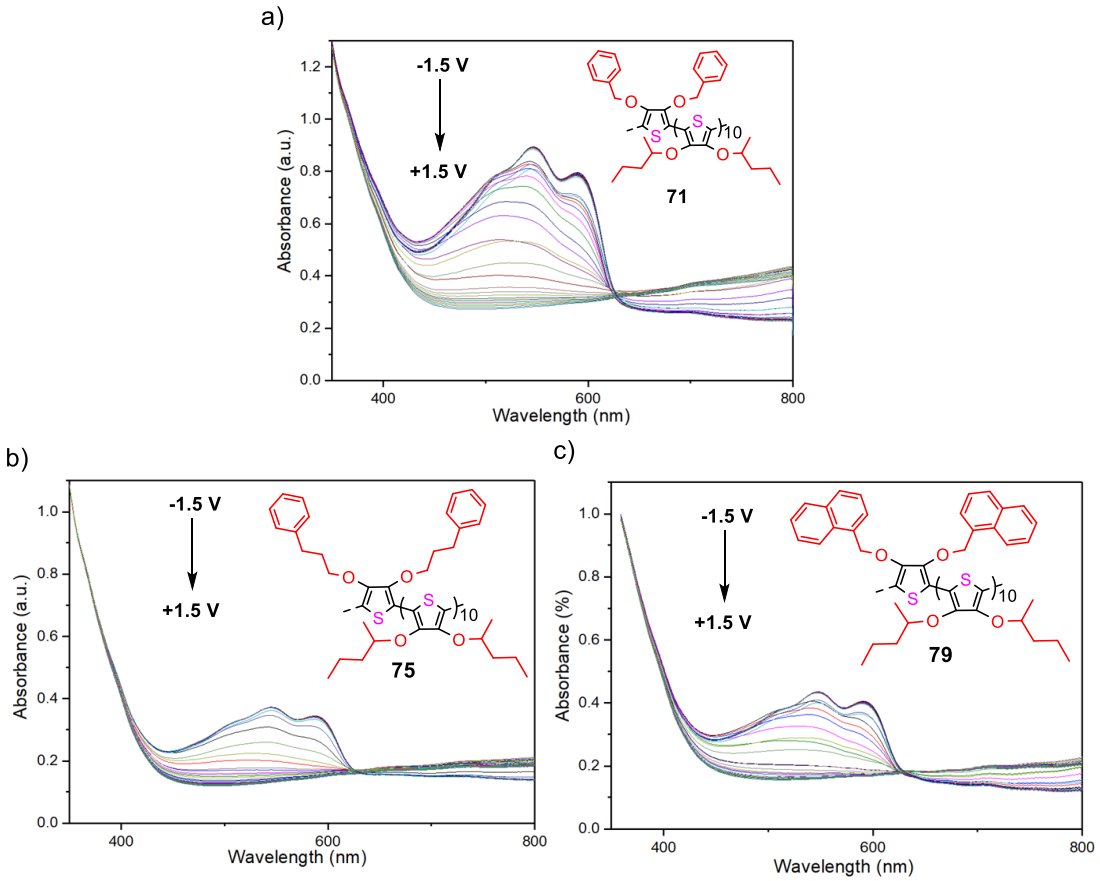

Figure 32: Spectroelectrochemistry of a) copolymer **71** film, b) copolymer **75** film and c) copolymer **79** film on ITO/PET slide between − 1.5 V and + 1.5 V with incremental potentials. The selected absorbance spectrums range from 350 nm to 800 nm.

It is worth noting the spectroelectrochemistry of copolymers **68** and **70** (Figure 33). Copolymer **68** reaches a maximum of absorption wavelength of 542 nm at a voltage of −1.4 V. As it can be seen in Figure 33a right, the small square in the middle of the fabricated ECD is the working electrode, where the outer square frame section is the counter electrode. The device of **68** switches between light red colour in the neutral state (− 1.5 V) and transparent grey in its oxidised state (+ 1.5 V). As for copolymer **70**, at the potential of − 0.6 V, it has stronger absorbance at λ_{max} = 495 nm. In Figure 33b right, the device of **70** exhibited a red colour in the neutral state and light red when oxidised. The significant wavelength difference between copolymers **68** and **70** at their maximum absorption is due to the different steric interactions between copolymer structures. Compared to copolymer **68**, which has a linear side chain on the thiophene unit, copolymer **70** with branched chains displays larger steric hindrance, which makes the structure become more twisted. The more twisted structure of the copolymer results a blue shift of the neutral state absorption.

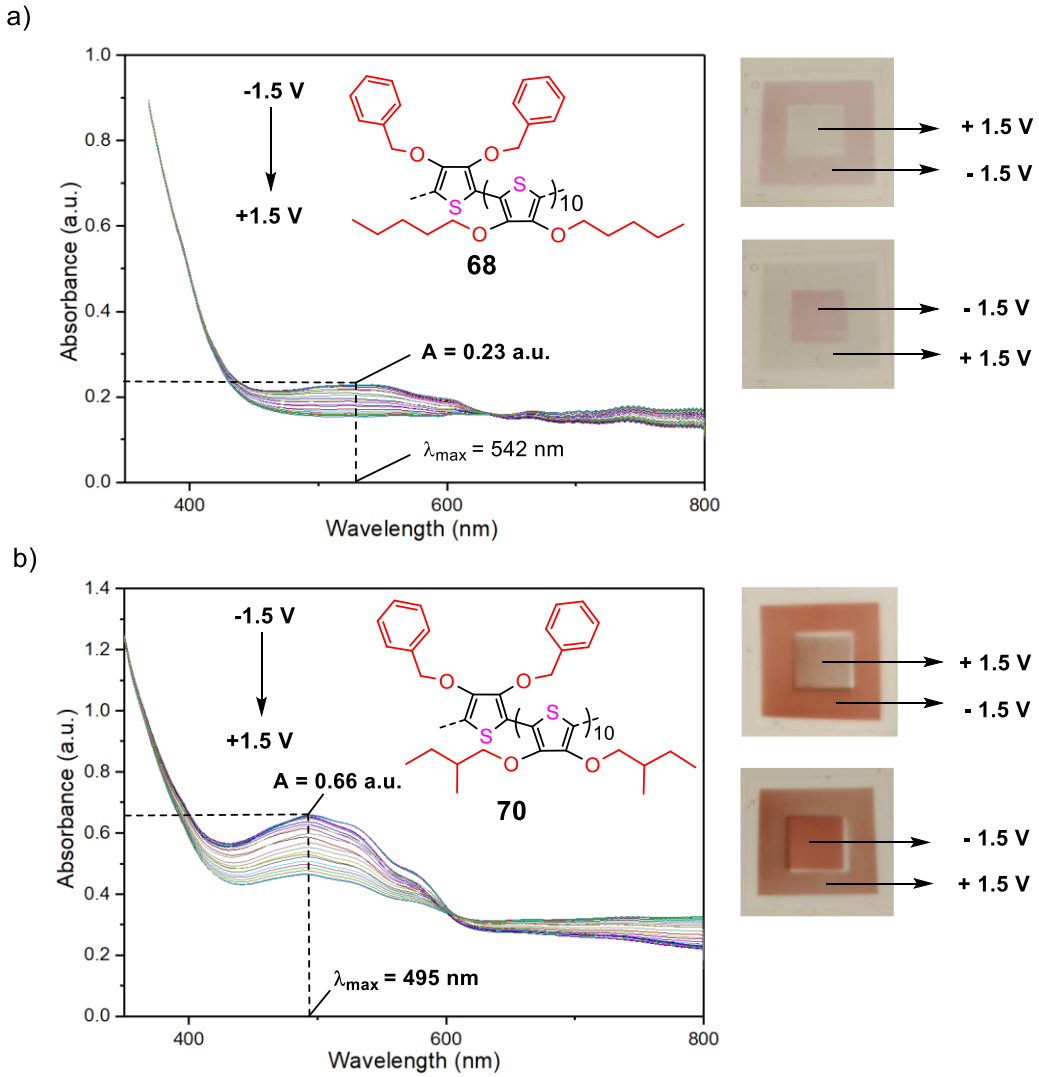

Figure 33: Spectroelectrochemistry of copolymer **68** film − 1.5 V ~ + 1.5 V with incremental potentials (a, left). Photo of copolymer **68** film at − 1.5 V and + 1.5 V (a, right). Spectroelectrochemistry of copolymer **70** film at − 1.5 V ~ + 1.5 V with incremental potentials (b, left). Photo of copolymer **70** film at − 1.5 V and + 1.5 V (b, right). The selected absorbance spectrums range from 350 nm to 800 nm.

In Figure 34a left, when applying a potential of + 1.5 V, the copolymer **73** still has an absorption band in the visible range, indicating that the copolymer absorbs in the oxidised state. However, homopolymer **64** has no absorption band in the visible region at incremental potential from − 1.5 to + 1.5 V. Therefore, the colour of **64** does not change with the applied voltage. In Figure 34a right, copolymer **73** demonstrated a colour change from its purple neutral state (− 1.5 V) to light purple in its oxidised state (+ 1.5 V). Compared with homopolymer **64**, copolymer **73** which contains alkyl branched thiophene units decreases the steric hindrance of the polymer backbone, resulting in a change in the absorption of the structure. Therefore, with the increase of potential, a change in the absorption of copolymer **73** can be seen in Figure 34a.

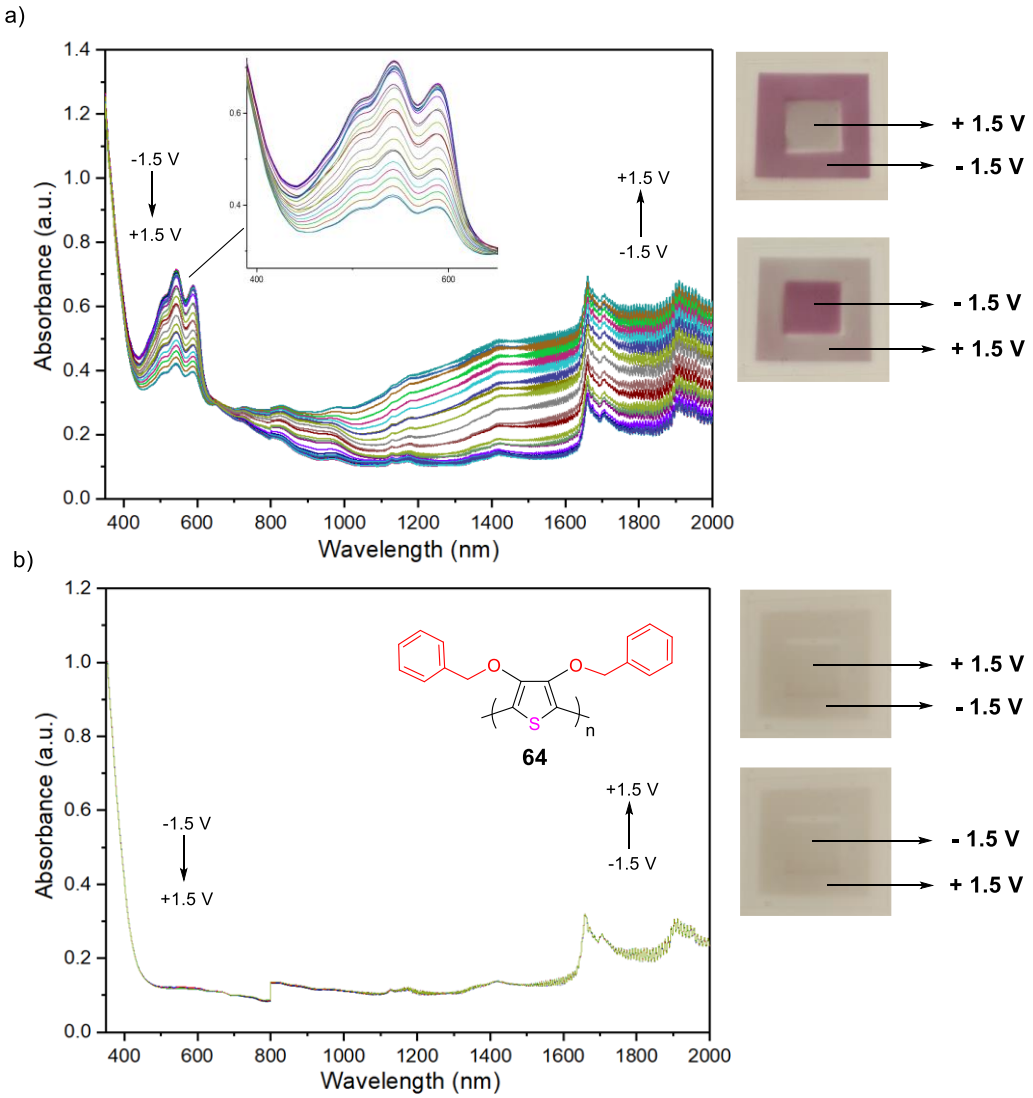

Figure 34: (a, left) Spectroelectrochemistry of copolymer **73** film − 1.5 V ~ + 1.5 V with incremental potentials. (a, right) Photo of copolymer **73** film at − 1.5 V and + 1.5 V. (b, left) Spectroelectrochemistry of copolymer **64** film −1.5 V ~ +1.5 V with incremental potentials. (b, right) Photo of copolymer **64** film at − 1.5 V and + 1.5 V.

Figure 35a exhibits the full spectrum electrochemical behaviour of copolymer **75** which was investigated by varying the external voltage applied to the film. When applying potentials from – 1.5 V to − 0.6 V, the maxima absorption of wavelength is 545 nm (λ_{max}), which can be ascribed to π to π* transition of the neutral copolymer. As the process of oxidation occurs, the amount of polarons and bipolarons starts to change: the generation of polarons reaches a peak and then starts to decline, while the generation of bipolarons is consistently increasing. The variation is reflected in Figure 35a, the value of absorption of copolymer **75** gradually decreases in the visible range, with increasing values of absorption in the infrared region.

The reason why polymer **75** deserves special attention is that it can be fully oxidised at

a very low potential. It can be identified by analysing images of the applied voltage and the degree of absorption of copolymer **75** in Figure 35b. At voltages of + 1.5 to + 1.1 V, the slope of the tangent line is almost zero, indicating that the polymer is fully oxidised. The device of copolymer **75** exhibits low oxidation potential and fast switching times (0.6 s). It switches between purple colour in the neutral state and colourless in its bleached state (Figure 35c).

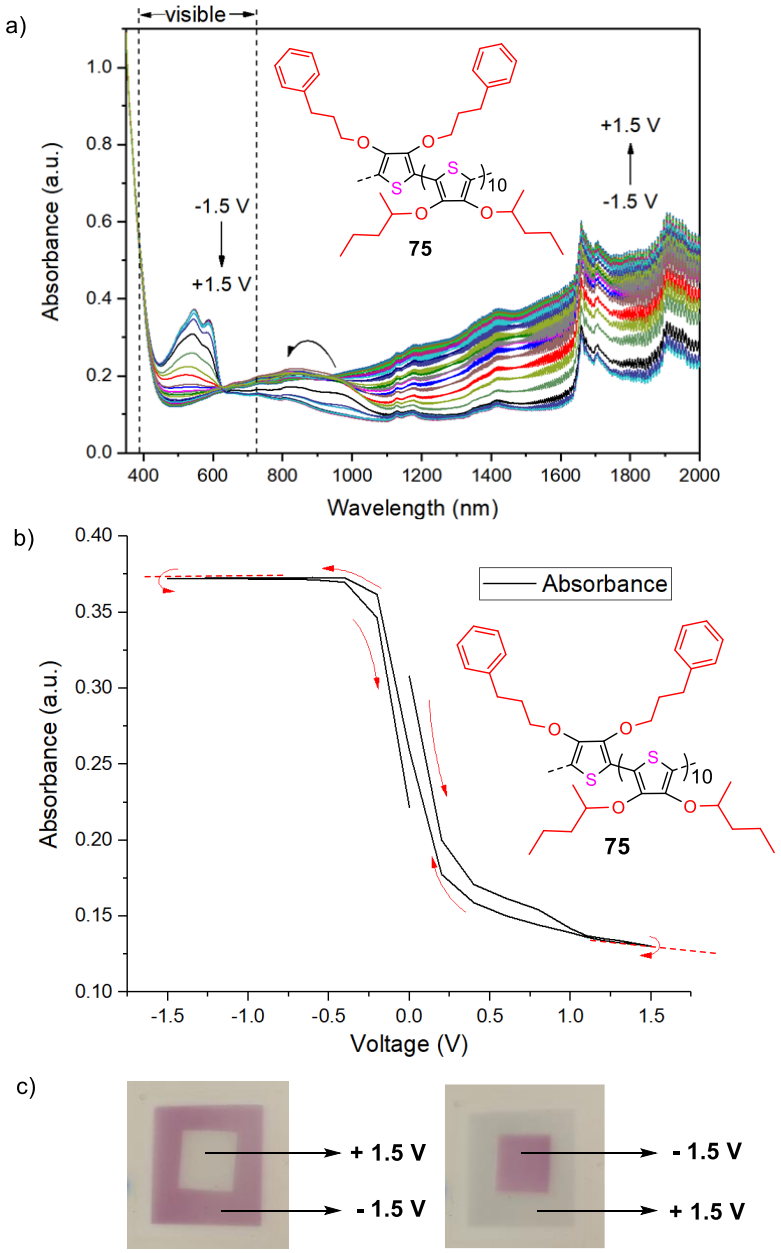

Figure 35: a) Spectroelectrochemistry of copolymer **75** film − 1.5 V ~ + 1.5 V with incremental potentials. b) Diagram of the relationship between applied potential and absorbance of copolymer **75**. c) Photo of copolymer **75** ECD at − 1.5 V and + 1.5 V.

Compared to copolymer **79**, copolymer **83** have a higher oxidation potential. As for copolymer **79**, it exhibited a purple-red colour in its neutral state and a highly

transparent light grey in its bleached state. After reaching + 1.5 V, as the voltage decreases, the curve of **83** does not return to the same path as the original voltage increase. In Figure 36b, copolymer **83** still has high tangent slope values at + 1.5 ~ + 1.1 V, indicating that copolymer **83** is not fully oxidised at + 1.5 V. A comparison of Figure 36a and Figure 36b demonstrates that copolymer **79** has a relatively lower oxidation potential, which allows it to reach a fully oxidised state at low applied voltages.

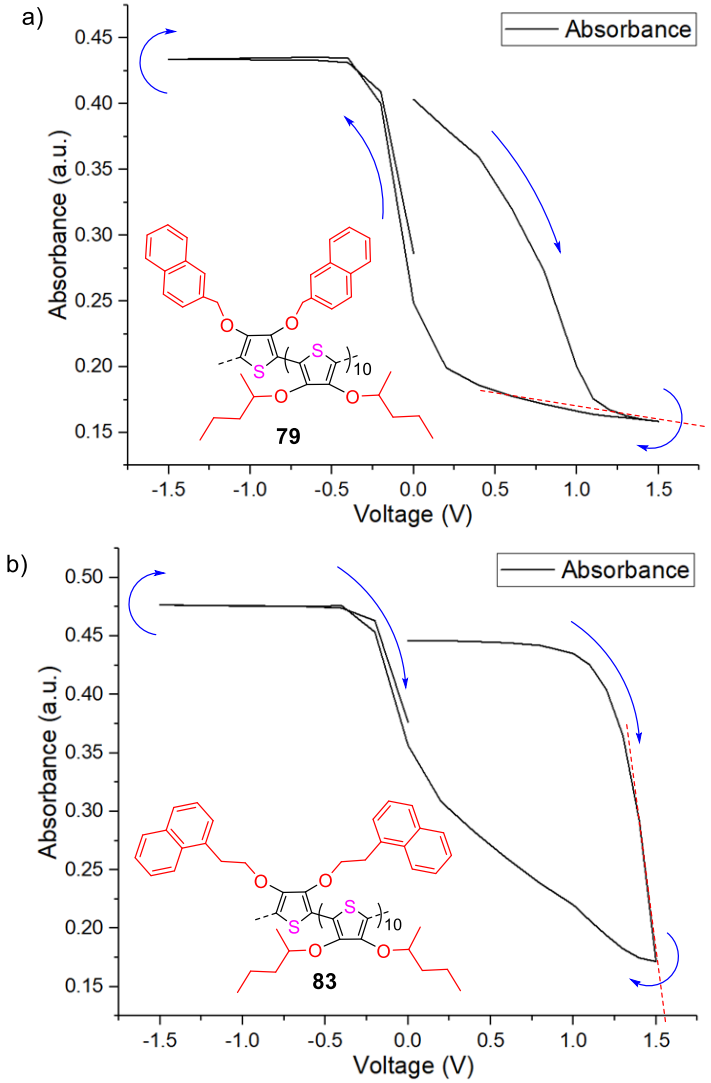

Figure 36: a) Diagram of the relationship between applied potential and absorbance of copolymer **79** and **83**.

2.2.3. Copolymer switching time studies

In order to evaluate the switching speed of the copolymers more accurately, the transmittance values of copolymers **74** and **82** at the maximum wavelength were used from the collected data for comparison. Furthermore, the time required for their redox states were also analysed. Figure 37a shows the results for copolymer **74** at maximum

wavelength of 499 nm, exhibiting a fast switching speed. During the bleaching process, polymer **74** reached 90% of the full transmittance contrast after 1.6 s (from T = 40.4% to T = 63.5% transmittance), while the reduction process completed 90% of the full transmittance contrast after 1 s (from T = 63.3% to T = 40.3%).

The switching time of copolymer **82** is longer compared to polymer **74**, as it can be seen in Figure 37b. Upon oxidation, **82** reached 90% of the full transmittance contrast after 4.3 s, and the reduction completed 90% of the full transmittance contrast after 1.6 s. The values of the ΔT% for the two states of oxidation and reduction were very similar (from T = 35.0% to T = 62.6% in oxidised state, from T = 62.5% to T = 36.8% in reduction state respectively). Therefore, the transmittance contrast of copolymer **74** is smaller than that of copolymer **82**. Furthermore, the absorbance of copolymer **74** is 0.42 a.u. at λ_{max} = 499 nm and 0.52 a.u. at λ_{max} = 527 nm for copolymer **82**. Compared to copolymer **74**, **82** has a much-increased conjugation, which makes the spectrum redshift.

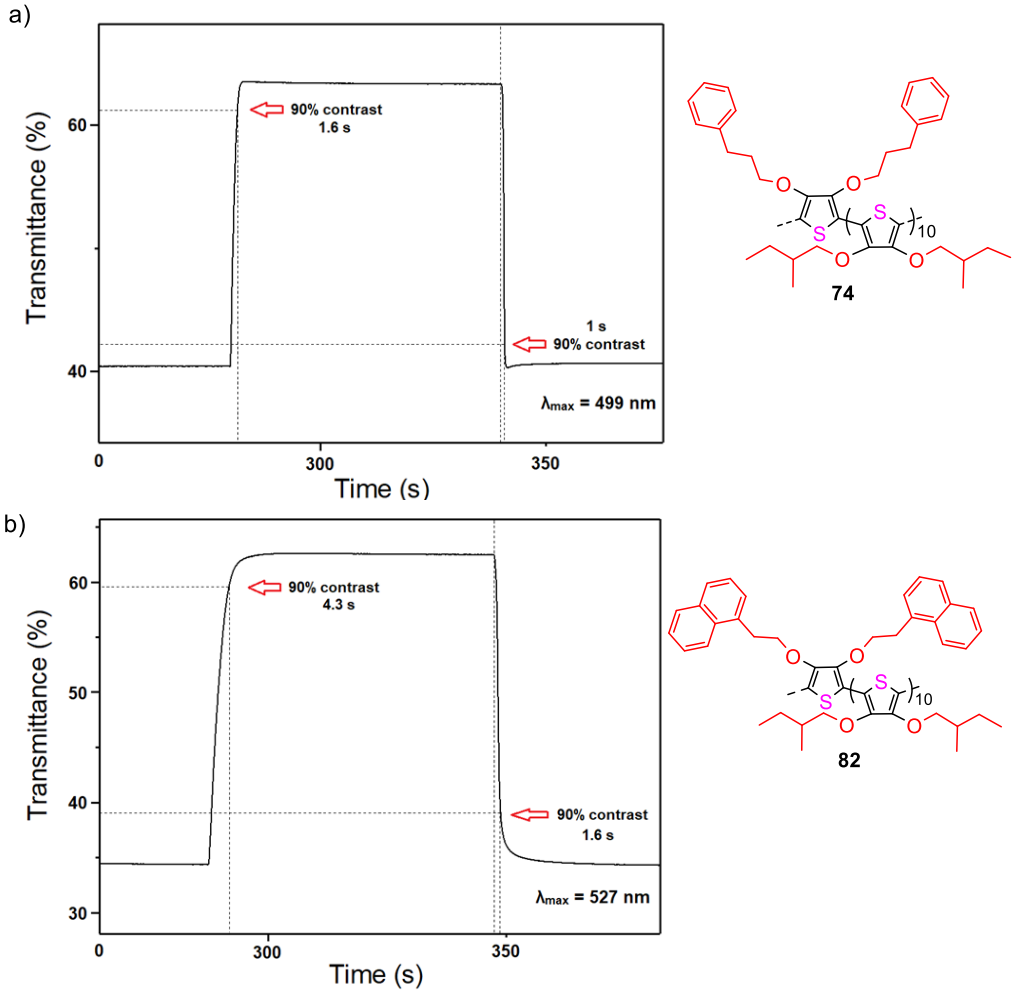

Figure 37: Time dependence of (a) copolymer **74** at 499 nm, (b) copolymer **82** at 527 nm with an applied 60 s potential squarewave from − 1.5 V to +1.5 V.

3. Conclusion

Four novel 3- and 4-substituted alkoxybenzyl/alkoxynaphthyl thiophene monomers soluble in organic solvents were synthesised by substitution reactions using the corresponding commercially available alcohol R-group with p-toluenesulfonic acid as a catalyst. Corresponding alkoxybenzyl/alkoxynaphthyl thiophene (3 and 4 position) homopolymers were synthesised using the four monomers with iron (III) chloride as the catalyst. Sixteen novel organic solvent-soluble and spray-treatable copolymers were synthesised from these alkoxybenzyl/alkoxynaphthyl thiophene (3 and 4 position) monomers through reaction with the four known alkoxy thiophene (3 and 4 position) monomers. As the groups introduced at the 3 and 4 positions become bulkier (from the benzene ring to the naphthalene ring), the solubility of the monomer in organic solvents becomes smaller gradually. The steric hindrance of the synthesised polymers will also change with the different bulky groups of monomers. To be specific, by varying the position of the substituent of alkoxy thiophene (3 and 4 position) monomers, the steric hindrance of the copolymer can be subtle changed, and thus precisely modulate the colour of the copolymers. All of the copolymers were fully characterised, including the spectroelectrochemical properties and switching time. It was found that the devices made using copolymer **75** and copolymer **79** have excellent electrochromic properties, and can be fully oxidised with low potential. As for copolymer **75**, it exhibited a purple colour in the neutral state and a highly transparent colour in its oxidised state. For copolymer **79**, it switched between a purple-red in the neutral state and a transparent colour in its oxidised state. Besides, they also exhibited fast switching times between − 1.5 V to + 1.5 V (0.6 s for **75** and 0.7 s for **79** during oxidation; 0.6 s for **75** and 0.4 s for **79** during reduction). Compared to the remaining copolymers with long switching times (above 3 s), most copolymers have fast switching times (0.5 to 2 s) but exhibit high oxidation potentials. For instance, copolymer **74** and **83** possess moderate switching times (1.6 s for **74** and 1.3 s for **83** during oxidation; 1 s for **74** and 0.6 s for **83** during reduction). However, the disadvantage is that copolymer **74** and **83** both require a relatively high oxidation potential and cannot be fully oxidised at + 1.5 V. Therefore, as electrochromic materials with fast switching time, low oxidation potential, and high solubility, copolymer **75** and **79** are excellent potential candidates for the application of electrochromic devices.

4. Experimental Part

General Remarks:

Thin layer chromatography (TLC) was performed using pre-coated aluminium sheets using 0.20 mm silica gel 60 with fluorescent indicator F254 manufactured by Merck. **Column chromatography** was carried out using silica gel 60 (particle size 40-60 μm) from Sigma Aldrich. **Melting Points (mp)** were measured on a Stuart SMP1 analogue melting point apparatus. **Nuclear Magnetic Resonance (NMR)** spectra were recorded using a Bruker Fourier 300 MHz spectrometer equipped with a dual (^{13}C, ^{1}H) probe or Bruker Fourier 400 MHz equipped with a broadband multinuclear (BBO) probe. ^{1}H spectra were obtained at 400 MHz or 300MHz and ^{13}C at 100 MHz or 75 MHz with complete decoupling for proton. All spectra were obtained at room temperature unless otherwise specified. Chemical shifts were reported in ppm according to the solvent residual signal ($CDCl_3$). The splitting of peaks is described as s (singlet), d (doublet), t (triplet), dd (doublet of doublets), and m (multiplet). **Infrared spectra (IR)** were recorded using a Shimadzu IR Affinity 1S FTIR spectrometer. **Mass Spectrometry (MS):** High resolution ESI mass spectra (HRMS) were performed on a Waters LCT HR TOF mass spectrometer in the positive or negative ion mode. All analyses above were carried out at Cardiff University.

General Procedure for the Synthesis of Thiophene Monomers Using 3,4-dimethoxythiophene and Benzyl/Naphthyl alcohol

3,4-dimethoxythiophene (1 eq.) along with benzyl/naphthyl alcohol (4 eq.) were weighted into a 50 mL round bottom flask. The flask was flushed with nitrogen and dry toluene (60 mL) was added, followed by PTSA (0.2 eq.). The reaction mixture was stirred and heated to 110 ℃ for 24 h. Methanol is removed from the solution twice per hour during the day and reacts overnight. After that, the reaction was cooled to room temperature, water (20 mL) was added and the phases were separated. The organic phase was washed by water (2 x 20 mL) and dried over $NaSO_4$ and then concentrated *in vacuo*. The crude material was purified by silica gel column chromatography (PE/DCM: 80/20 to 60/40).

3,4-bis(benzyloxy)thiophene (51):

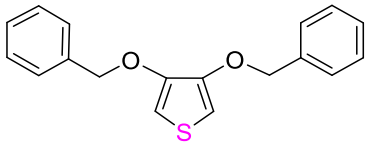

3,4-dimethoxythiophene (601 mg, 4.163 mmol) was coupled with benzyl alcohol (1880 mg, 17.187 mmol) to give 370 mg of 3,4-bis(benzyloxy)thiophene (30 % yield) as a white solid after chromatography. **M.p.**: 78 - 80 °C; **^{1}H NMR** (300 MHz, $CDCl_3$) δ 7.45-7.30 (m, 10H), 6.21 (s, 2H), 5.10 (s, 4H); **^{13}C NMR** (75 MHz, $CDCl_3$) δ 147.1, 136.8, 128.6, 128.0, 127.5, 98.5, 72.4; **HRMS** (ES m/z): $[M + Na]^+$ calc. for $C_{18}H_{16}O_2S$: 319.0769, found: 319.0779. **IR** ν (cm^{-1}): 1556.55, 1489.05, 1465.90, 1452.40, 1363.67, 1267.23, 1220.94, 1197.79, 1138.00, 1082.07, 1018.41, 999.13, 985.62, 914.26, 885.33, 862.18, 846.75, 744.52, 698.23, 636.51, 628.79, 607.58, 584.43, 499.56, 489.92, 468.70, 455.20, 422.41, 406.98.

3,4-bis(3-phenylpropoxy)thiophene (55):

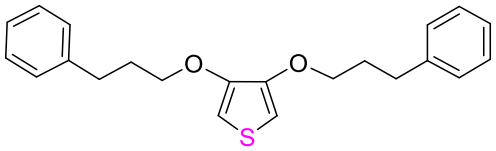

Commercially available 3,4-dimethoxythiophene (400 mg, 2.775 mmol) was coupled with 3-phenyl-1-propanol (1580 mg, 11.658 mmol) to give 392 mg of 3,4-bis(3-phenylpropoxy)thiophene (40 % yield) as a white solid after chromatography. **M.p.**: 50 - 51 °C; **^{1}H NMR** (300 MHz, $CDCl_3$) δ 7.31-7.15 (m, 10H), 6.14 (s, 2H), 4.00 (t, 4H, *J* = 6.5 Hz), 2.83-2.78 (t, 4H), 2.20-2.10 (m, 4H); **^{13}C NMR** (75 MHz, $CDCl_3$) δ 147.4, 141.5, 128.5, 128.4, 126.0, 97.2, 69.5, 32.1, 30.6; **HRMS** (ES m/z): $[M + H]^+$ calc. for $C_{22}H_{25}O_2S$: 353.1575, found: 353.1582. **IR** ν (cm^{-1}): 1602.85, 1560.41, 1494.83, 1467.83, 1452.40, 1394.53, 1375.25, 1365.60, 1242.16, 1203.58, 1151.50, 1091.71, 1078.21, 1062.78, 1014.56, 931.62, 886.04, 806.25, 750.31, 742.59, 700.16, 636.51, 592.15, 569.00, 557.43, 493.78, 480.28, 418.55.

3,4-bis(naphthalen-2-ylmethoxy)thiophene (56):

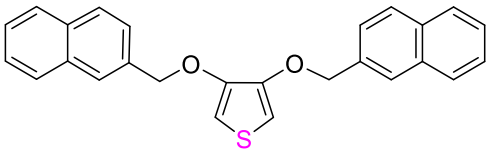

3,4-dimethoxythiophene (203 mg, 1.387 mmol) was coupled with 2-naphthalenemethanol (921 mg, 5.829 mmol) to give 95 mg of 3,4-bis(naphthalen-2-ylmethoxy)thiophene (17 % yield) as a white solid after chromatography. **M.p.**: 118 - 121 °C; **^{1}H NMR** (300 MHz, $CDCl_3$) δ 7.90-7.79 (m, 8H), 7.58 (dd, 2H, J = 8.4, 1.7 Hz), 7.51-7.45 (m, 4H), 6.27 (s, 2H), 5.29 (s, 4H); **^{13}C NMR** (75 MHz, $CDCl_3$) δ 147.2, 134.3, 133.3, 133.1, 128.4, 128.0, 127.8, 126.5, 126.2, 126.1, 125.3, 98.8, 72.7; **HRMS** (ES m/z): $[M + H]^+$ calc. for $C_{26}H_{21}O_2S$: 397.1262, found: 397.1260; **IR** ν (cm^{-1}): 1598.99, 1554.63, 1485.19, 1462.04, 1438.90, 1363.67, 1348.24, 1271.09, 1195.87, 1174.65, 1139.93, 1124.50, 1093.64, 1018.41, 1001.06, 968.27, 952.84, 898.83, 881.47, 856.39, 815.89, 775.38, 744.52, 619.15, 578.64, 476.42, 466.77, 412.77.

3,4-bis(2-(naphthalen-1-yl)ethoxy)thiophene (59):

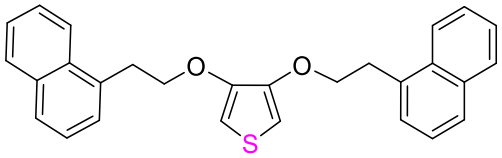

3,4-dimethoxythiophene (502 mg, 3.469 mmol) was coupled with 2-(naphthalen-1-yl)ethan-1-ol (2507 mg, 14.569 mmol) to give 472 mg of 3,4-bis(2-(naphthalen-1-yl)ethoxy)thiophene (32 % yield) as a white solid after chromatography. **M.p.**: 122 - 124 °C; **^{1}H NMR** (300 MHz, $CDCl_3$) δ 7.95-7.92 (m, 2H), 7.71-7.68 (dd, 2H, *J* = 1.9 Hz), 7.62-7.57 (m, 2H), 7.39-7.28 (m, 8H), 5.96 (s, 2H), 4.13 (t, 4H, *J* = 7.4 Hz), 3.46 (t, 4H, *J* = 7.4 Hz); **^{13}C NMR** (75 MHz, $CDCl_3$) δ 147.0, 133.9, 133.8, 132.1, 128.9, 127.5, 127.2, 126.2, 125.7, 125.6, 123.7, 97.5, 70.6, 32.8; **HRMS** (ES m/z): $[M + H]^+$ calc. for $C_{28}H_{25}O_2S$: 425.1575, found: 425.1578. **IR** ν (cm^{-1}): 1595.13, 1564.27, 1502.55, 1458.18, 1429.25, 1396.46, 1363.67, 1265.30, 1201.65, 1153.43, 1080.14, 1047.35, 1020.34, 997.20, 918.12, 898.83, 854.47, 842.89, 798.53, 788.89, 775.38, 740.67, 694.37, 621.08, 580.57, 567.07, 551.64, 484.13, 464.84, 435.91, 428.20, 405.05.

3,4-bis(pentyloxy)thiophene (60):[93]

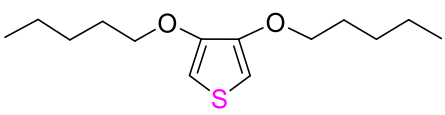

3,4-dimethoxythiophene (401 mg, 2.775 mmol) was coupled with pentan-1-ol (1027 mg, 11.658 mmol) to give 305 mg of 3,4-bis(pentyloxy)thiophene (43 % yield) as a transparent oil after chromatography. **^{1}H NMR** (300 MHz, $CDCl_3$) δ 6.15 (s, 2H), 3.97

(t, 4H, *J* = 6.8 Hz), 1.87-1.77 (m, 4H), 1.47-1.30 (m, 8H), 0.85 (t, 6H, *J* = 4.7 Hz); **^{13}C NMR** (75 MHz, $CDCl_3$) δ 147.5, 96.8, 70.6, 28.7, 28.2, 22.5, 14.1. **HRMS** (ES m/z): $[M]^+$ calc. for $C_{14}H_{24}O_2S$: 256.1492, found: 256.1480.

3,4-bis(isopentyloxy)thiophene (61):[93]

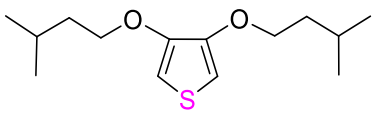

Commercially available 3,4-dimethoxythiophene (603 mg, 4.163 mmol) was coupled with 3-methylbutan-1-ol (1542 mg, 17.487 mmol) to give 343 mg of 3,4-bis(isopentyloxy)thiophene (32 % yield) as a transparent oil after chromatography. **^{1}H NMR** (300 MHz, $CDCl_3$) δ 6.16 (s, 2H), 4.00 (t, 4H, *J* = 6.8 Hz), 1.87-1.76 (m, 2H), 1.76-1.67 (m, 4H), 0.96 (d, 12H, *J* = 6.4 Hz); **^{13}C NMR** (75 MHz, $CDCl_3$) δ 147.6, 96.8, 69.0, 37.7, 25.1, 22.7. **HRMS** (ES m/z): $[M]^+$ calc. for $C_{14}H_{24}O_2S$: 256.1492, found: 256.1483.

3,4-bis(2-methylbutoxy)thiophene (62):[93, 95]

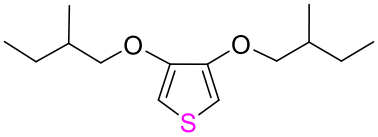

3,4-dimethoxythiophene (502 mg, 3.469 mmol) was coupled with 2-methylbutan-1-ol (1284 mg, 14.573 mmol) to give 249 mg of 3,4-bis(2-methylbutoxy)thiophene (28 % yield) as a transparent oil after chromatography. **^{1}H NMR** (300 MHz, $CDCl_3$) δ 6.16 (s, 2H), 3.86 (dd, 2H, *J* = 9.1, 6.1 Hz), 3.76 (dd, 2H, *J* = 9.1, 6.1 Hz), 1.96-1.85 (m, 2H), 1.62-1.48 (m, 2H), 1.32-1.17 (m, 2H), 1.01 (d, 6H, *J* = 6.7 Hz), 0.96 (t, 6H, *J* = 7.4 Hz); **^{13}C NMR** (75 MHz, $CDCl_3$) δ 147.9, 96.9, 75.4, 34.6, 26.2, 16.6, 11.4. **HRMS** (ES m/z): $[M]^+$ calc. for $C_{14}H_{24}O_2S$: 256.1492, found: 256.1487.

3,4-bis(pentan-2-yloxy)thiophene (63):[93]

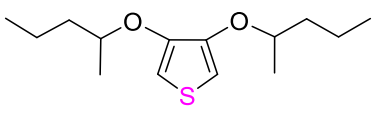

3,4-dimethoxythiophene (605 mg, 4.163 mmol) was coupled with DL-2-pentanol (1542 mg, 17.487 mmol) to give 365 mg of 3,4-bis(pentan-2-yloxy)thiophene (34 % yield) as a transparent oil after chromatography. **^{1}H NMR** (300 MHz, $CDCl_3$) δ 6.18 (d, 2H, J =

4.1 Hz), 4.25-4.15 (m, 2H), 1.83-1.36 (m, 8H), 1.33-1.29 (m, 6H), 0.95 (td, 6H, *J* = 7.2, 1.9 Hz); **^{13}C NMR** (75 MHz, $CDCl_3$) δ 147.5, 99.1, 76.8, 38.6, 19.7, 18.8, 14.1. **HRMS** (ES m/z): $[M]^+$ calc. for $C_{14}H_{24}O_2S$: 256.1492, found: 256.1481.

General Procedure for the Synthesis of Thiophene Homopolymers Using Benzyl/Naphthyl Thiophene Monomer

In a round-bottomed flask, benzyl/naphthyl thiophene monomer (1 eq.) were dissolved in ethyl acetate (1.2 ml). Iron (III) chloride (3 eq.) was dissolved in ethyl acetate (3.6 ml) and then added to the stirred solution of monomer. The reaction mixture was stirred for 24 hours at room temperature. After that, the reaction was stopped and quenched with chloroform (20 mL) and water (20 mL). The mixture of the round bottom flask was transferred to separatory funnel. Methanol (20 mL) was added and the phases were separated. The aqueous phase was extracted by chloroform (2 x 20 mL). The organic phase was washed with mixture of water and methanol (1:1, 3 x 40 mL). The crude polymer in solution of chloroform was concentrated *in vacuo*. Finally, the desired polymer was obtained after washing with methanol (3 x 25 mL) using sonicator.

Homopolymer (64):

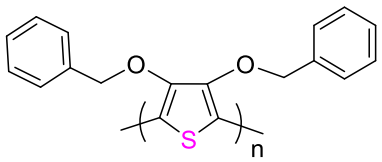

3,4-bis(benzyloxy)thiophene (70.13 mg, 0.236 mmol), Iron (III) chloride (115.03 mg, 0.708 mmol) and ethyl acetate (4.8 ml) were used in this polymerisation. This gave the polymer in 20 % (14 mg) yield of purple solid.

Homopolymer (65):

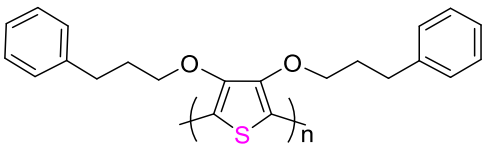

3,4-bis(3-phenylpropoxy)thiophene (69.82 mg, 0.198 mmol), Iron (III) chloride (96.72 mg, 0.596 mmol) and ethyl acetate (4.3 ml) were used in this polymerisation, giving 15 mg of homopolymer **65** (22 % yield) as a purple solid after purification.

Homopolymer (66):

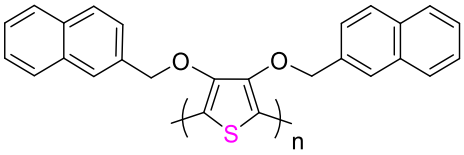

3,4-bis(naphthalen-2-ylmethoxy)thiophene (60.1 mg, 0.151 mmol), Iron (III) chloride (73.7 mg, 0.453 mmol) and ethyl acetate (4.3 ml) were used in this polymerisation, giving the designed compound as a dark brown solid in 14 % yield (8 mg).

Homopolymer (67):

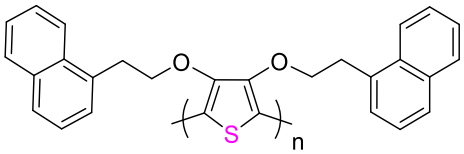

3,4-bis(2-(naphthalen-1-yl)ethoxy)thiophene (70.2 mg, 0.165 mmol), Iron (III) chloride (80.3 mg, 0.495 mmol) and ethyl acetate (3.91 ml) were used in this polymerisation. This gave the polymer in 12 % (8 mg) yield of dark grey solid.

General Procedure for the Synthesis of Thiophene Copolymers Using Alkyl Thiophene Monomer and Benzyl/Naphthyl Thiophene Monomer

Alkyl thiophene monomer (10 eq.) and benzyl/naphthyl thiophene monomer (1 eq.) were dissolved in ethyl acetate (1.05 ml). Iron (III) chloride (33 eq.) was dissolved in ethyl acetate (3.15 ml) and then added to the stirred solution of two monomers. The reaction mixture was stirred for 24 hours at room temperature. After that, the reaction was stopped and quenched with chloroform (20 mL) and water (20 mL). The mixture in flask was transferred to separatory funnel. Methanol (20 mL) was added and the phases were separated. The aqueous phase was extracted by chloroform (2 x 20 mL). The organic phase was washed with mixture of water and methanol (1:1, 3 x 40 mL). Subsequently, two organic phases were combined and concentrated *in vacuo*. Finally, the crude polymer was washed with methanol (3 x 25 mL) using sonicator to yield the designed compound.

Copolymer (68):

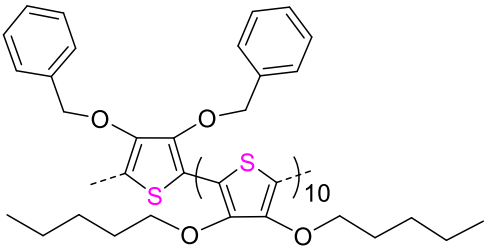

3,4-bis(pentyloxy)thiophene (59.99 mg, 0.234 mmol), 3,4-bis(benzyloxy)thiophene (6.93 mg, 0.0234 mmol), Iron (III) chloride (113.3 mg, 0.702 mmol) and ethyl acetate (4.2 ml) were used in this copolymerisation, giving 8 mg of copolymer **68** (12 % yield) as a dark purple-red solid after purification.

Copolymer (69):

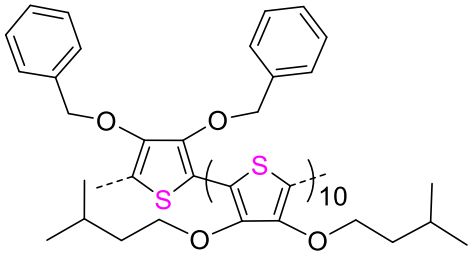

3,4-bis(isopentyloxy)thiophene (60.01 mg, 0.234 mmol), 3,4-bis(benzyloxy)thiophene (6.91 mg, 0.0234 mmol), Iron (III) chloride (113.8 mg, 0.702 mmol) and ethyl acetate (4.2 ml) were used in this copolymerisation. This gave the copolymer in 17 % (11 mg) yield of purple solid.

Copolymer (70):

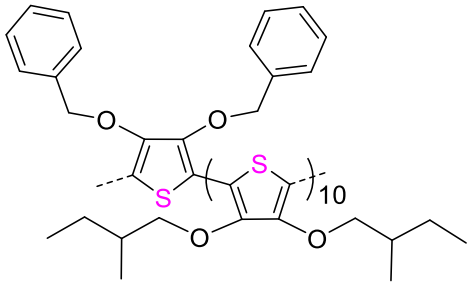

3,4-bis(2-methylbutoxy)thiophene (59.93 mg, 0.234 mmol), 3,4-bis(benzyloxy)thiophene (6.71 mg, 0.0234 mmol), Iron (III) chloride (113.1 mg, 0.702 mmol) and ethyl acetate (4.2 ml) were used in this copolymerisation. This gave the copolymer in 18 % (12 mg) yield of brown-red solid.

Copolymer (71):

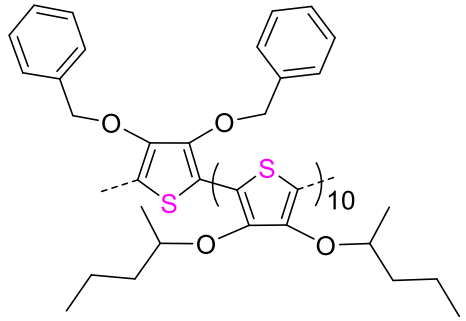

3,4-bis(pentan-2-yloxy)thiophene (60.13 mg, 0.234 mmol), 3,4-bis(benzyloxy)thiophene (7.03 mg, 0.0234 mmol), Iron (III) chloride (113.2 mg, 0.702 mmol) and ethyl acetate (4.2 ml) were used in this copolymerisation, giving 10 mg of copolymer **71** (15 % yield) as a purple solid after purification.

Copolymer (72):

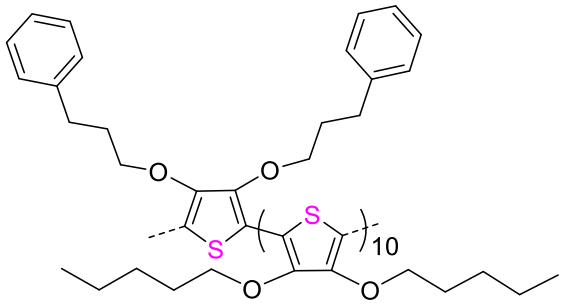

3,4-bis(pentyloxy)thiophene (60.08 mg, 0.234 mmol), 3,4-bis(3-phenylpropoxy)thiophene (8.25 mg, 0.0234 mmol), Iron (III) chloride (113.9 mg, 0.702 mmol) and ethyl acetate (4.2 ml) were used in this copolymerisation, giving the designed compound as a purple-red solid in 19 % yield (13 mg).

Copolymer (73):

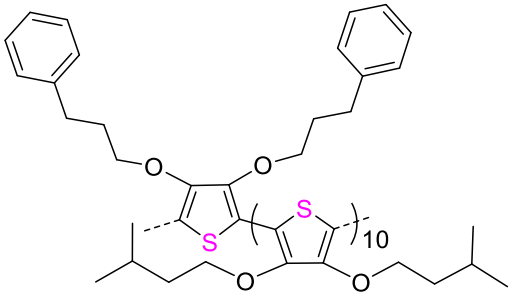

3,4-bis(isopentyloxy)thiophene (60.17 mg, 0.234 mmol), 3,4-bis(3-phenylpropoxy)thiophene (8.28 mg, 0.0234 mmol), Iron (III) chloride (113.7 mg, 0.702

mmol) and ethyl acetate (4.2 ml) were used in this copolymerisation. This gave the copolymer in 16 % (11 mg) yield of purple solid.

Copolymer (74):

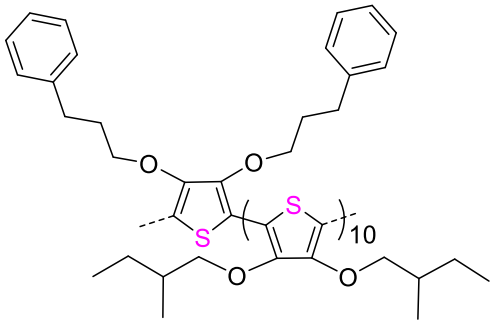

3,4-bis(2-methylbutoxy)thiophene (60.06 mg, 0.234 mmol), 3,4-bis(3-phenylpropoxy)thiophene (8.17 mg, 0.0234 mmol), Iron (III) chloride (113.7 mg, 0.702 mmol) and ethyl acetate (4.2 ml) were used in this copolymerisation, giving the designed compound of brown solid in 15 % yield (10 mg).

Copolymer (75):

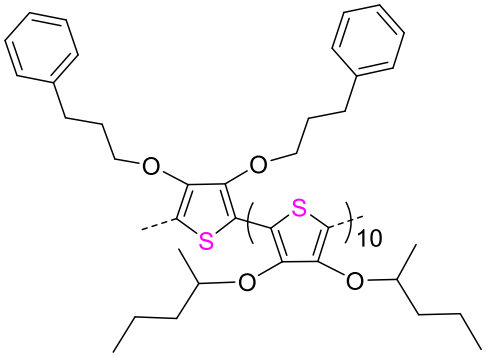

3,4-bis(pentan-2-yloxy)thiophene (59.94 mg, 0.234 mmol), 3,4-bis(3-phenylpropoxy)thiophene (8.30 mg, 0.0234 mmol), Iron (III) chloride (113.8 mg, 0.702 mmol) and ethyl acetate (4.2 ml) were used in this copolymerisation. This gave the copolymer in 18 % (12 mg) yield of purple solid.

Copolymer (76):

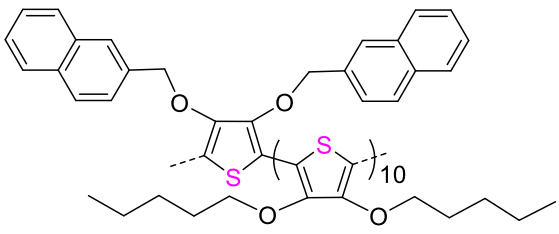

3,4-bis(pentyloxy)thiophene (60.02 mg, 0.234 mmol), 3,4-bis(naphthalen-2-ylmethoxy)thiophene (9.23 mg, 0.0234 mmol), Iron (III) chloride (113.9 mg, 0.702 mmol) and ethyl acetate (4.2 ml) were used in this copolymerisation. This gave the copolymer of purple solid in 13 % (9 mg) yield.

Copolymer (77):

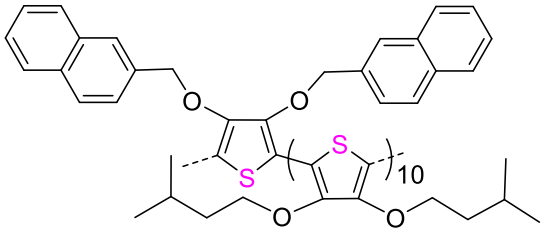

3,4-bis(isopentyloxy)thiophene (60.02 mg, 0.234 mmol), 3,4-bis(naphthalen-2-ylmethoxy)thiophene (9.29 mg, 0.0234 mmol), Iron (III) chloride (113.6 mg, 0.702 mmol) and ethyl acetate (4.2 ml) were used in this copolymerisation, giving 10 mg of copolymer **77** (15 % yield) as a purple solid after purification.

Copolymer (78):

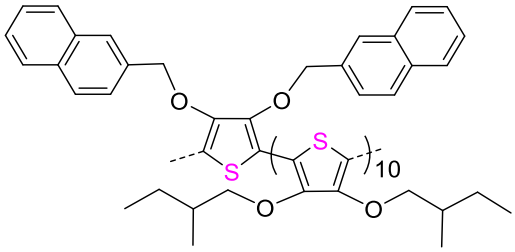

3,4-bis(2-methylbutoxy)thiophene (60.05 mg, 0.234 mmol), 3,4-bis(naphthalen-2-ylmethoxy)thiophene (9.29 mg, 0.0234 mmol), Iron (III) chloride (113.7 mg, 0.702 mmol) and ethyl acetate (4.2 ml) were used in this copolymerisation, giving 11 mg of copolymer **78** (16 % yield) as a brown solid after purification.

Copolymer (79):

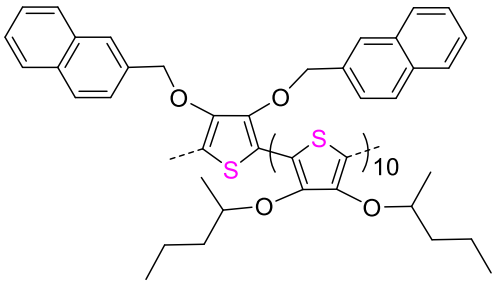

3,4-bis(pentan-2-yloxy)thiophene (60.02 mg, 0.234 mmol), 3,4-bis(naphthalen-2-ylmethoxy)thiophene (9.29 mg, 0.0234 mmol), Iron (III) chloride (113.9 mg, 0.702 mmol) and ethyl acetate (4.2 ml) were used in this copolymerisation, giving the designed compound of purple-red solid in 17 % yield (12 mg).

Copolymer (80):

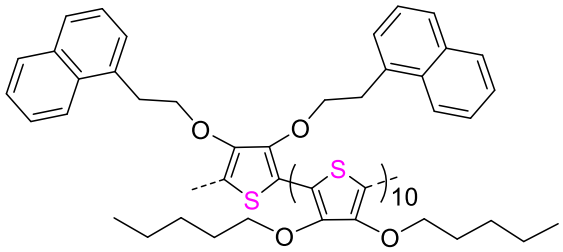

3,4-bis(pentyloxy)thiophene (60.04 mg, 0.234 mmol), 3,4-bis(2-(naphthalen-1-yl)ethoxy)thiophene (9.97 mg, 0.0234 mmol), Iron (III) chloride (113.6 mg, 0.702 mmol) and ethyl acetate (4.2 ml) were used in this copolymerisation, giving 10 mg of copolymer **80** (14 % yield) as a purple solid after purification.

Copolymer (81):

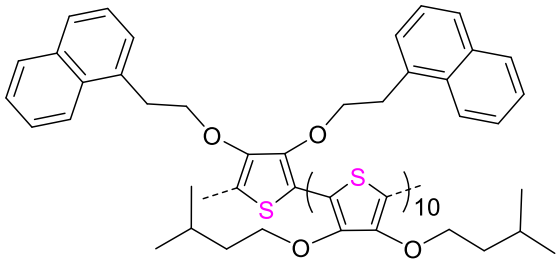

3,4-bis(isopentyloxy)thiophene (60.07 mg, 0.234 mmol), 3,4-bis(2-(naphthalen-1-yl)ethoxy)thiophene (9.90 mg, 0.0234 mmol), Iron (III) chloride (113.9 mg, 0.702 mmol) and ethyl acetate (4.2 ml) were used in this copolymerisation. This gave the copolymer of purple solid in 19 % (13 mg) yield.

Copolymer (82):

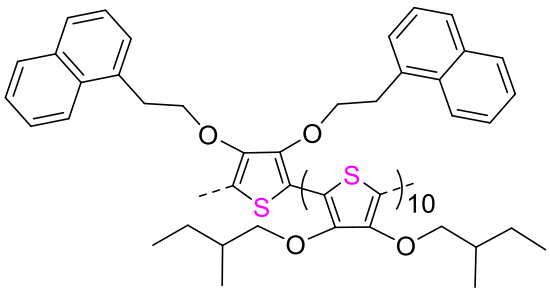

3,4-bis(2-methylbutoxy)thiophene (60.03 mg, 0.234 mmol), 3,4-bis(2-(naphthalen-1-yl)ethoxy)thiophene (10.06 mg, 0.0234 mmol), Iron (III) chloride (113.8 mg, 0.702 mmol) and ethyl acetate (4.2 ml) were used in this copolymerisation, giving 12 mg of copolymer **82** (17 % yield) as a brown solid after purification.

Copolymer (83):

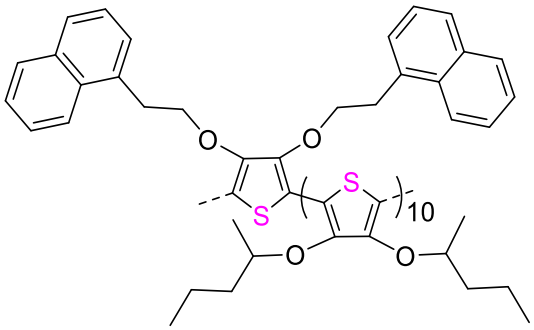

3,4-bis(pentan-2-yloxy)thiophene (60.03 mg, 0.234 mmol), 3,4-bis(2-(naphthalen-1-yl)ethoxy)thiophene (9.97 mg, 0.0234 mmol), Iron (III) chloride (113.5 mg, 0.702 mmol) and ethyl acetate (4.2 ml) were used in this copolymerisation, giving the designed compound of purple solid in 17 % yield (12 mg).

NMR Spectra of Synthesised Compounds:

3,4-bis(benzyloxy)thiophene (51)

^{1}H NMR (400 MHz, $CDCl_3$) of **51**

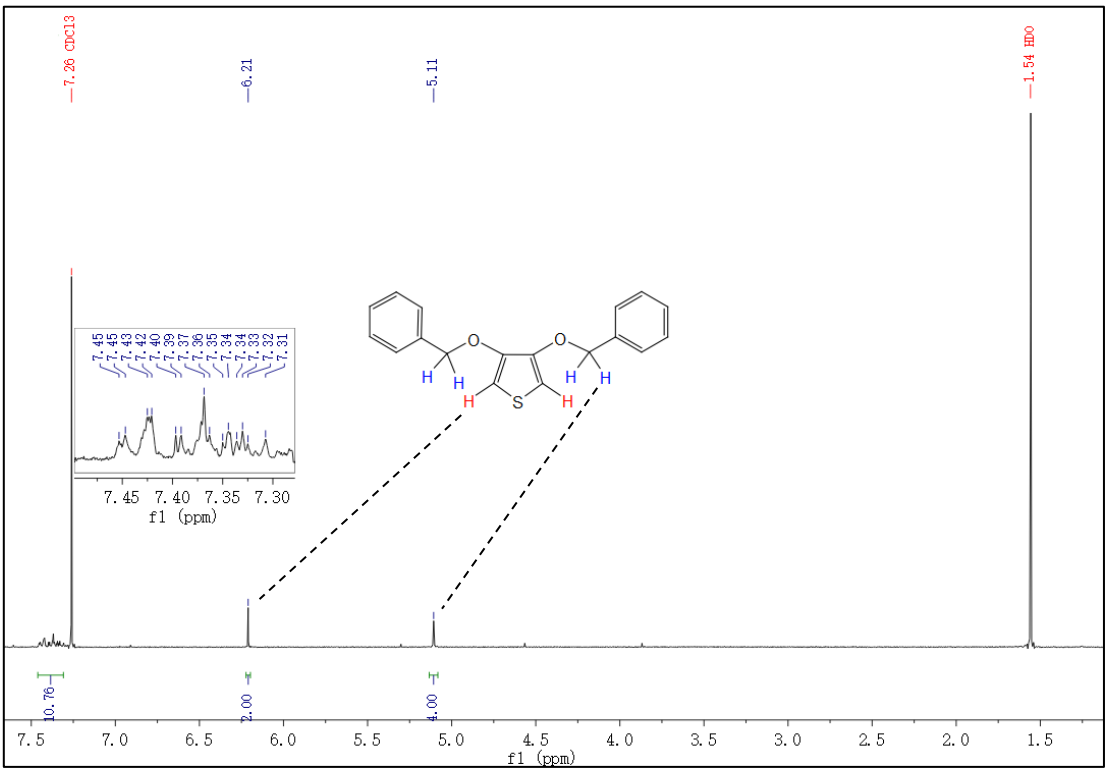

^{13}C NMR (75 MHz, $CDCl_3$) of **51**

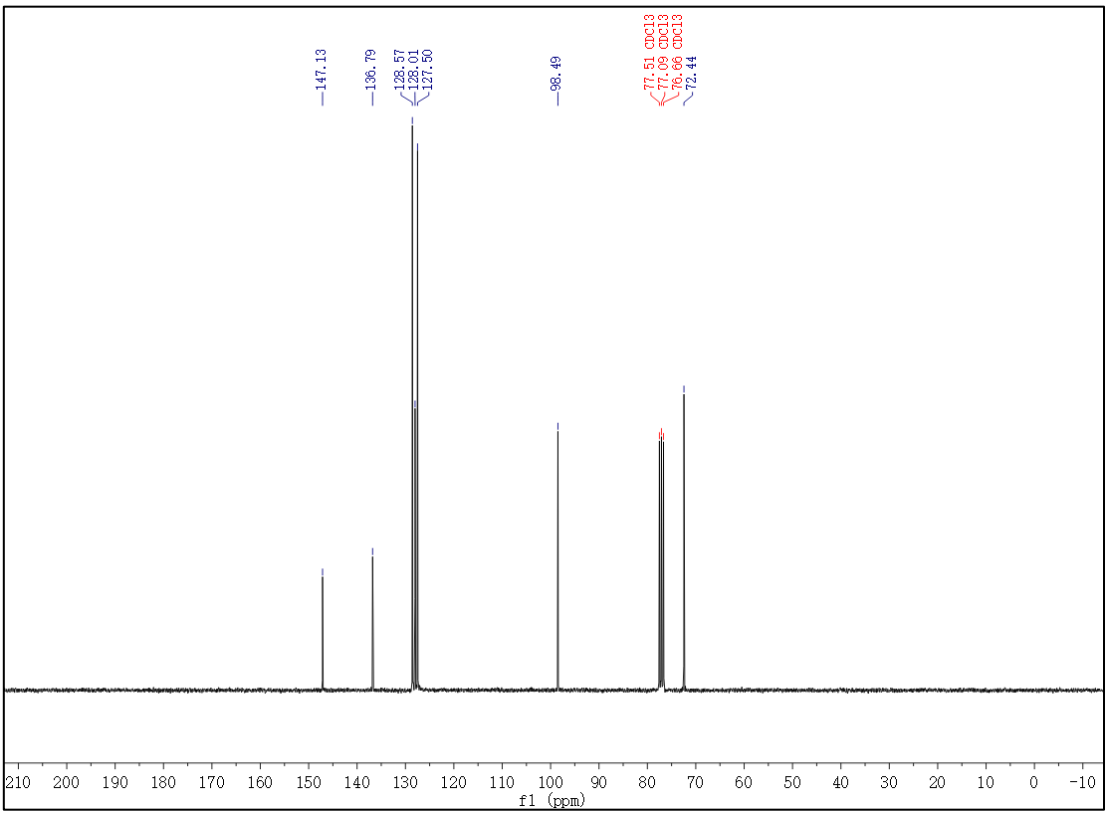

3,4-bis(3-phenylpropoxy)thiophene (55)

^{1}H NMR (300 MHz, $CDCl_3$) of **55**

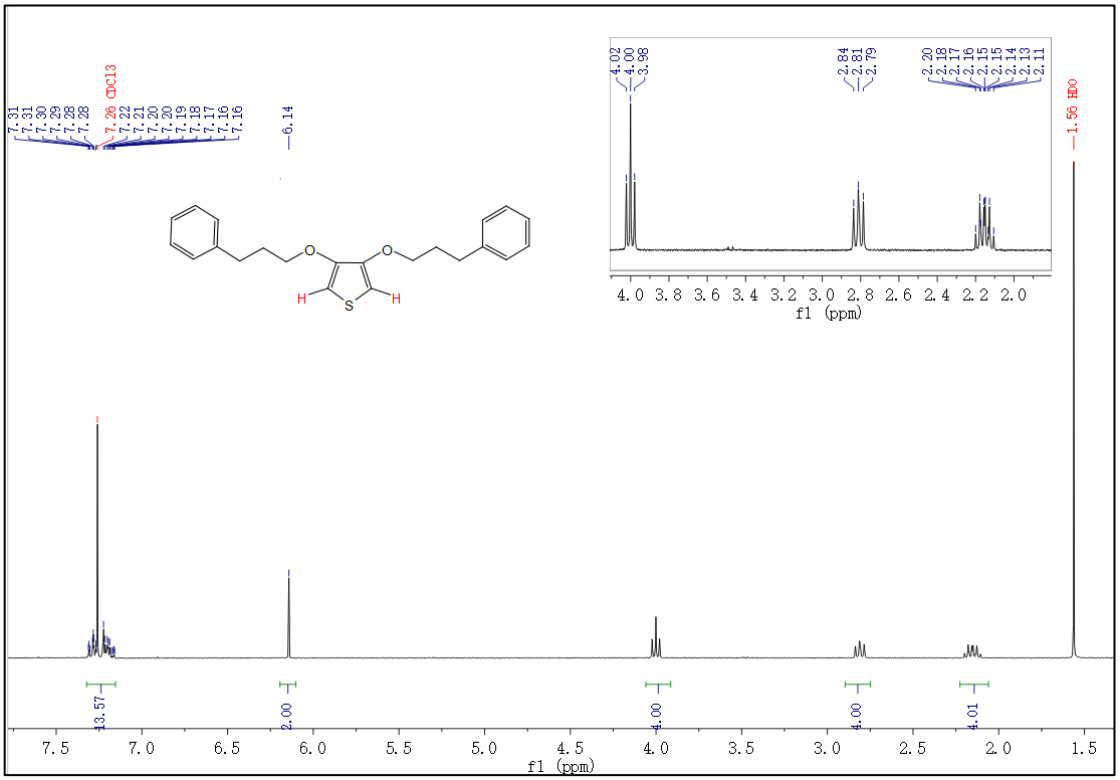

^{13}C NMR (75 MHz, $CDCl_3$) of **55**

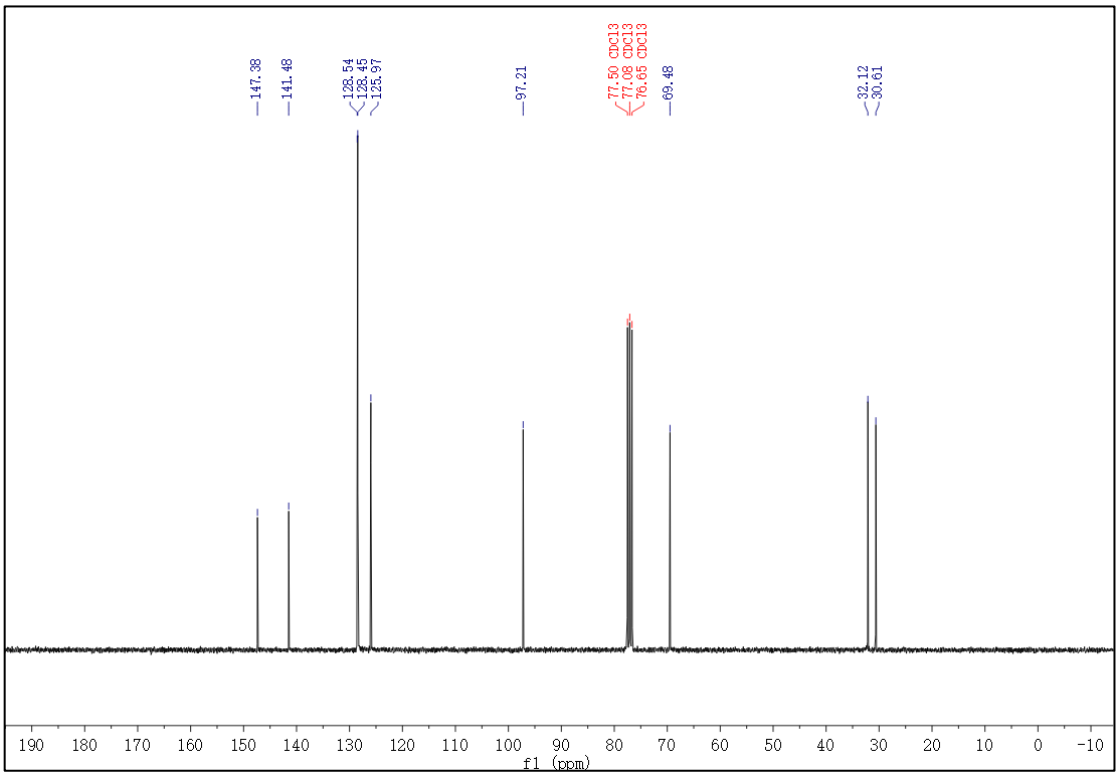

3,4-bis(naphthalen-2-ylmethoxy)thiophene (56)

^{1}H NMR (300 MHz, $CDCl_3$) of **56**

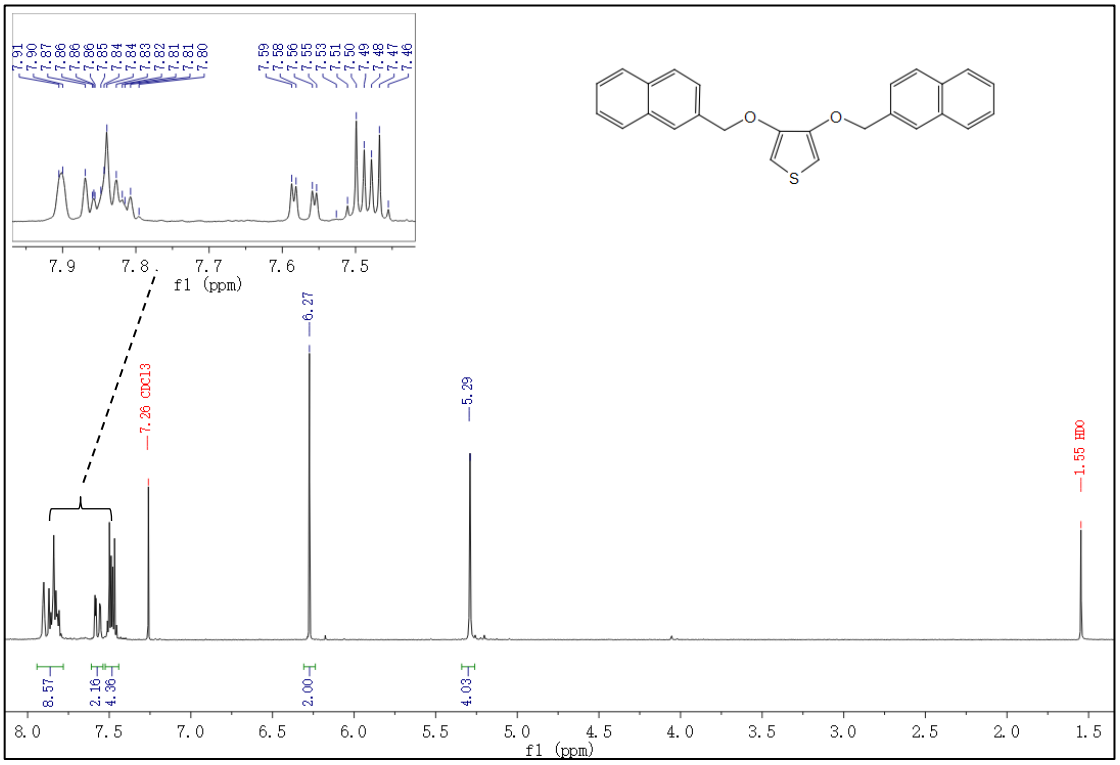

^{13}C NMR (75 MHz, $CDCl_3$) of **56**

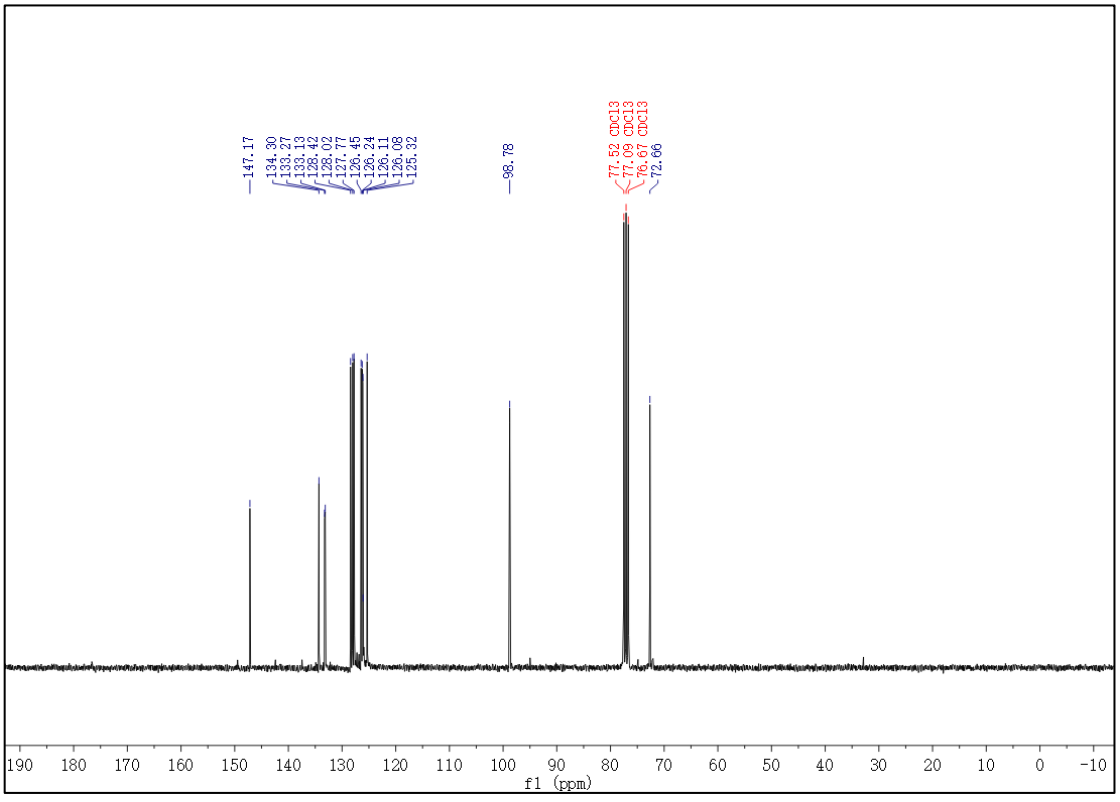

3,4-bis(2-(naphthalen-1-yl)ethoxy)thiophene (59)

^{1}H NMR (300 MHz, $CDCl_3$) of **59**

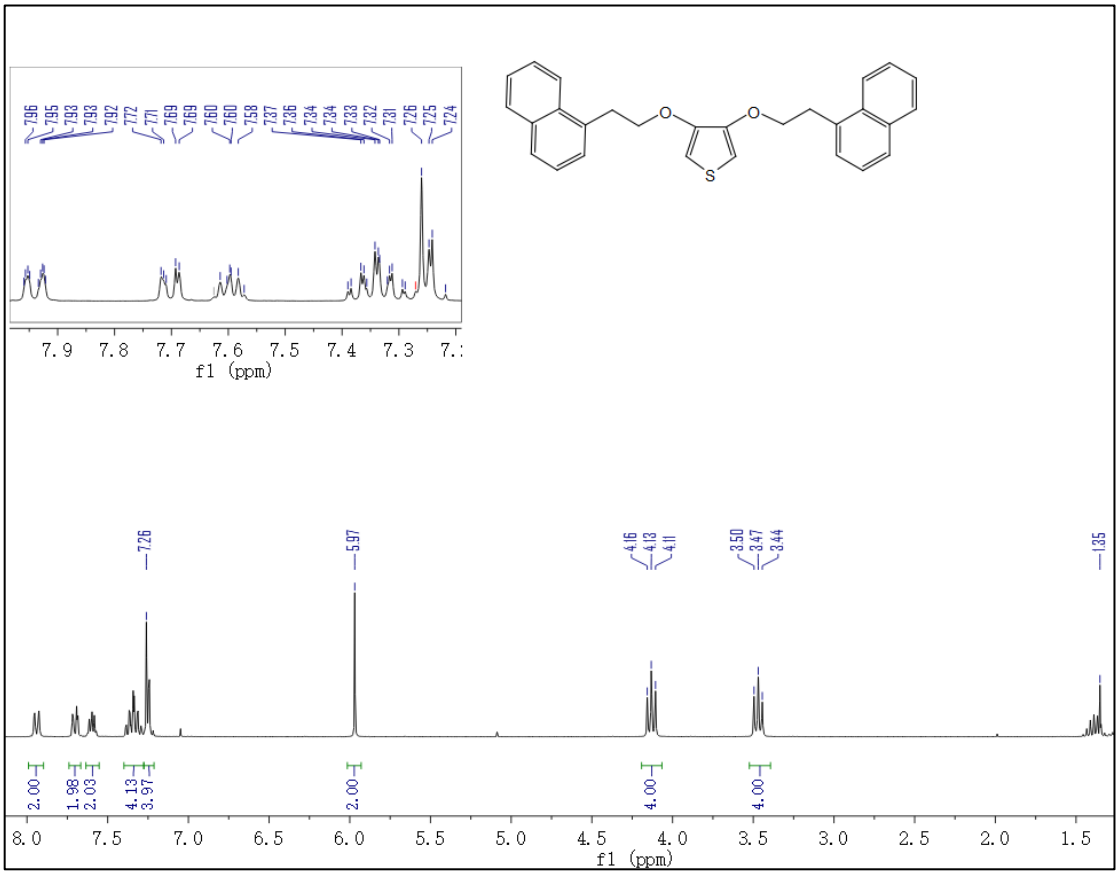

^{13}C NMR (75 MHz, $CDCl_3$) of **59**

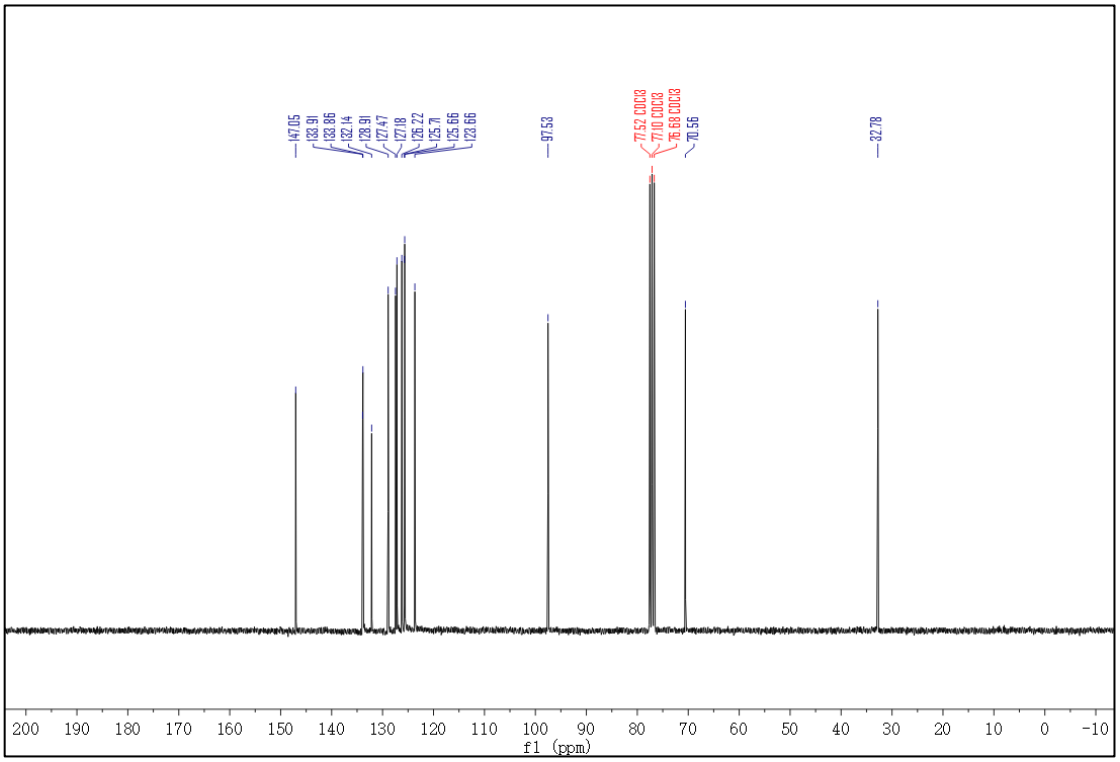

3,4-bis(pentyloxy)thiophene (60)

^{1}H NMR (300 MHz, $CDCl_3$) of **60**

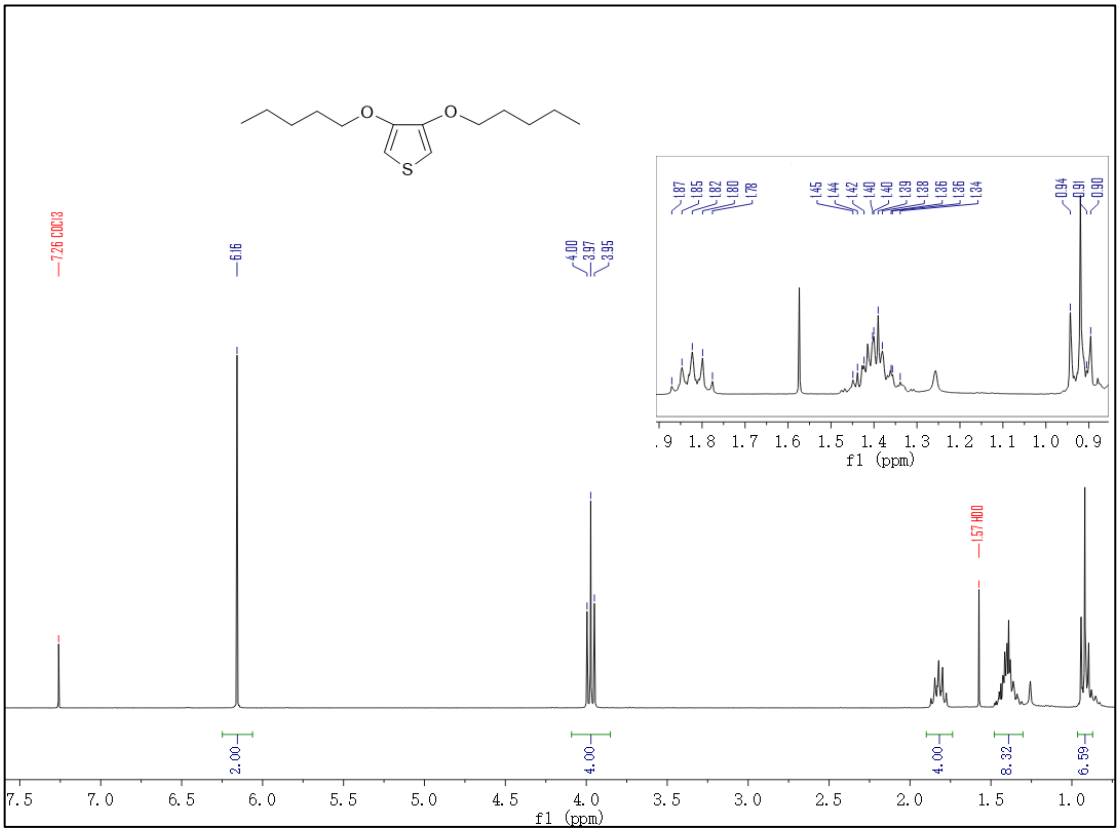

^{13}C NMR (75 MHz, $CDCl_3$) of **60**

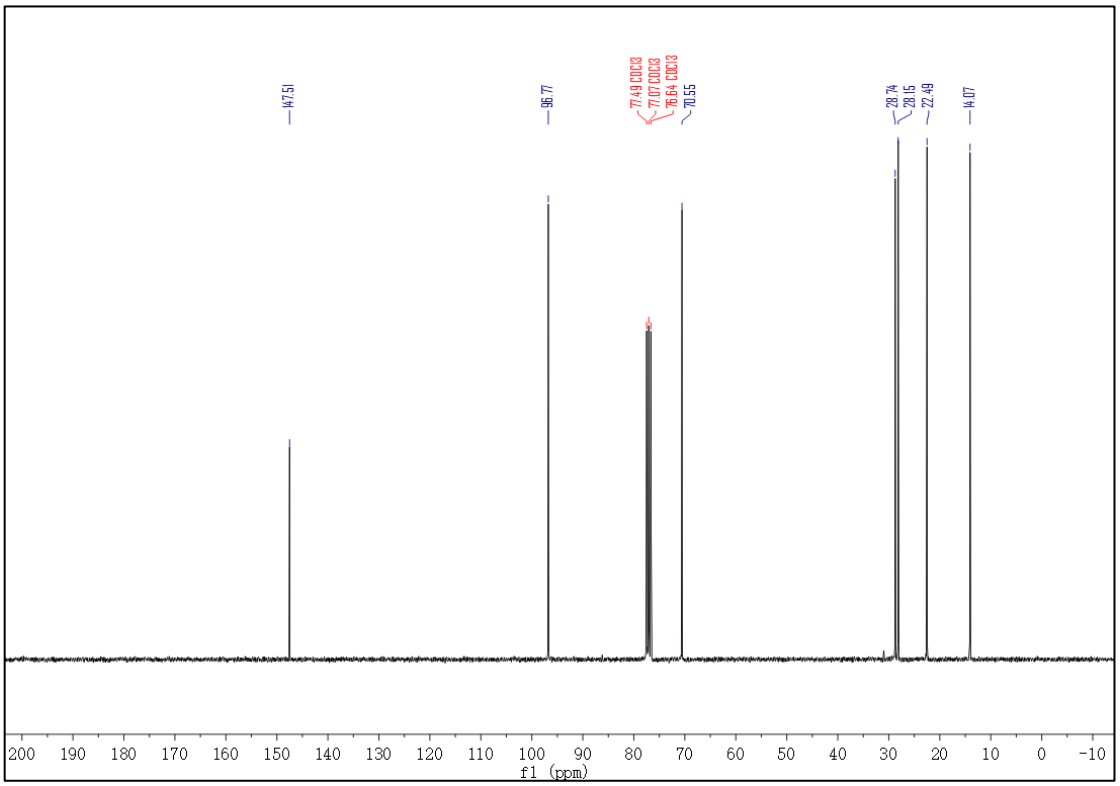

3,4-bis(isopentyloxy)thiophene (61)

^{1}H NMR (300 MHz, $CDCl_3$) of **61**

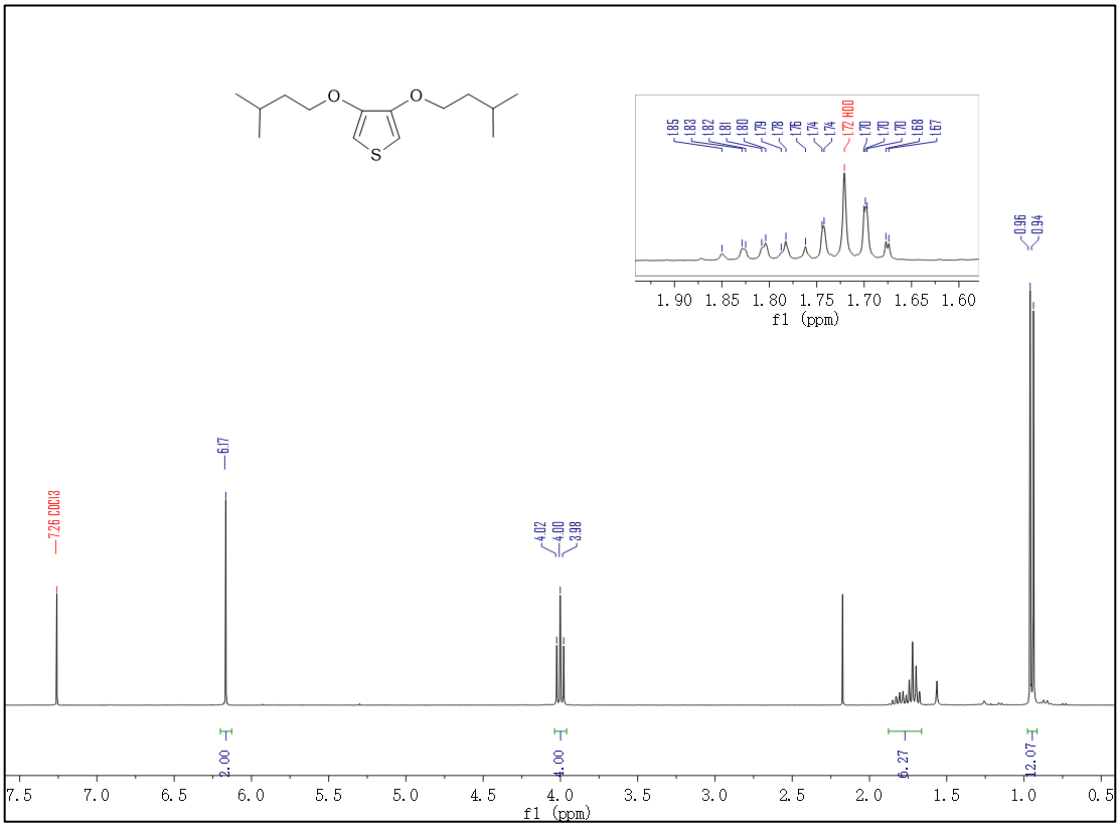

^{13}C NMR (75 MHz, $CDCl_3$) of **61**

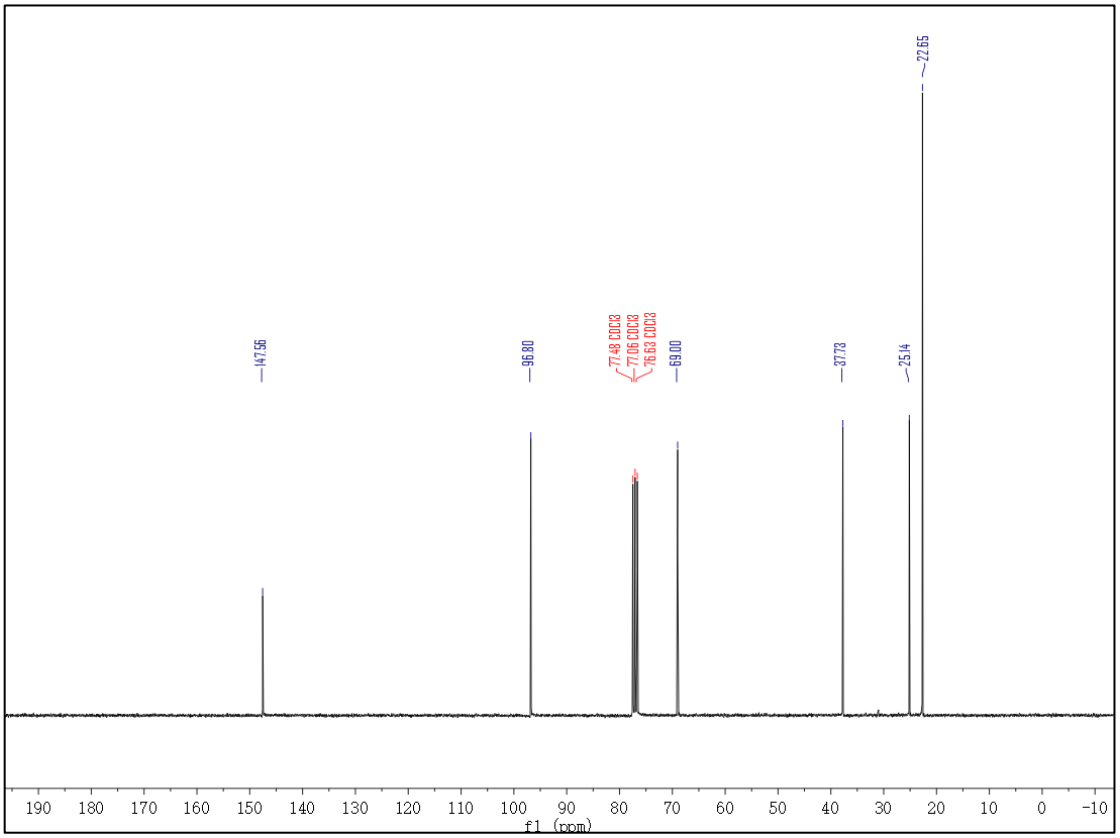

3,4-bis(2-methylbutoxy)thiophene (62)

^{1}H NMR (300 MHz, $CDCl_3$) of **62**

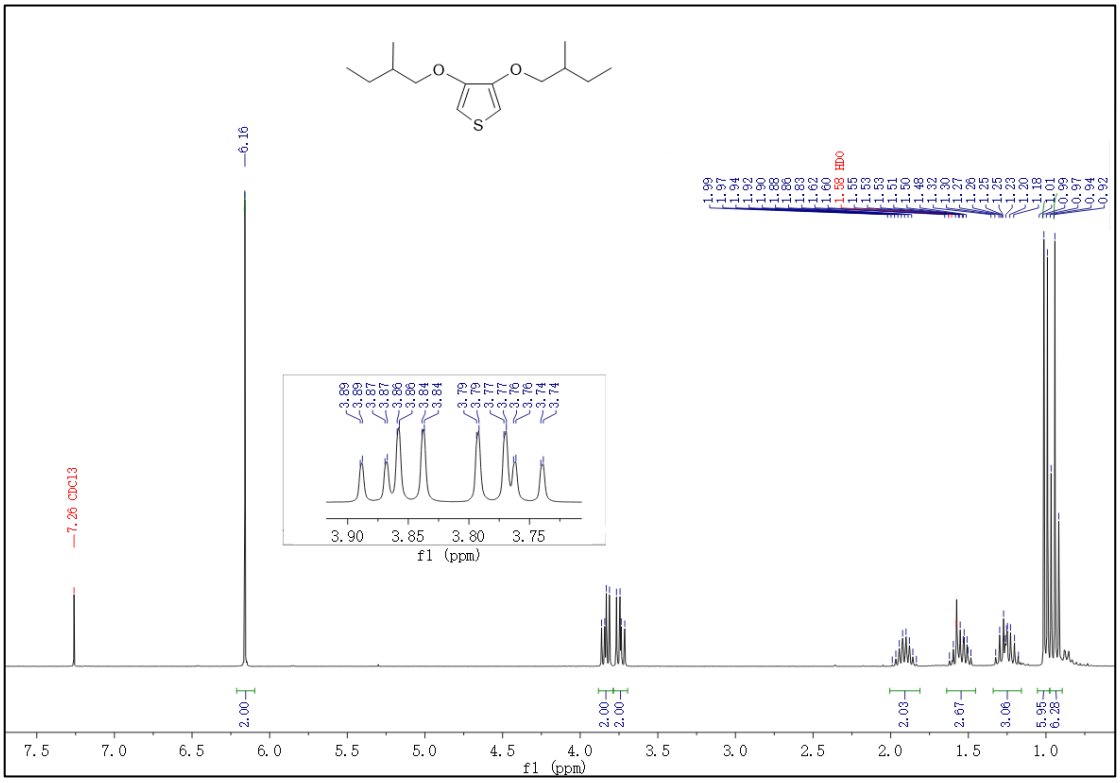

^{13}C NMR (75 MHz, $CDCl_3$) of **62**

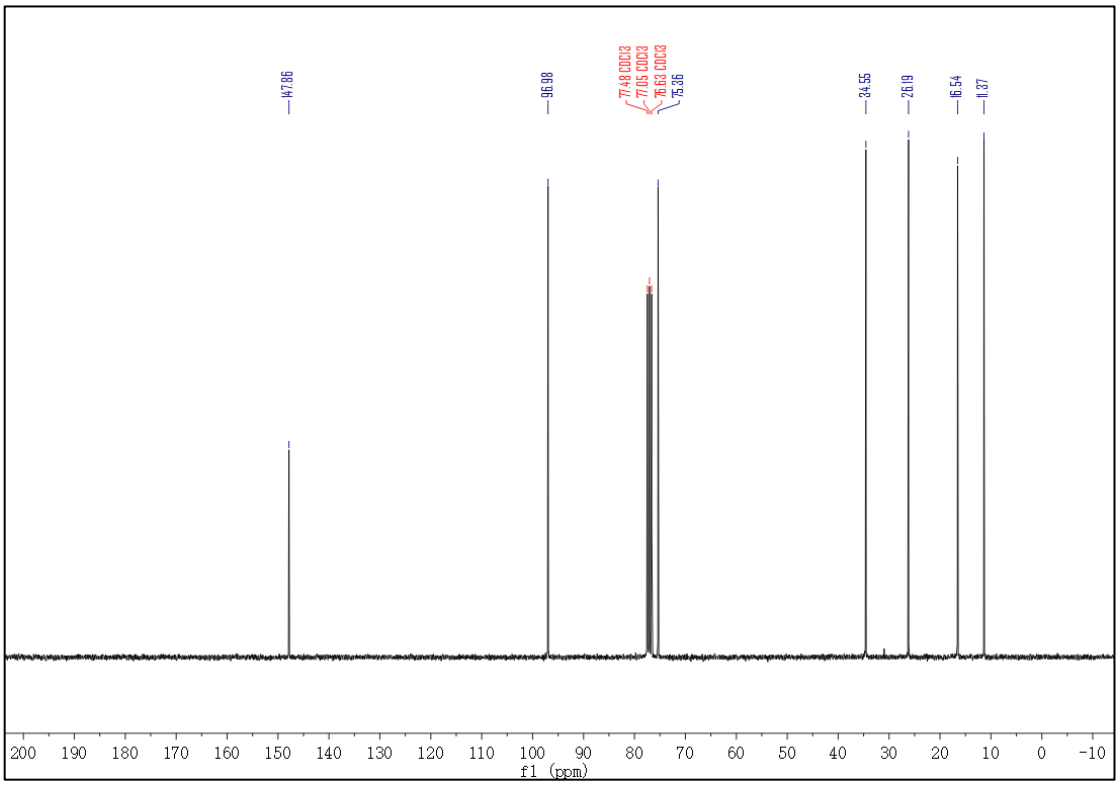

3,4-bis(pentan-2-yloxy)thiophene (63)

^{1}H NMR (300 MHz, $CDCl_3$) of **63**

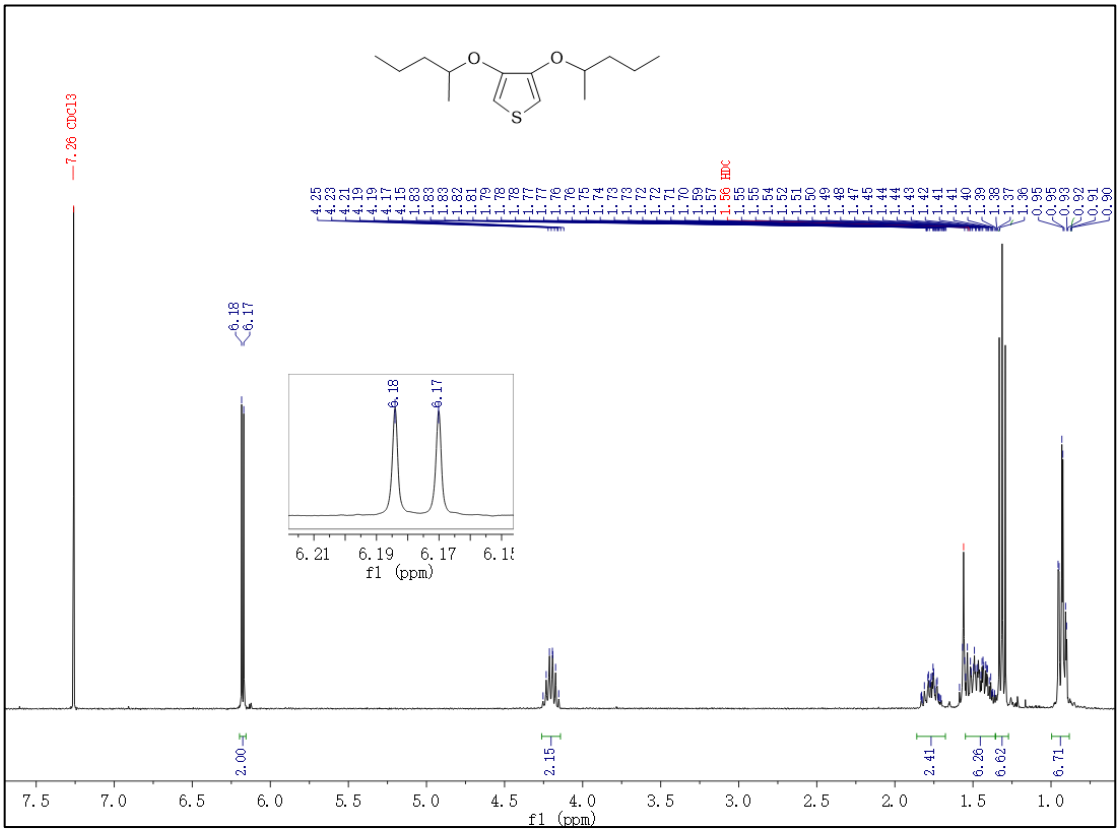

^{13}C NMR (75 MHz, $CDCl_3$) of **63**

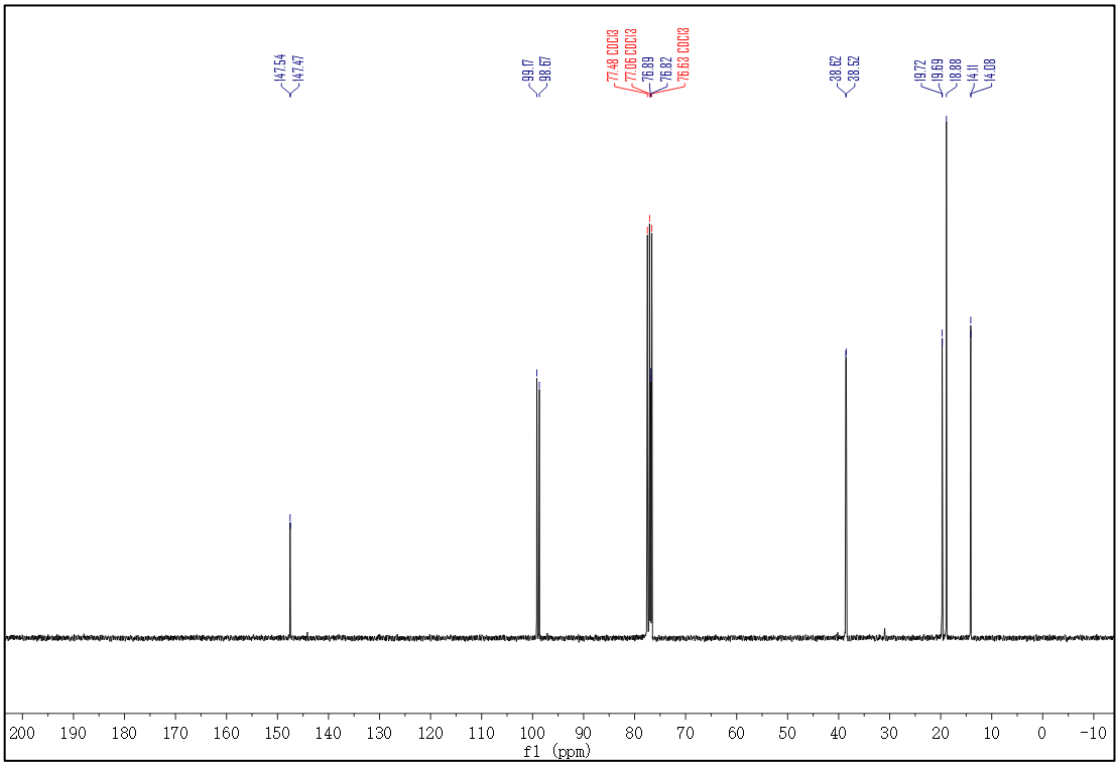

Homopolymer (64)

^{1}H NMR (300 MHz, $CDCl_3$) of **64**

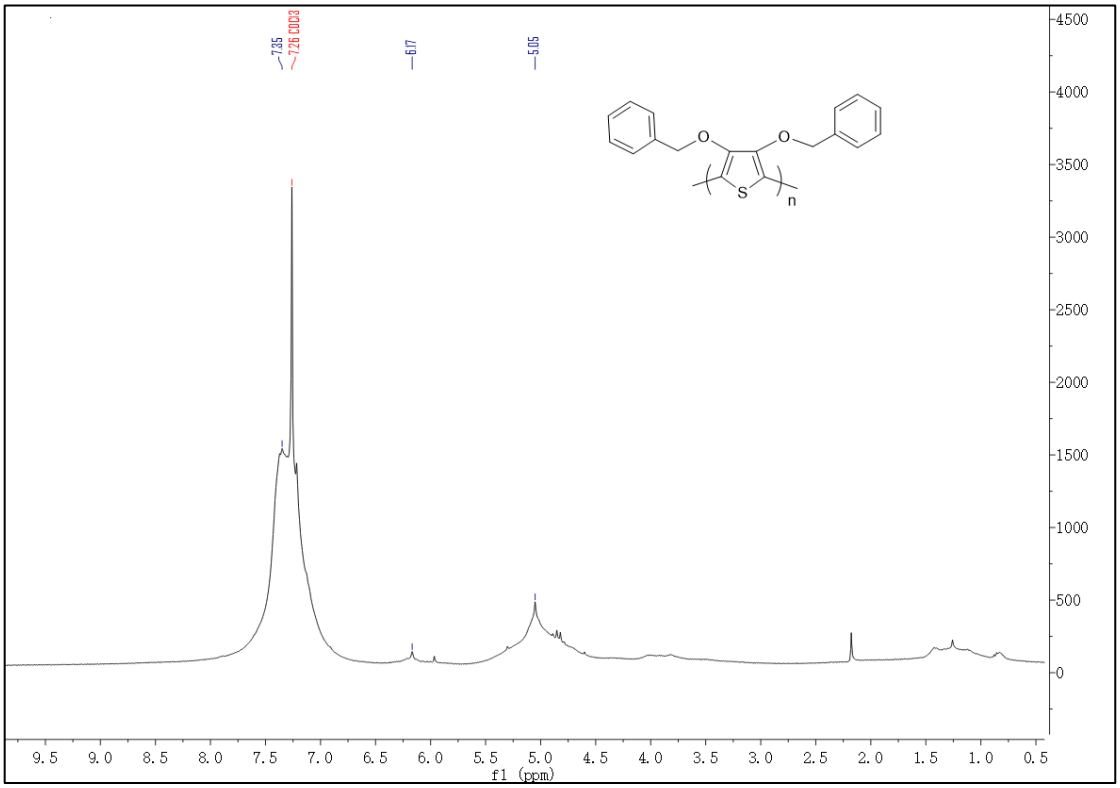

Homopolymer (65)

^{1}H NMR (300 MHz, $CDCl_3$) of **65**

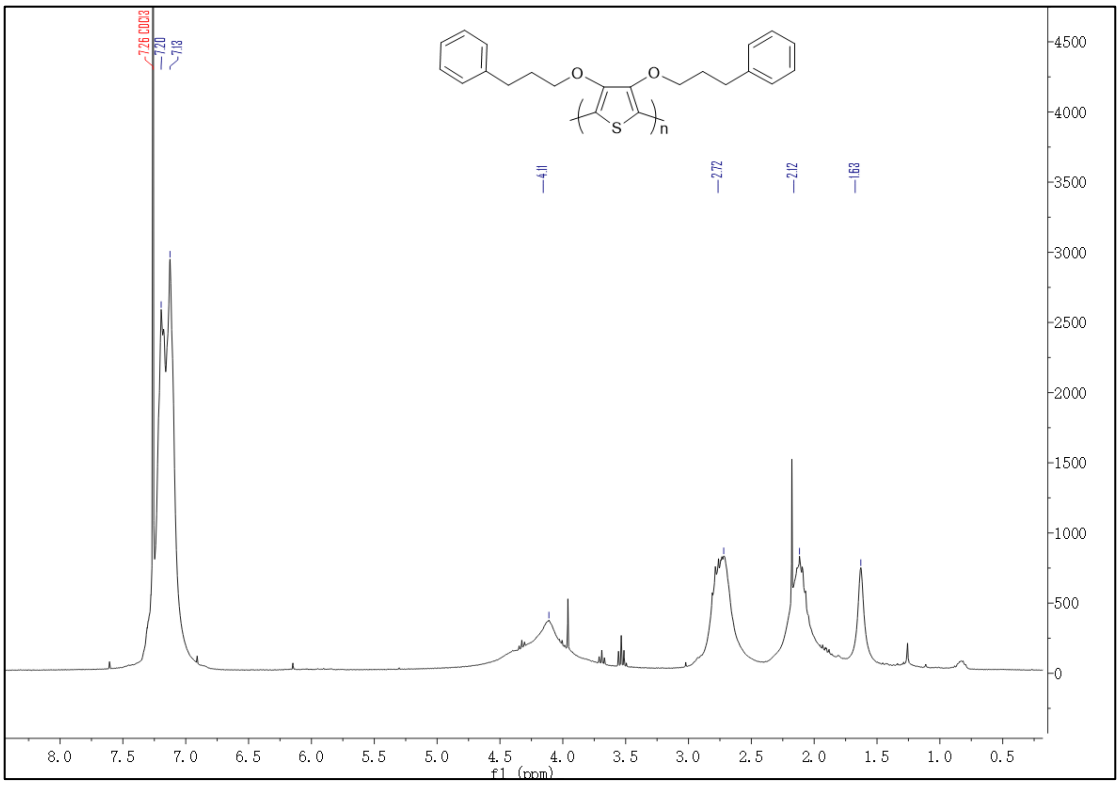

Homopolymer (66)

^{1}H NMR (300 MHz, $CDCl_3$) of **66**

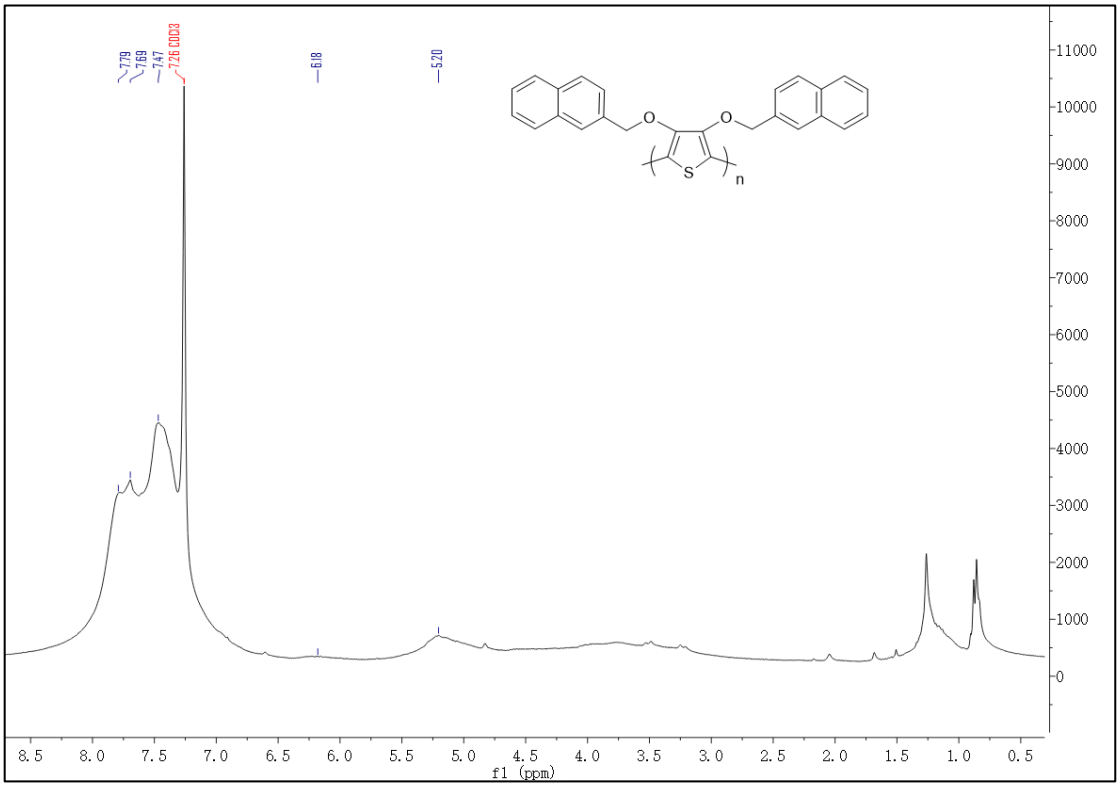

Homopolymer (67)

^{1}H NMR (300 MHz, $CDCl_3$) of **67**

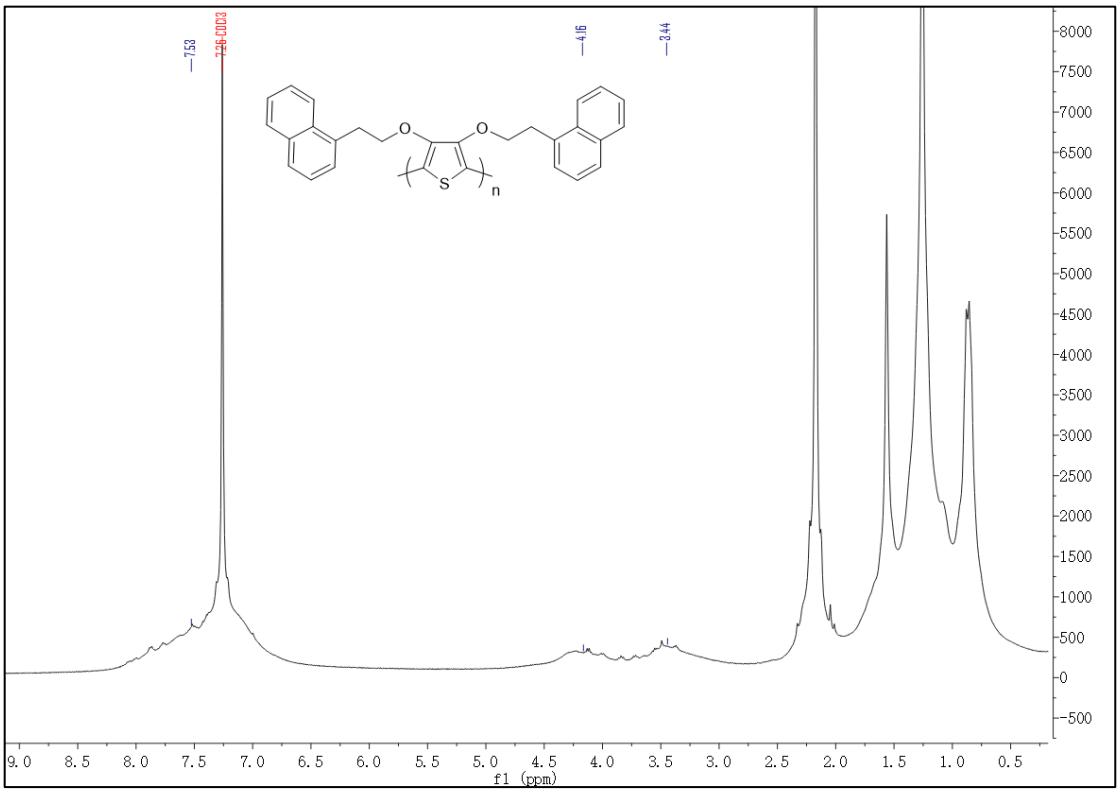

Copolymer (68)

^{1}H NMR (300 MHz, $CDCl_3$) of **68**

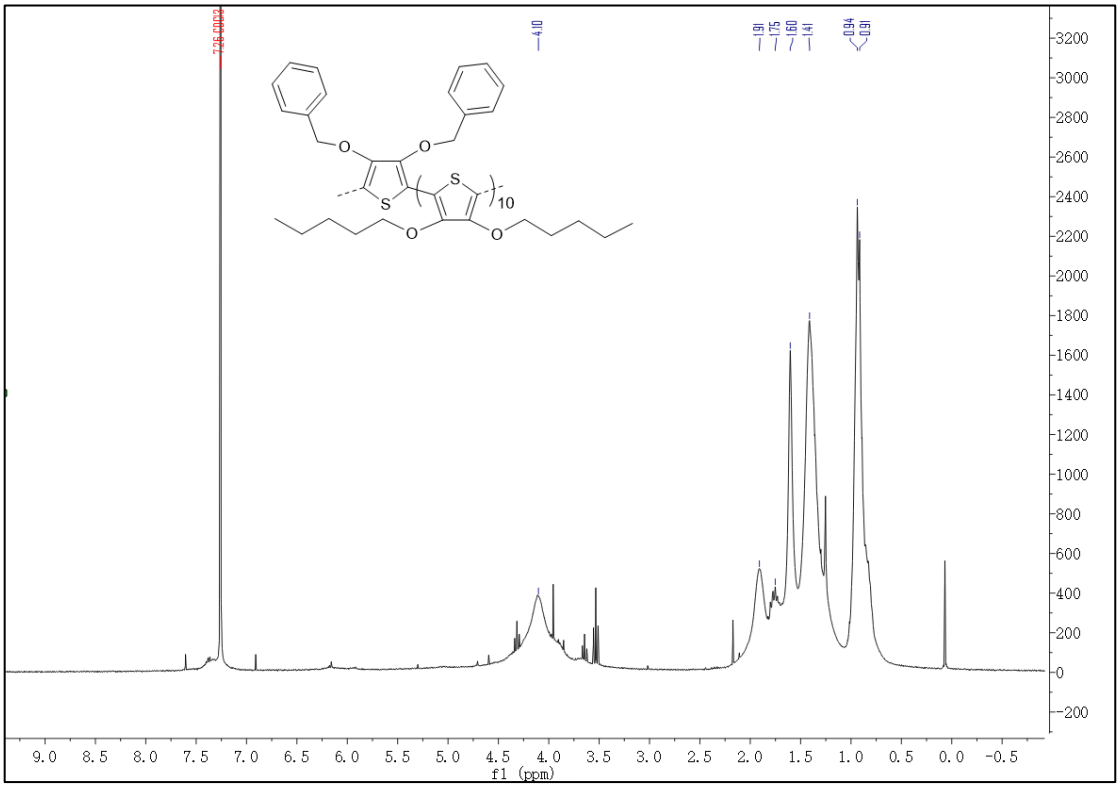

Copolymer (69)

^{1}H NMR (300 MHz, $CDCl_3$) of **69**

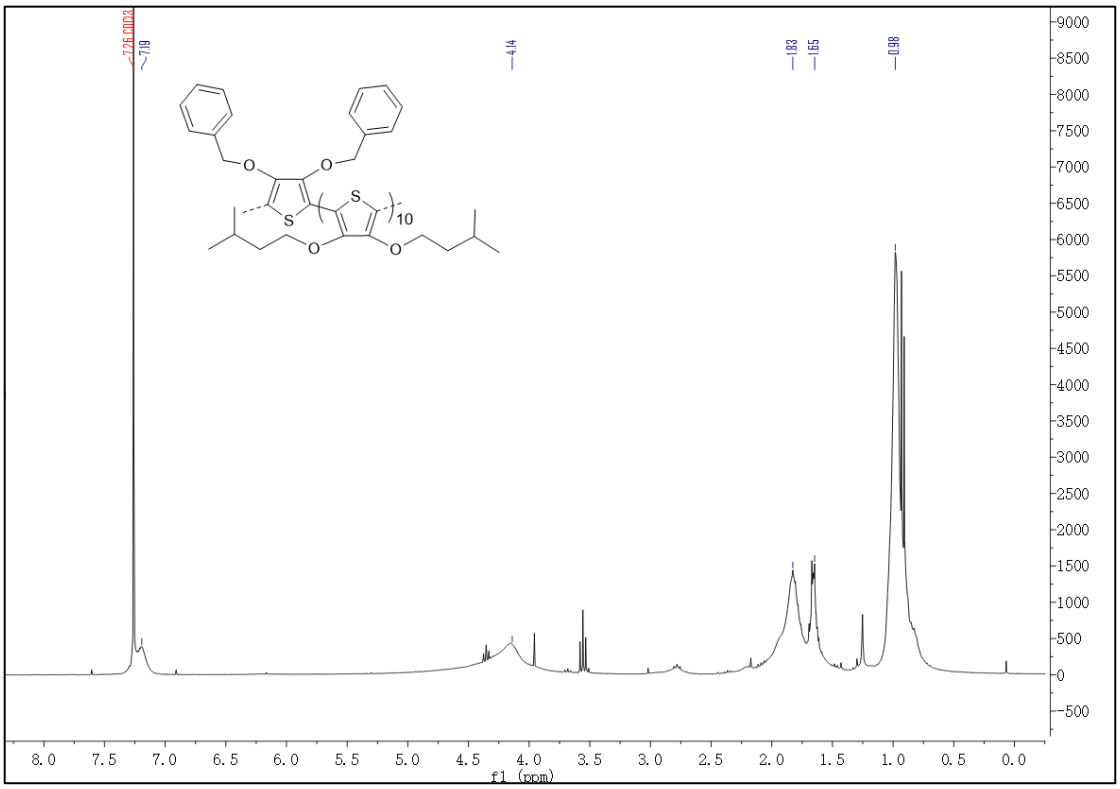

Copolymer (70)

^{1}H NMR (300 MHz, $CDCl_3$) of **70**

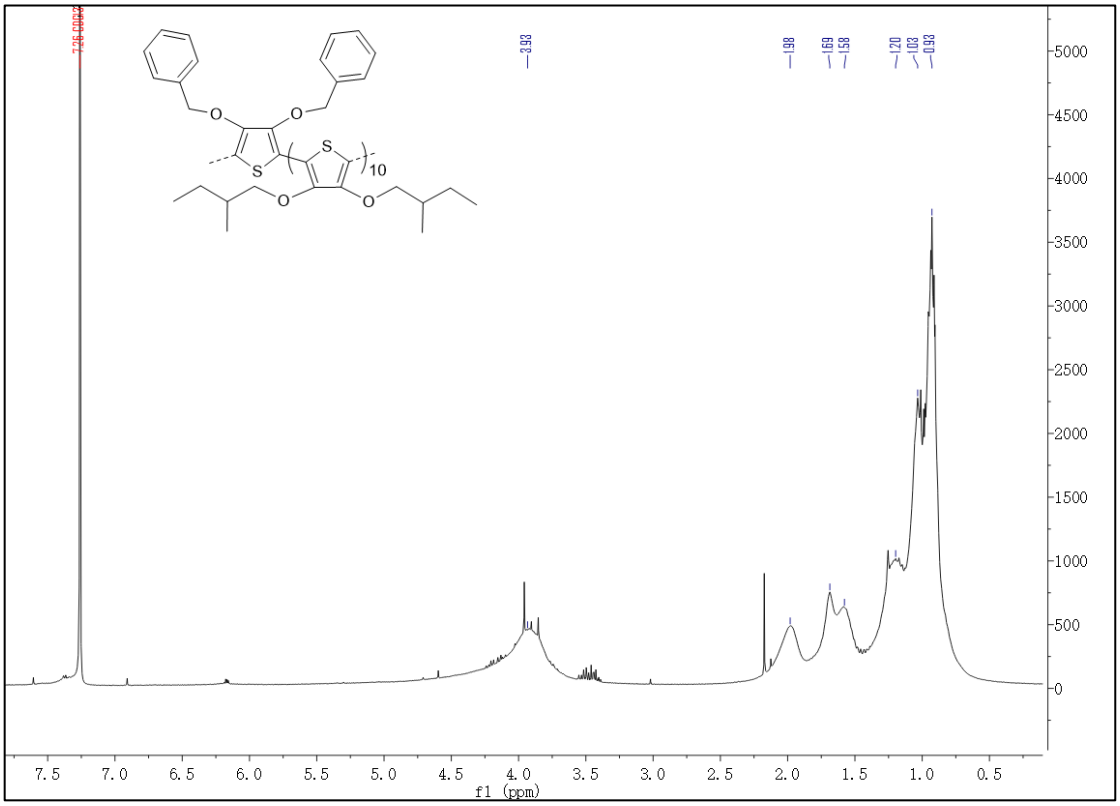

Copolymer (71)

^{1}H NMR (300 MHz, $CDCl_3$) of **71**

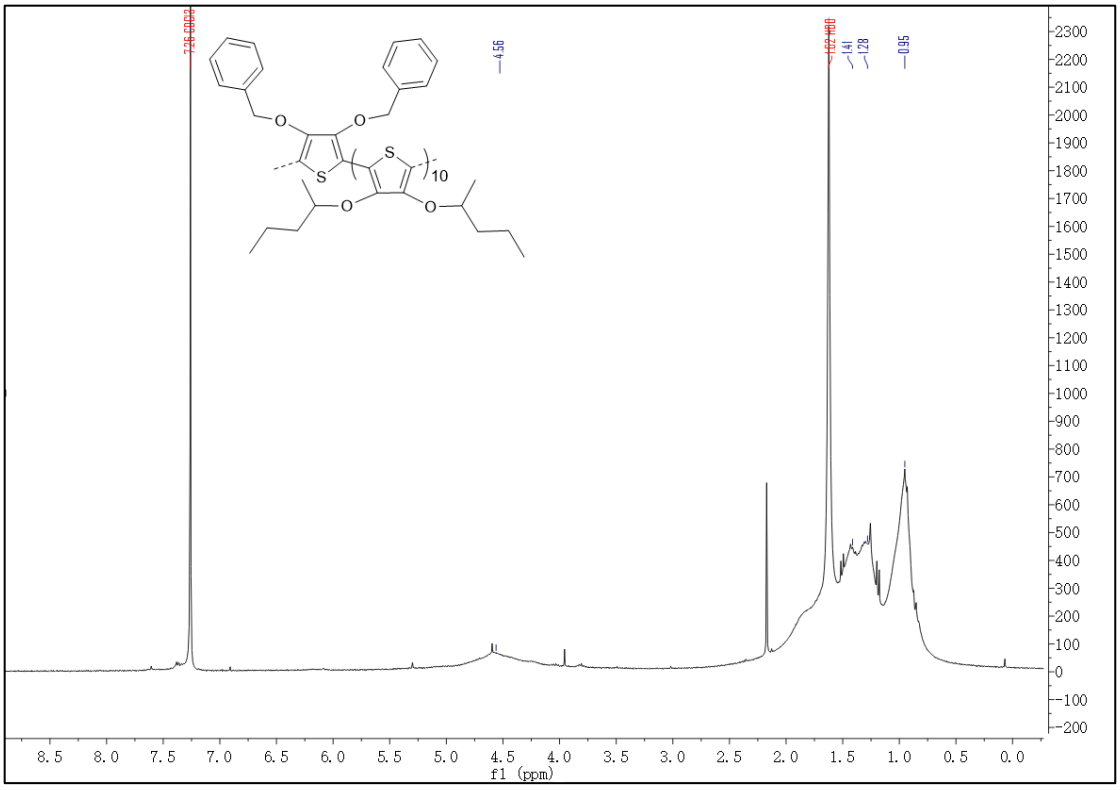

Copolymer (72)

^{1}H NMR (300 MHz, $CDCl_3$) of **72**

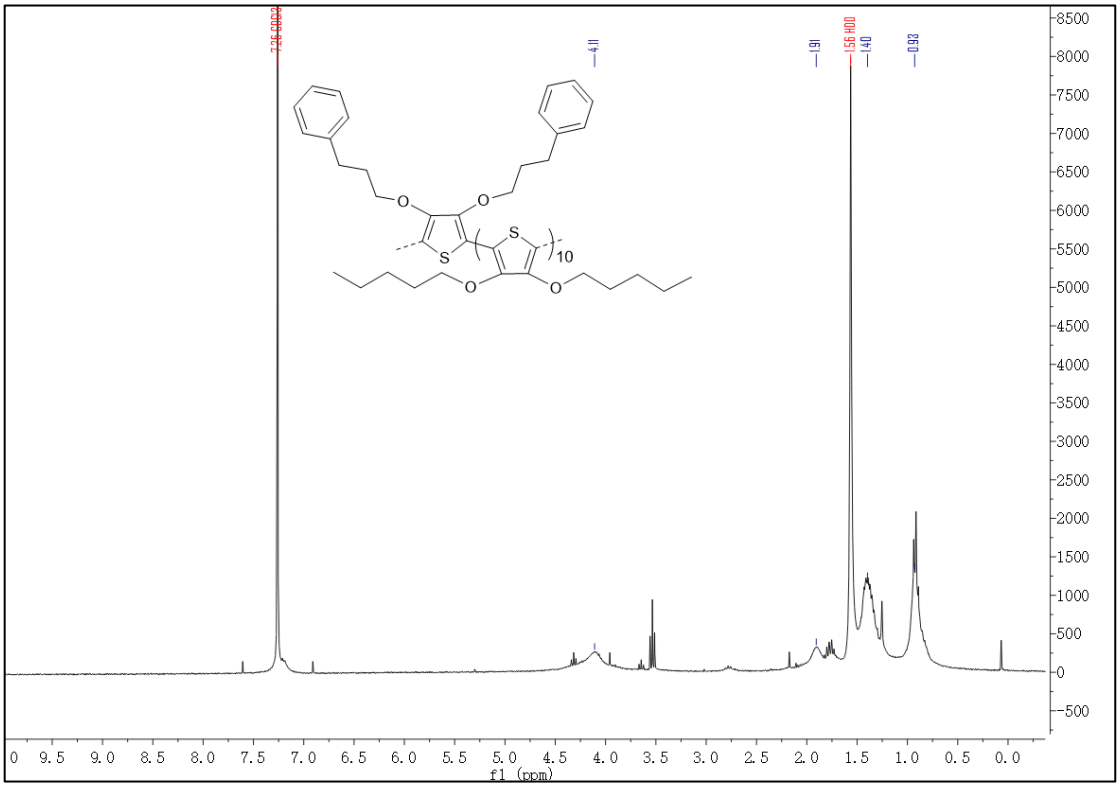

Copolymer (73)

^{1}H NMR (300 MHz, $CDCl_3$) of **73**

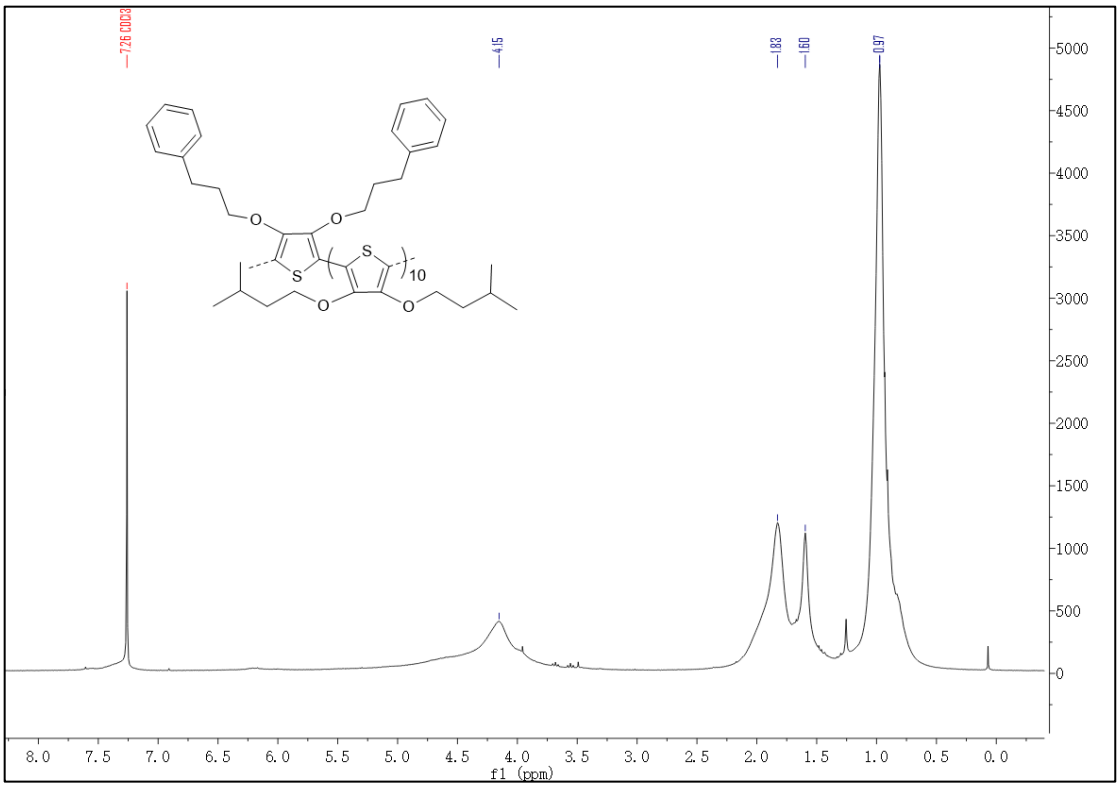

Copolymer (74)

^{1}H NMR (300 MHz, $CDCl_3$) of **74**

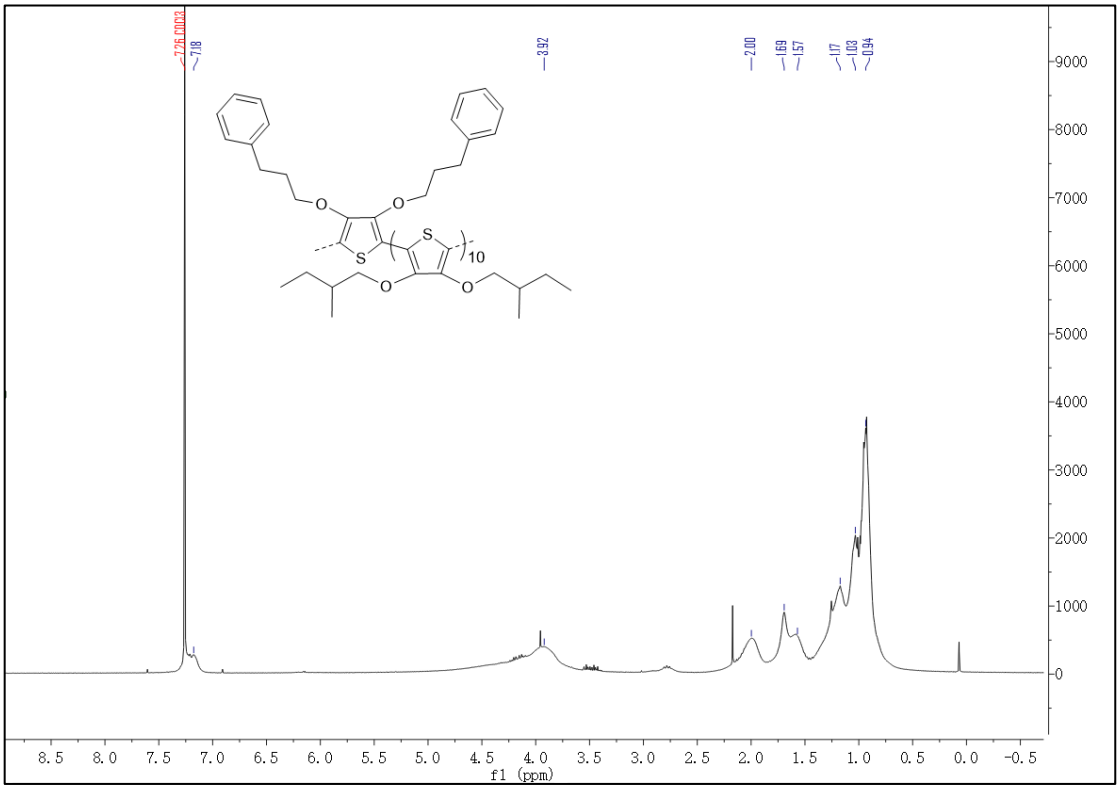

Copolymer (75)

^{1}H NMR (300 MHz, $CDCl_3$) of **75**

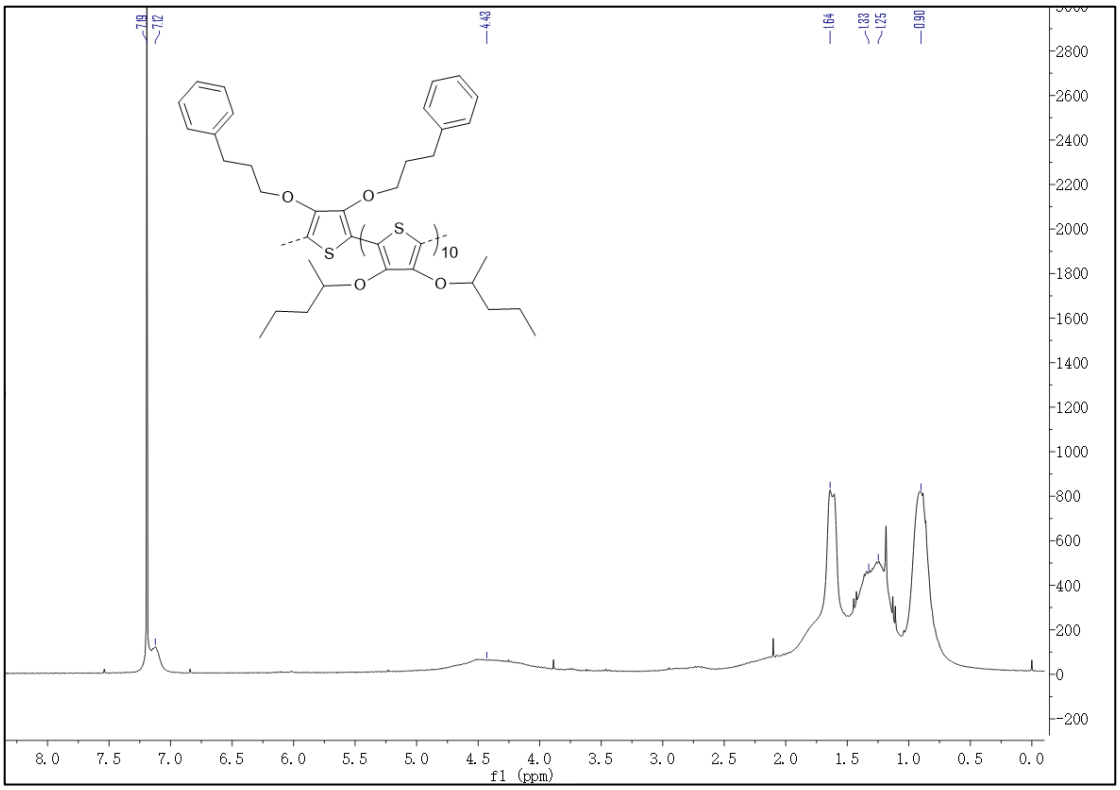

Copolymer (76)

^{1}H NMR (300 MHz, $CDCl_3$) of **76**

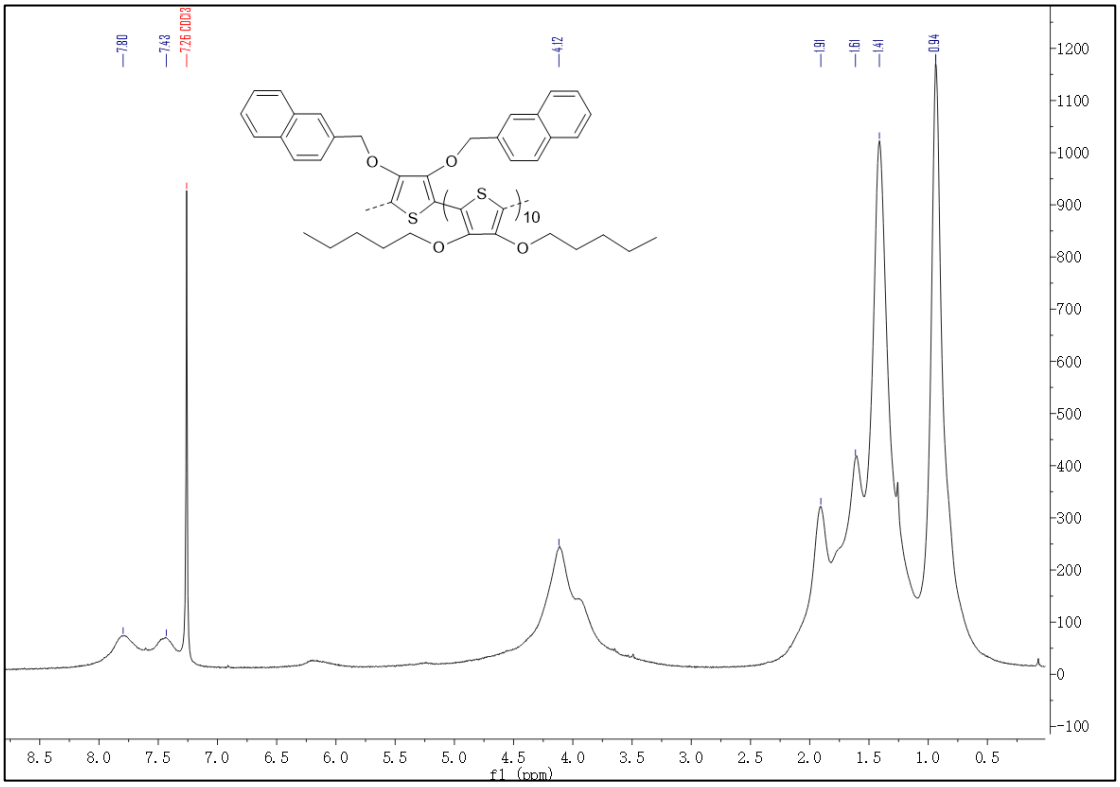

Copolymer (77)

^{1}H NMR (300 MHz, $CDCl_3$) of **77**

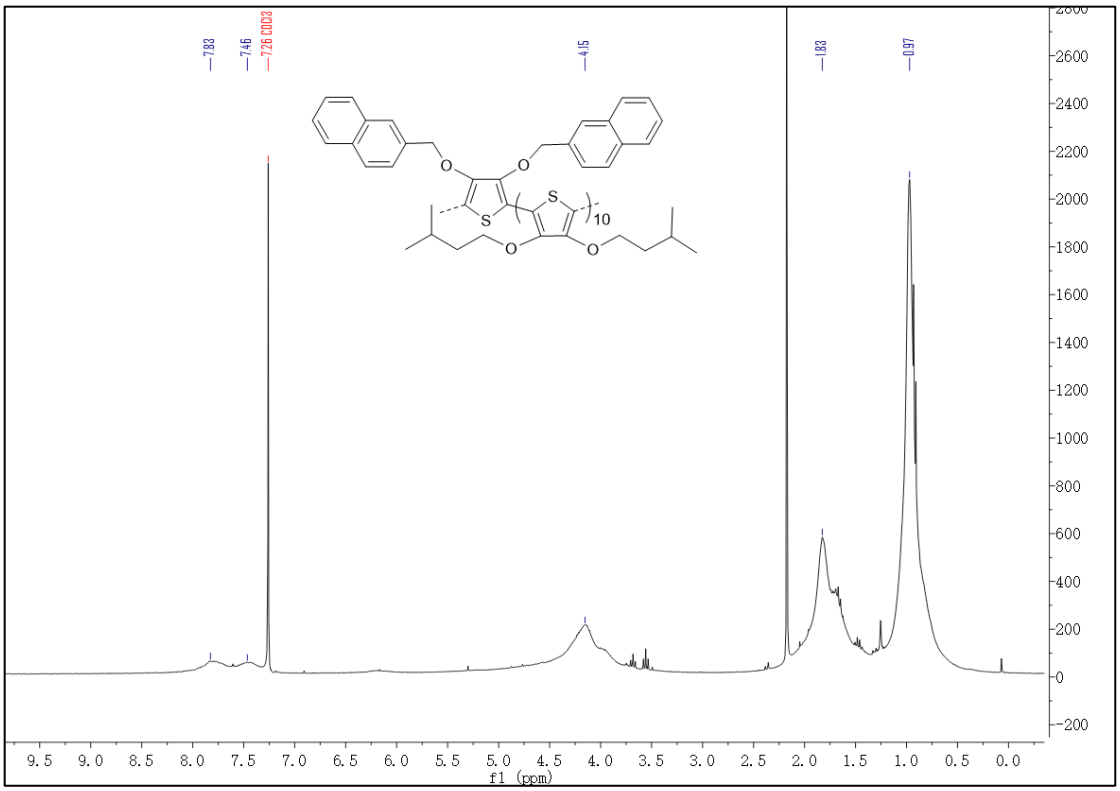

Copolymer (78)

^{1}H NMR (300 MHz, $CDCl_3$) of **78**

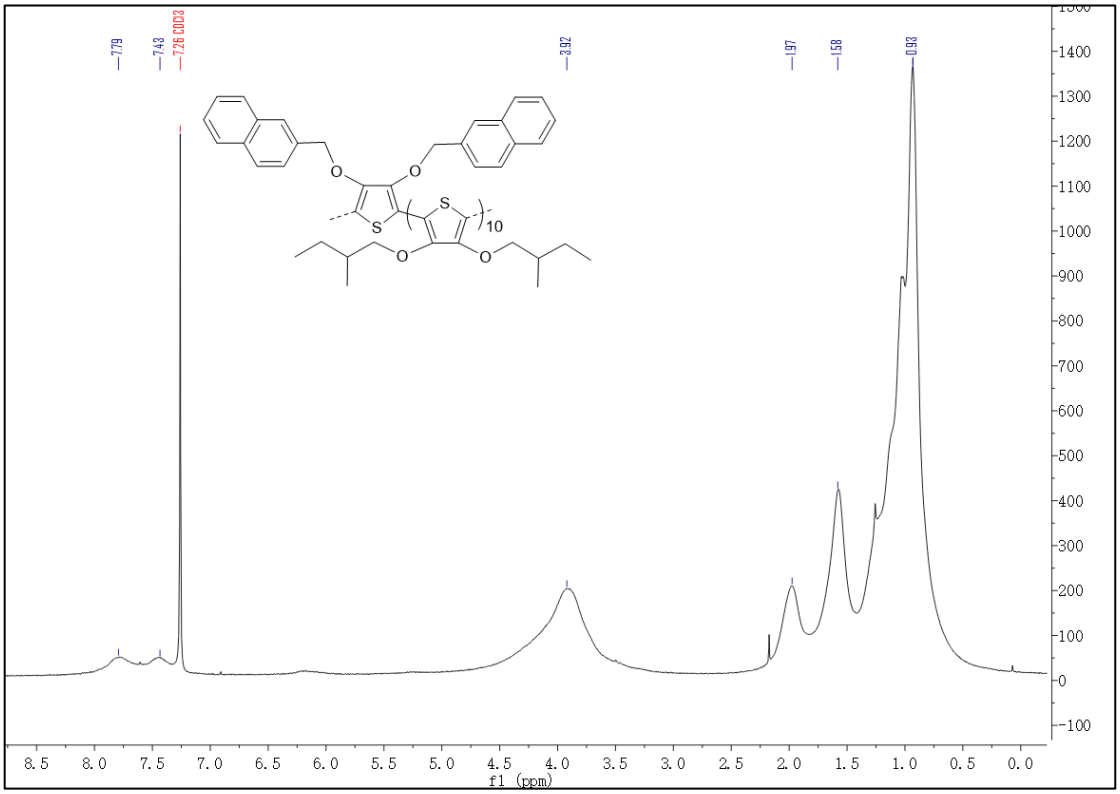

Copolymer (79)

^{1}H NMR (300 MHz, $CDCl_3$) of **79**

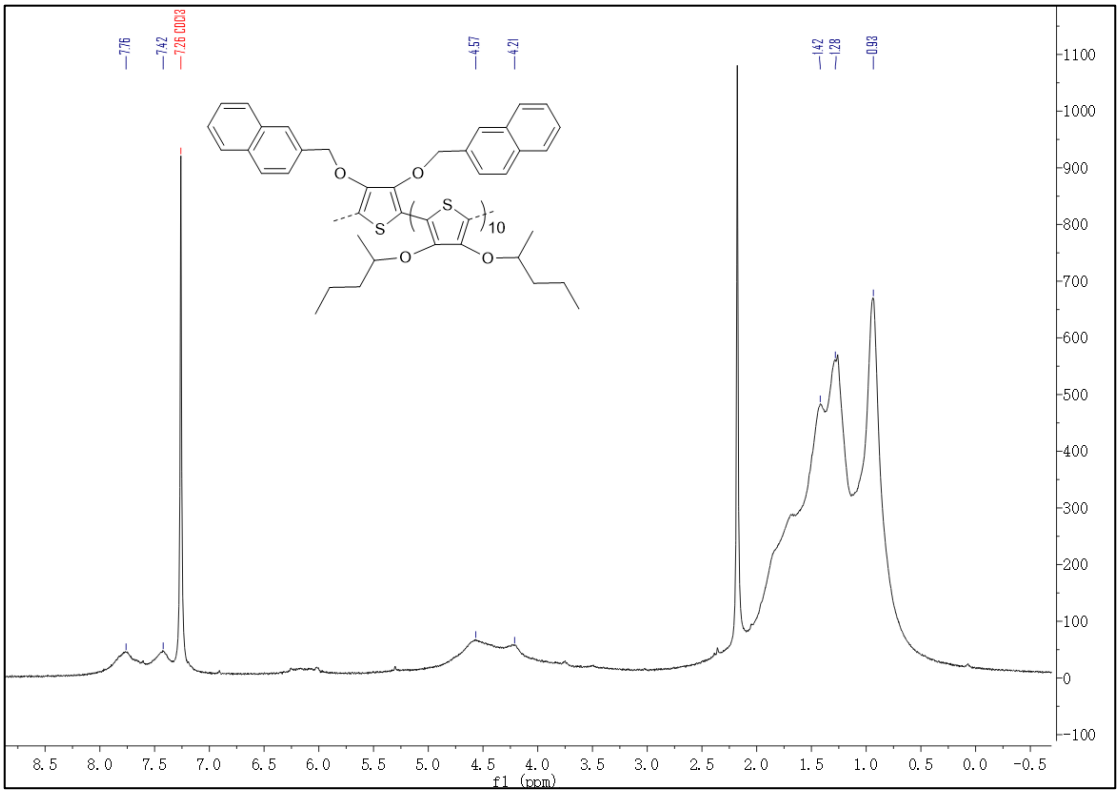

Copolymer (80)

^{1}H NMR (300 MHz, $CDCl_3$) of **80**

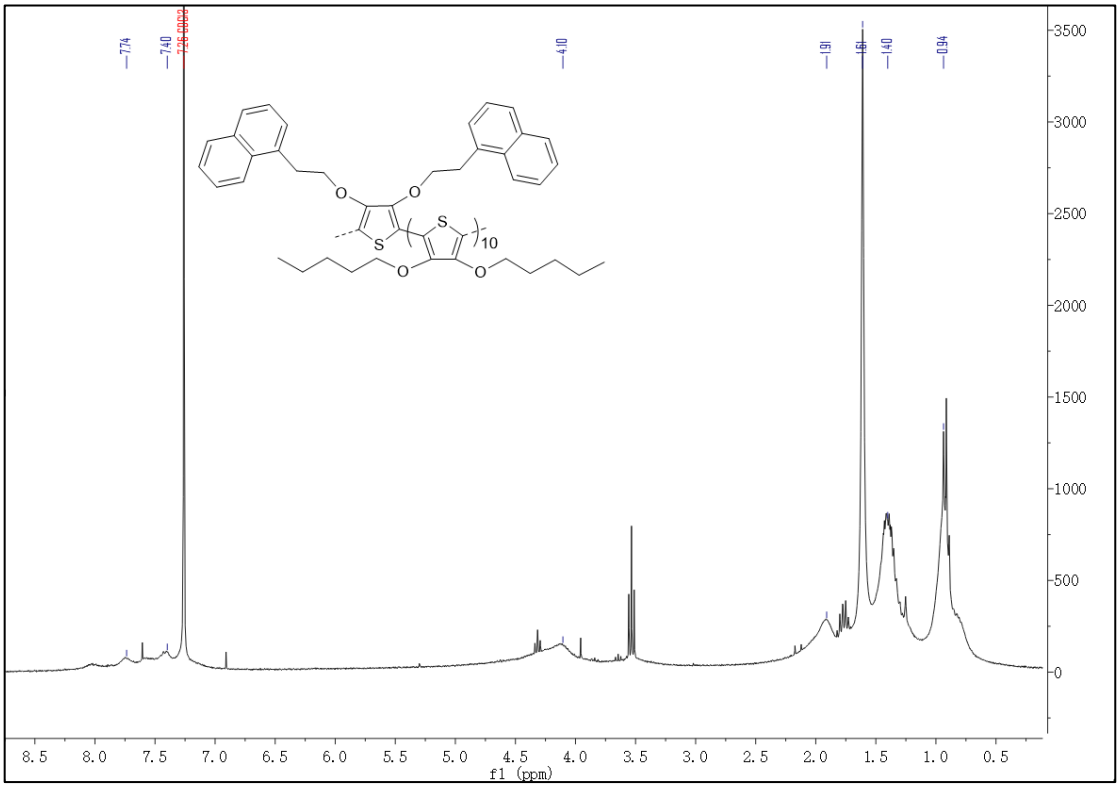

Copolymer (81)

^{1}H NMR (300 MHz, $CDCl_3$) of **81**

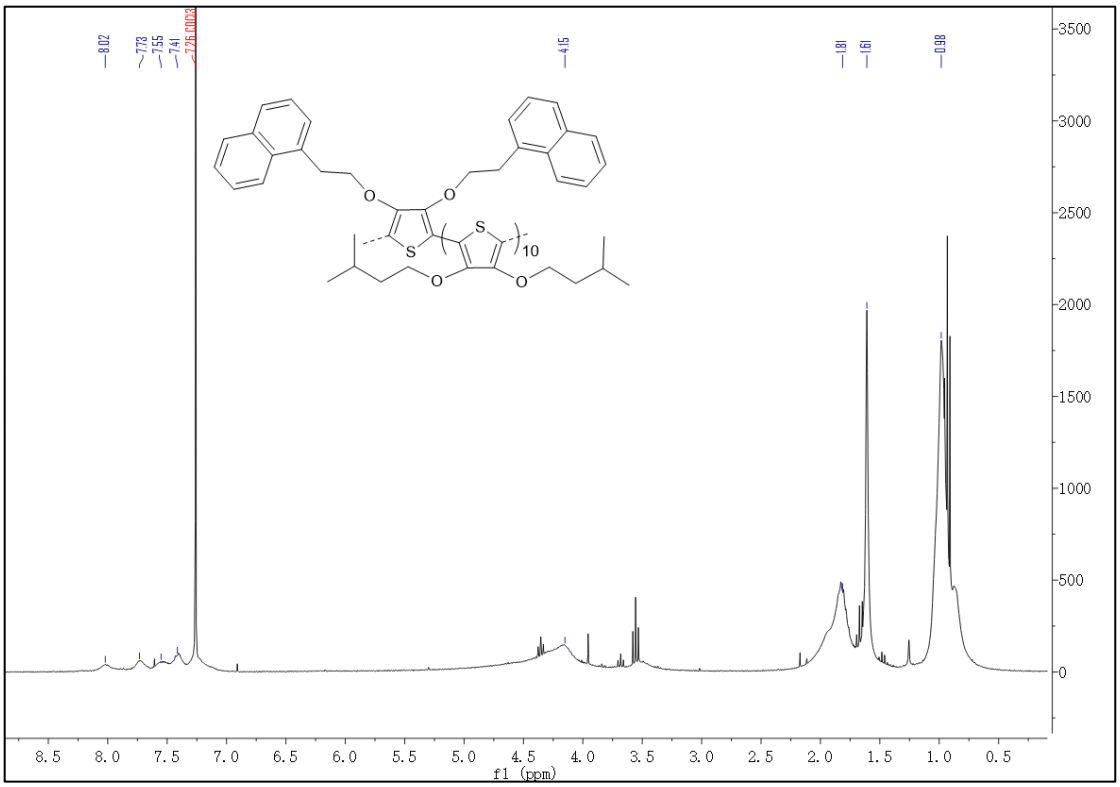

Copolymer (82)

^{1}H NMR (300 MHz, $CDCl_3$) of **82**

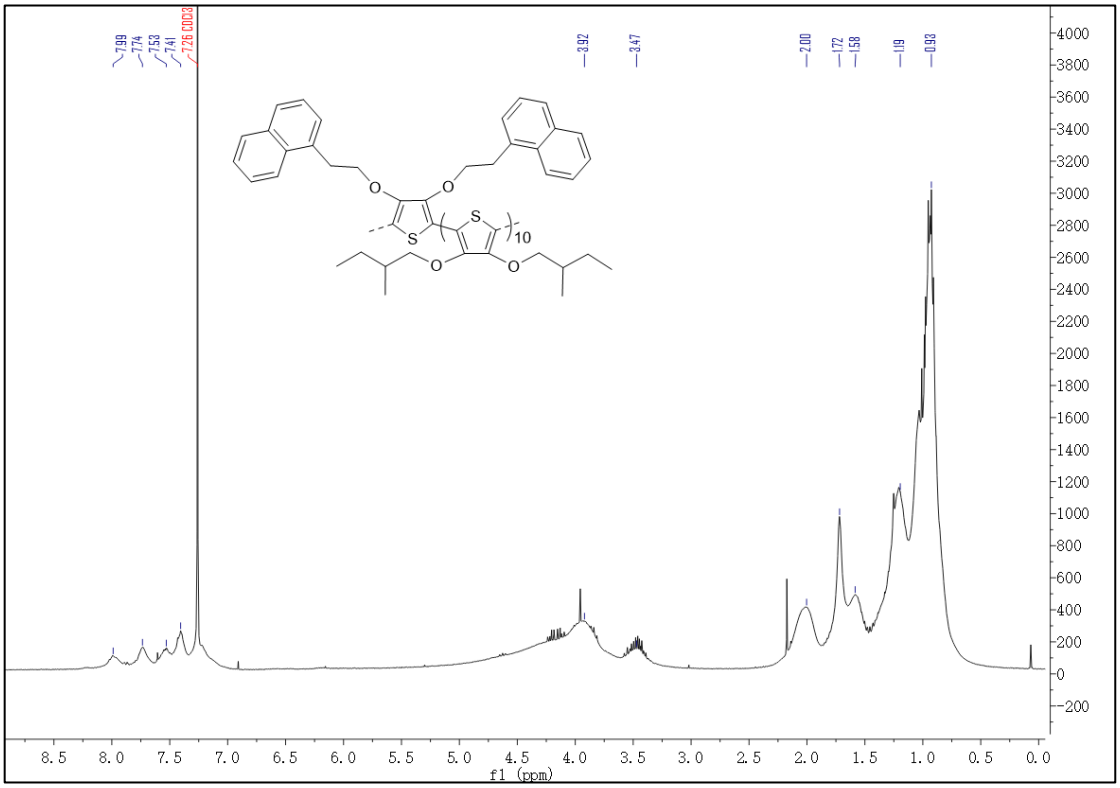

Reference

1 Z. Tong, S. Liu, X. Li, J. Zhao, Y. Li, *Nanoscale Horiz*, **2018**, *3*, 261-292.

2 C. G. Granqvist, M. A. Arvizu, İ. Bayrak Pehlivan, H. Y. Qu, R. T. Wen, G. A. Niklasson, *Electrochim. Acta*, **2018**, *259*, 1170-1182.

3 G. Kaur, R. Adhikari, P. Cass, M. Bown, P. Gunatillake, *RSC Adv*., **2015**, *5*, 37553-37567.

4 X. Li, K. Perera, J. He, A. Gumyusenge, J. Mei, *J. Mater. Chem. C*, **2019**, *7*, 12761-12789.

5 S. K. Deb, *Appl. Opt*, **1969**, *8*, 192-195.

6 A. Malti, R. Brooke, X. Liu, D. Zhao, P. Andersson Ersman, M. Fahlman, M. P. Jonsson, M. Berggren, X. Crispin, *Journal of Materials Chemistry C* **2016**, *4*, 9680-9686.

7 M. D. F. Albuquerque, E. Santos, R. R. T. Perdone, R. A. Simao, *Thin Solid Films* **2014**, *564*, 73-78.

8 E. Turac, E. Sahmetlioglu, L. Toppare, H. Yuruk, *Des Monomers Polym,* **2010**, *13*, 261-275.

9 Ynvisible - things alive, https://www.ynvisible.com/products/segment-display, (accessed 15 April 2020).

10 W. T. Neo, Q. Ye, S.-J. Chua, J. Xu, *J. Mater. Chem. C*, **2016**, *4*, 7364-7376.

11 P. M. Beaujuge, J. R. Reynolds, *Chem. Rev.*, **2010**, *110*, 268-320.

12 J. A. Kerszulis, R. H. Bulloch, N. B. Teran, R. M. W. Wolfe, J. R. Reynolds, *Macromolecules* **2016**, *49*, 6350-6359.

13 Y. Huang, E.-L. Hsiang, M.-Y. Deng, S.-T. Wu, *Light Sci. Appl*., **2020**, *9*, 105.

14 R. S. Berns, D. M. Reiman, **2002**, *27*, 360-373.

15 W. K. Backhaus, R.; Werner, J. S., in *Book Color Vision: Perspectives from Different Disciplines*, **1998**.

16 A. Valberg, *Light Vision Color*. Editor, **2005**.

17 in *Book color grab(color detection)*.

18 in *Book Tricky Squares: Can you spot the different color?*

19 Q. Zhang, C.-Y. Tsai, L.-J. Li, D.-J. Liaw, *Nat. Commun*., **2019**, *10*, 1239.

20 J. Jensen, M. Hösel, A. L. Dyer, F. C. Krebs, *Adv. Funct. Mater*., **2015**, *25*, 2073-2090.

21 I. Schwendeman, C. L. Gaupp, J. M. Hancock, L. Groenendaal, J. R. Reynolds, **2003**, *13*, 541-547.

22 Y. Chen, Z. Bi, X. Li, X. Xu, S. Zhang, X. Hu, *Electrochim. Acta*., **2017**, *224*, 534-540.

23 P. Camurlu, *RSC Adv*., **2014**, *4*, 55832-55845.

24 K. Iqbal, degree of Master. **2010**.

25 L. D. Burke, E. J. M. O'Sullivan, *J. Electroanal. Chem. Interf. Electrochem*., **1978**, *93*, 11-18.

26 L. D. Burke, D. P. Whelan, *J. Electroanal. Chem. Interf. Electrochem*., **1979**, *103*, 179-187.

27 L. D. Burke, O. J. Murphy, *J. Electroanal. Chem. Interf. Electrochem*., **1980**, *112*, 39-50.

28 V. K. Thakur, G. Ding, J. Ma, P. S. Lee, X. Lu, *Adv. Mater*., **2012**, *24*, 4071-4096.

29 A. Kumar, D. M. Welsh, M. C. Morvant, F. Piroux, K. A. Abboud, J. R. Reynolds, *Chem. Mater*., **1998**, *10*, 896-902.

30 S. A. Sapp, G. A. Sotzing, J. R. Reynolds, *Chem. Mater*., **1998**, *10*, 2101-2108.

31 J. Roncali, *Chem. Rev.*, **1997**, *97*, 173-206.

32 P. K. H. Ho, D. Stephen, Thomas, R. H. Friend, N. Tessler, *Science* **1999**, *285*, 233.
33 G. J. Stec, A. Lauchner, Y. Cui, P. Nordlander, N. J. Halas, *ACS Nano*, **2017**, *11*, 3254-3261.
34 G. A. Corrente, E. Fabiano, F. Manni, G. Chidichimo, G. Gigli, A. Beneduci, A.-L. Capodilupo, *Chem. Mater*., **2018**, *30*, 5610-5620.
35 T. P. Kaloni, G. Schreckenbach, M. S. Freund, *Sci. Rep*., **2016**, *6*, 36554.
36 A. Çirpan, S. y. Alkan, L. Toppare, Y. m. Hepuzer, Y. Yağci, **2002**, *40*, 4131-4140.
37 T. Johansson, W. Mammo, M. Svensson, M. R. Andersson, O. Inganäs, *J. Mater. Chem*., **2003**, *13*, 1316-1323.
38 R. Ansari, *E-J Chem*, **2006**, *3*, 860413.
39 A. F. Diaz, K. K. Kanazawa, G. P. Gardini, *Chem. Commun*., **1979**, 635-636.
40 A. F. Diaz, J. I. Castillo, J. A. Logan, W.-Y. Lee, *J. Electroanal. Chem. Interf. Electrochem*., **1981**, *129*, 115-132.
41 J. R. Reynolds, P. A. Poropatic, R. L. Toyooka, *Synth. Met*., **1987**, *18*, 95-100.
42 J. R. Reynolds, P. A. Poropatic, R. L. Toyooka, *Macromolecules* **1987**, *20*, 958-961.
43 P. Bujak, I. Kulszewicz-Bajer, M. Zagorska, V. Maurel, I. Wielgus, A. Pron, *Chem. Soc. Rev*., **2013**, *42*, 8895-8999.
44 C. Gatti, G. Frigerio, T. Benincori, E. Brenna, F. Sannicolò, G. Zotti, S. Zecchin, G. Schiavon, *Chem. Mater*., **2000**, *12*, 1490-1499.
45 A. Cihaner, *J. Macromol. Sci*., **2006**, *43*, 1379-1386.
46 A. Cihaner, *J. Electroanal. Chem*., **2007**, *605*, 8-14.
47 M. Ak, M. S. Ak, L. Toppare, **2006**, *207*, 1351-1358.
48 F. Garnier, G. Tourillon, M. Gazard, J. C. Dubois, *J. Electroanal. Chem. Interf. Electrochem*., **1983**, *148*, 299-303.
49 M. Gazard, J. Dubois, C., M. Champagne, F. Garnier, G. J. J. P. C. Tourillon, **1983**, *44*, C3-537-C3-542.
50 G. Sonmez, C. K. F. Shen, Y. Rubin, F. Wudl, **2004**, *43*, 1498-1502.
51 G. Heywang, F. Jonas, **1992**, *4*, 116-118.
52 M. Mastragostino, C. Arbizzani, A. Bongini, G. Barbarella, M. Zambianchi, *Electrochim. Acta*, **1993**, *38*, 135-140.
53 C. Arbizzani, A. Bongini, M. Mastragostino, A. Zanelli, G. Barbarella, M. Zambianchi, **1995**, *7*, 571-574.
54 R. L. Elsenbaumer, K. Y. Jen, G. G. Miller, L. W. Shacklette, *Synth. Met*., **1987**, *18*, 277-282.
55 I. Osaka, R. D. McCullough, *Acc. Chem. Res*., **2008**, *41*, 1202-1214.
56 J. C. Gustafsson-Carlberg, O. Inganäs, M. R. Andersson, C. Booth, A. Azens, C. G. Granqvist, *Electrochim. Acta*, **1995**, *40*, 2233-2235.
57 D. M. Welsh, A. Kumar, M. C. Morvant, J. R. Reynolds, *Synth. Met*., **1999**, *102*, 967-968.
58 A. Kumar, J. R. Reynolds, *Macromolecules* **1996**, *29*, 7629-7630.
59 G. Sonmez, H. B. Sonmez, C. K. F. Shen, F. Wudl, **2004**, *16*, 1905-1908.
60 M. Dietrich, J. Heinze, G. Heywang, F. Jonas, *J. Electroanal. Chem*., **1994**, *369*, 87-92.
61 C. L. Gaupp, D. M. Welsh, J. R. Reynolds, **2002**, *23*, 885-889.
62 D. M. Welsh, A. Kumar, E. W. Meijer, J. R. Reynolds, *Adv Mater*., **1999**, *11*, 1379-1382.
63 D. M. Welsh, L. J. Kloeppner, L. Madrigal, M. R. Pinto, B. C. Thompson, K. S.

Schanze, K. A. Abboud, D. Powell, J. R. Reynolds, *Macromolecules* **2002**, *35*, 6517-6525.
64 B. D. Reeves, C. R. G. Grenier, A. A. Argun, A. Cirpan, T. D. McCarley, J. R. Reynolds, *Macromolecules* **2004**, *37*, 7559-7569.
65 J. Roncali, *Chemical Reviews* **1992**, *92*, 711-738.
66 G. Daoust, M. Leclerc, *Macromolecules* **1991**, *24*, 455-459.
67 A. L. Dyer, M. R. Craig, J. E. Babiarz, K. Kiyak, J. R. Reynolds, *Macromolecules* **2010**, *43*, 4460-4467.
68 B. Kuei, E. D. Gomez, *Soft Matter* **2017**, *13*, 49-67.
69 M. J. Kim, A. R. Jung, M. Lee, D. Kim, S. Ro, S.-M. Jin, H. D. Nguyen, J. Yang, K.-K. Lee, E. Lee, M. S. Kang, H. Kim, J.-H. Choi, B. Kim, J. H. Cho, *ACS Appl. Mater. Interfaces*., **2017**, *9*, 40503-40515.
70 K.-H. Yim, G. L. Whiting, C. E. Murphy, J. J. M. Halls, J. H. Burroughes, R. H. Friend, J.-S. Kim, **2008**, *20*, 3319-3324.
71 J. Mei, Z. Bao, *Chem. Mater*., **2014**, *26*, 604-615.
72 T. Adachi, J. Brazard, P. Chokshi, J. C. Bolinger, V. Ganesan, P. F. Barbara, *J. Phys. Chem. C*., **2010**, *114*, 20896-20902.
73 B. J. Schwartz, **2003**, *54*, 141-172.
74 S. L. Pittelli, M. De Keersmaecker, J. F. Ponder Jr, A. M. Österholm, M. A. Ochieng, J. R. Reynolds, *J. Mater. Chem. C*., **2020**, *8*, 683-693.
75 A. M. Österholm, D. E. Shen, J. A. Kerszulis, R. H. Bulloch, M. Kuepfert, A. L. Dyer, J. R. Reynolds, *ACS Appl. Mater. Interfaces*., **2015**, *7*, 1413-1421.
76 C. M. Amb, A. L. Dyer, J. R. Reynolds, *Chem. Mater*., **2011**, *23*, 397-415.
77 K. Cao, D. E. Shen, A. M. Österholm, J. A. Kerszulis, J. R. Reynolds, *Macromolecules* **2016**, *49*, 8498-8507.
78 J. A. Kerszulis, Ph.D., Georgia Institute of Technology, **2014**.
79 L. A. Estrada, J. J. Deininger, G. D. Kamenov, J. R. Reynolds, *ACS Macro Lett*., **2013**, *2*, 869-873.
80 C. Sanchez, P. Belleville, M. Popall, L. Nicole, *Chem. Soc. Rev*., **2011**, *40*, 696-753.
81 L. Ma, Y. Li, X. Yu, Q. Yang, C.-H. Noh, *Sol. Energy Mater Sol. Cells*, **2008**, *92*, 1253-1259.
82 A. C. Sonavane, A. I. Inamdar, D. S. Dalavi, H. P. Deshmukh, P. S. Patil, *Electrochim. Acta*., **2010**, *55*, 2344-2351.
83 X. H. Xia, J. P. Tu, J. Zhang, X. H. Huang, X. L. Wang, W. K. Zhang, H. Huang, *Electrochem. commun*., **2009**, *11*, 702-705.
84 H. Elzanowska, E. Miasek, V. I. Birss, *Electrochim. Acta*., **2008**, *53*, 2706-2715.
85 Y.-C. Nah, S.-S. Kim, J.-H. Park, H.-J. Park, J. Jo, D.-Y. Kim, *Electrochem. commun*., **2007**, *9*, 1542-1546.
86 M. A. G. Namboothiry, T. Zimmerman, F. M. Coldren, J. Liu, K. Kim, D. L. Carroll, *Synth. Met*., **2007**, *157*, 580-584.
87 S. Bhandari, M. Deepa, A. K. Srivastava, A. G. Joshi, R. Kant, *J. Phys. Chem. B*., **2009**, *113*, 9416-9428.
88 B. N. Reddy, M. Deepa, A. G. Joshi, A. K. Srivastava, *J. Phys. Chem. C*., **2011**, *115*, 18354-18365.
89 S. Bhandari, M. Deepa, S. N. Sharma, A. G. Joshi, A. K. Srivastava, R. Kant, *J. Phys. Chem. C*., **2010**, *114*, 14606-14613.
90 A. P. Saxena, M. Deepa, A. G. Joshi, S. Bhandari, A. K. Srivastava, *ACS Appl. Mater. Interfaces*., **2011**, *3*, 1115-1126.
91 C. Bounioux, E. A. Katz, R. Yerushalmi – Rozen, *Polym. Adv. Technol*., **2012**,

23, 1129-1140.
92 D. Bonifazi, D. Mosca, C. Laia, J. Parola, F. Pina, C. Pinherio, WO 2018/073598 Al, **2018**.
93 Z. J. Qi, B. Wei, Y. M. Sun, X. M. Wang, F. Kang, M. X. Hong, L. L. Tang, *Polym. Bull*., **2011**, *66*, 905-915.
94 M. P. C. A. P. B. Ana Clara Lopes Marques, Freibrug (DE); Jorge Araujo, Barcelos (PT) US 9.625,782 B2 **Apr. 18, 2017**
95 J. Liu, Y. Shi, J. Wu, M. Li, J. Zheng, C. Xu, *RSC Adv*., **2017**, *7*, 25444-25449.